

宮崎大学大学院
博士学位論文

**Study on Degradation Diagnostic Technique of
Silicone Rubber**

(シリコンゴムの劣化診断技術の開発に関する研究)

September, 2024

Interdisciplinary Graduate School of Agriculture and
Engineering,
Department of Materials and Informatics
University of Miyazaki, Miyazaki, Japan

MAY THIN KHAING

Acknowledgement

First of all, the author is deeply grateful to her supervisor Professor Tatsuya SAKODA, Faculty of Engineering, University of Miyazaki, Japan. His precious support, kindness, optimism, encouragement, enthusiasm, motivation and immense knowledge helped her a lot in the progress of her research. Without his great instructions and patience, this thesis would not be easily succeeded in practical. Moreover, he gave her a lot of excellent advice, guidance and supervision on her research, and taught her a collection of knowledge on her research field that she had never known before. By following to his treasured supervision, guidance and instructions, she is really developed into a worthy doctoral degree student.

The author would like to express her gratitude to the Board of Examiners, Professor Aya NISHIWAKI, Faculty of Agriculture, Professor Koichi TANNO, Faculty of Engineering, Associate Professor Masanori KAKU, Faculty of Engineering and Associate Professor Yasuyuki OTA, Faculty of Engineering, University of Miyazaki for their helpful suggestions, valuable time, and fruitful discussion throughout this study.

The author is extremely grateful to Mr. Shigehiko Goto, Mr. Tomikazu Anjiki, Mr. Tomoki Chiba, and Mr Yasunori Kasuga, Hamakawasaki Operations Toshiba Energy Systems & Solutions Corporation, Tokyo, for sharing their helpful idea, valuable suggestions and support, knowledge and experience throughout this study.

The author also wishes to express her sincere thanks to Mr. Uki Kanenari, Mr. Yusuke Nishihiro, Mr. Junki Oasa, Mr. Shoichi Higashiyama, and Mr. Yuko Inaoka, Kansai Transmission and Distribution, Inc., Osaka, for sharing priceless suggestions, ideas, motivation and encouragement help her a lot in this study.

The author is very thankful to Dr. Takuma MIYAKE, Department of Engineering, University of Miyazaki for his technical guidance, invaluable suggestions and support. The author also wishes to appreciate the collaborative attitude of all the former and present laboratory members for their warmest welcome, awesome kindness, generous hospitality and truthful friendship with her. Especially, she would like to give her special gratitude to polymer team members, Mr. Kosei YOSHIMURA, Mr. Kenji KODA, Mr. Sora OTANI and Mr. Takaaki NAKAYAMA, for their kind support, cooperation and for spending their time with all the requirements whatever she needed their supports while doing the experiment for

the research. Moreover, the author wishes to extend her gratefulness to Mr. Takafumi UTO for taking care, giving kindness and the requirements whenever she needed his supports during living in Japan. She also wishes to bear vast thanks to her laboratory members because she received gladly amazing atmosphere and an adorable life from them.

The author would like to express her sincere gratitude to the Rotary Yoneyama Scholarship Foundation for financial support while studying in Japan and Japan Power Academy for supporting the research fund while doing this research.

The author is deeply grateful to her lovely parents, Mr. Win Shein and Ms. Myint Myint Kyi, and her lovely brothers, Dr. Okkar Min and Mr. Aung Chit Moe for supporting her spiritually throughout her life, never-ending love and words of comfort.

Last but not least, the author overcame difficult problems related to her research and daily life in Japan with the strong and active support of her laboratory members and lovely friends from Myanmar. The author would like to extend her special thanks to her lovely best friends, Ms. Sane Lai Lai Win, Mr. Chan Myae Ko Ko and Mr. Theik Tun Aung for giving her great physical and mental support of comfort whenever/whatever she needs, never-ending kindness, and staying beside her throughout her life and while studying in Japan.

Study on Degradation Diagnostic Technique of Silicone Rubber (シリコーンゴムの劣化診断技術の開発に関する研究)

MAY THIN KHAING

*Doctoral Course in Advanced Materials and Energy,
Interdisciplinary Graduate School of Agriculture and Engineering,
University of Miyazaki*

Submitted on May 31 2024

Abstract

Recently, silicone rubber (SiR) insulators have emerged as popular outdoor applications for high-voltage overhead transmission and distribution lines. SiR insulators have various advantages such as lightweight design, inherent hydrophobicity characteristics and mechanical strength. However, the hydrophobicity property of SiR insulators may be degraded by multiple stresses and, it may be recovered by low molecular weight (LMW) dispersion from the bulk to the surface. The hydrophobicity losses and their recovery repeatedly occur over time, and eventually, it may lead to dry banding arcing. Therefore, if the degradation degree of SiR insulators can be measured, it may contribute to the long-term maintenance of SiR insulators. To collect aged SiR insulators with different numbers of years in use, which is for developing a degradation diagnostic technique of SiR, is difficult. Therefore, it is desired to make degraded SiR surface, which has similar characteristics to the actual aged SiR surfaces. To realize the fabrication, the surfaces of specimens cut out from 22 kV line post SiR insulators used in the coastal area for 10 and 20 years are first characterized. The results show that to introduce fine particles into the surface is necessary for making degraded surface having the minute surface roughness. Additionally, it was found that to activate the dispersion of LMW with foreign matters is also necessary.

Based on the results of characterization on aged SiR insulators, one fabrication cycle (1-cycle test) of 24 h and two fabrication cycle (2-cycle test) of 48 h are performed. In one fabrication cycle, a red clay adhesion process, an ultraviolet (UV) irradiation process, a surface heating process, a heat radiation process and a surface cleaning process are included. The effects of UV irradiation and surface heating are evaluated, and then, it was found that a combination of UV irradiation for breaking molecular structure and surface heating for promoting LMW dispersion play an important role in adhering red clay to SiR surface. In addition, the decreased rate of chemical structure on artificially degraded SiR surface made by 1-cycle test and 2-cycle test are similar to those of 10-year aged and 20-year aged SiR surfaces, respectively. Therefore, it can be considered that various degraded SiR surfaces can be made by changing the number of fabrication cycle.

To grasp the degradation degree on actual aged and artificially degraded SiR surfaces, a novel technique is proposed in which the surface discharge (SD) on SiR surface temporarily decreased the surface hydrophobicity and then, the hydrophobicity recovery times are measured. The SD treatments are performed against actual aged and artificially degraded SiR surfaces with the treatment time of 5 s to 25 s. After each SD treatment, the contact angle is evaluated at intervals of 10 min. As a result, the contact angle recovery times on actual aged and artificially degraded SiR surface are longer than that on an unused SiR surface, ie., the contact angle recovery time after SD treatment is useful for investigating the degradation degree. On the other hand, based on the results obtained by scanning electron microscope (SEM) and attenuated total reflection-Fourier transform infrared spectroscopy (ATR-FTIR) measurement, it is shown that SD treatment doesn't cause any physical or chemical damages to the surface of SiR specimens. In addition, the observed maximum SD current did not significantly differ from that obtained during the 20-time salt fog aging test. Moreover, it is confirmed that SD consists of filamentary discharge. In measurement of optical emissions, emissions with wavelength of less than 291 nm which can cut C-H bond of SiR aren't observed. Therefore, it is thought that the direct energy transfer from energetic particles with higher energy than the binding energy of C-H changes chemical characteristics and decreases the contact angle on SiR surface.

CONTENTS

	Page
ACKNOWLEDGEMENTS	i
ABSTRACT	iii
TABLE OF CONTENTS	v
LISTS OF FIGURES	viii
LISTS OF TABLES	xiii

CHAPTER TITLE

1	INTRODUCTION	1
	1.1 Background	1
	1.2 Aim and Objectives	2
	1.3 Methods	3
	1.3.1 Acceleration of Degraded SiR Surface	3
	1.3.2 Evaluation of Degradation Degree on SiR Surface	4
	1.4 Outlines of Thesis	6
2	CHARACTERISTICS OF AGED SILICONE RUBBER INSULATORS USED IN OUTDOORS FOR 20 YEARS	8
	2.1 Introduction	8
	2.2 Characteristics of SiR and Deterioration Factors	9
	2.2.1 Chemical Structure of SiR	9
	2.2.2 Hydrophobicity Characteristics of SiR	11
	2.2.2.1 Swedish Transmission Research Institute Method	11
	2.2.2.2 Hydrophobicity Loss and Recovery of SiR	14
	2.3 Experimental Methods	16
	2.3.1 Characterization of aged SiR specimen	16
	2.3.2 20-times Salt-fog Aging Test	19
	2.4 Experimental Results	23
	2.4.1 Surface Characterization	23
	2.4.2 Electric Characteristics	34
	2.4.3 Hydrophobicity Recovery Time	37

2.5	Discussions	40
2.6	Conclusions	41
3	SHORT-TIME FABRICATION OF DEGRADED SURFACE ON SILICONE RUBBER	42
3.1	Introduction	42
3.2	Features of Aged SiR	42
3.2.1	Surface Morphology of Aged SiR	44
3.2.2	Chemical Changes of Aged SiR	48
3.3	Short-Time Fabrication of Degraded Surface	50
3.4	Results and Discussions	54
3.4.1	UV Irradiation Effect	54
3.4.2	Heating Effect	56
3.4.3	Fabrication by Red Clay Adhesion, UV Ray Irradiation and Surface Heating	58
3.5	Conclusions	64
4	DEGRADATION DIAGNOSTIC TECHNIQUE OF SILICONE RUBBER	65
4.1	Introduction	65
4.2	Degradation Monitoring of SiR Used for Insulators	66
4.2.1	Methodology	66
4.2.1.1	Test Method of Chemical Structure Analysis	66
4.2.1.2	Experimental Setup of Salt-fog Aging Test	69
4.2.2	Results and Discussions	73
4.2.2.1	Chemical Structure Analysis	73
4.2.2.2	Salt-fog Aging Test	77
4.2.3	Conclusions of Degradation Monitoring of SiR Used for Insulators	81
4.3	Evaluation of Degradation Degree of SiR using Surface Discharge	81
4.3.1	Experimental Setup	81
4.3.2	Results and Discussions	85
4.3.2.1	Characteristics of Surface Discharge	85

	4.3.2.2	Recovery Characteristics of Hydrophobicity	88
	4.3.2.3	Analysis of Physical or Chemical Damages on SiR Specimens after SD Treatment	94
	4.3.3	Conclusions of Evaluation of Degradation Degree of SiR Using Surface Discharge	98
4.4		Characterization of SD used for Measuring Degradation Degree of SiR Insulator	99
	4.4.1	Experimental Setup	99
	4.4.2	Results and Discussions	101
	4.4.2.1	Characterization of SD	101
	4.4.2.2	Surface Temperature and Optical Emission of an SD electrode	105
	4.4.3	Conclusions of Characterization of SD Used for Measuring Degradation Degree of SiR Insulator	111
5		EVALUATION OF DEGRADATION DEGREE OF ARTIFICIALLY DEGRADED SIR SURFACE USING SURFACE DISCHARGE	112
	5.1	Introduction	112
	5.2	Experimental Method	112
	5.2.1	Surface Morphology of Aged SiR	112
	5.2.2	Surface Discharge Treatment	115
	5.3	Experimental Results and Discussions	118
	5.3.1	Physical Structure of Artificially Degraded SiR Surface	118
	5.3.2	Chemical Structure Change of Artificially Degraded SiR Surface	122
	5.3.3	Recovery Characteristics of Hydrophobicity after SD Treatment	125
	5.4	Conclusions	133
6		CONCLUSIONS AND RECOMMENDATIONS	134
	6.1	Conclusions	134
	6.2	Recommendation	136
		REFERENCES	137

LIST OF FIGURES

Figure	Page
2.1. Chemical Structure of SiR Bonding Model	10
2.2. Typical Examples of Surfaces with HC from 1 to 6	13
2.3. Water Repellency Recovery Mechanism	15
2.4. Appearance of a 22 kV-SiR Insulator Aged 20 years	17
2.5. SiR Specimens Cut Out from Figure 2.4 (Before Wiping with Alcohol)	18
2.6. Experimental Setup of a 20-times Salt-fog Aging Test	20
2.7. Test Cycles for Obtaining Leakage Current and Recovery Characteristics of Hydrophobicity in a 20-times Salt-fog Aging Test	21
2.8. Surface State of Aged Specimen after Applying Salt-fog for 2h and Partial Discharges during a Salt-fog Aging Test (a) After Applying Salt-fog for 2 h and (b) During a Salt-fog Aging Test.	22
2.9. Images of a Sprayed SiR Insulator for Investigating Hydrophobicity Class Before/After Wiping with Alcohol (a) Before Wiping and (b) After Wiping	25
2.10. Contact Angle of Upper Surfaces of Sheds and Surfaces of Body Portions before/after Wiping (a) Upper Surface of Shed and (b) Body	26
2.11. SEM Images of (a) Upper Surface of Shed 5, (b) Body 5, and (c) Unused Surface	27
2.12. Typical ATR-FTIR Spectra Obtained on Shed and Unused Specimens (a) Before Wiping off and (b) After Wiping off	29
2.13. Peak Intensity Ratios of Chemical Bonds on Shed Portions before Wiping off	30
2.14. Peak Intensity Ratios of Chemical Bonds on Shed Portions after Wiping off	31
2.15. Peak Intensity Ratios of Chemical Bonds on Body Portions before Wiping off	32
2.16. Peak Intensity Ratios of Chemical Bonds on Body Portions	

	after Wiping off	33
2.17.	Temporal Variations in Leakage Current (a)1st Cycle and (b) 20th Cycle In a 20-times Salt-fog Aging Test	35
2.18.	Cumulative Charge in Each Cycle	36
2.19.	Surface States (a) just after a 20-times Salt-fog Aging Test on Specimens Cut Out from Shed 5 and (b) after Hydrophobicity Recovery	38
2.20.	Hydrophobicity Recovery Times of Aged Shed Specimen and Unused SiR specimen	39
3.1.	Appearance of 22 kV-SiR Insulators (a) Aged 10 Years and (b) Aged 20 Years	43
3.2.	Images of Sprayed SiR Insulators for Investigating Hydrophobicity Class (a) Aged 10 Years and (b) Aged 20 Years	45
3.3.	Contact Angles on Unused and Aged SiR Specimens	46
3.4.	SEM Images of (a) Unused, (b) Aged 10 Years and (c) Aged 20 Years	47
3.5.	Peak Intensity Ratios of Chemical Bonds of (a) Aged 10 Years and (b) Aged 20 Years	49
3.6.	A Cycle Consisting of Red Clay Adhesion, UV Ray Irradiation and Surface Heating for Artificially Making Degraded Surface	52
3.7.	Contact Angle Recovery Rates under Various UV Irradiation Times without Step 3	55
3.8.	Contact Angle Recovery Rates under Various Heating Temperatures without Step 2	57
3.9.	SEM Images of (a) Untreated, (b) After Wiping off with Ionized Water, And (c) After Wiping off with Alcohol	59
3.10.	Comparison of Contact Angles of Fabricated SiR Surface after Wiping off with Ionized Water and Alcohol	60
3.11.	Contact Angle Recovery Rates on SiR Surfaces Fabricated with UV Ray Irradiation and Surface Heating	61
3.12.	Peak Intensity Ratios of Targeted Chemical Bonds of Fabricated SiR Surface	63

4.1.	20 Years Aged SiR Insulator used in Actual System	67
4.2.	Specimen Size of SiR	68
4.3.	Experimental Setup of Salt-fog Aging Test	70
4.4.	Test Cycles for Obtaining Leakage Current and Recovery Characteristics of Hydrophobicity	71
4.5.	ATR-FTIR Spectrum by ATR Method	74
4.6.	Peak Intensity Ratio (Specimen A and Shed)	75
4.7.	Peak Intensity Ratio (Specimen A and Body)	76
4.8.	Leakage Current of an Unused Specimen	78
4.9.	Leakage Current of 20 Years Aged Specimen	79
4.10.	Difference of Hydrophobicity Recovery Time between 20 Years Aged Specimen and an Unused Specimen	80
4.11.	Electrode Configuration for Generating SD	83
4.12.	Schematic Diagram of an Experimental Setup for SD Treatment	84
4.13.	Waveforms of Applied Voltage and Discharge Current in an SD Treatment	86
4.14.	Appearance of Uniformly Formed SD on a 150-mesh Plate	87
4.15.	Variations of Contact Angles on Unused, 10 and 20-year-aged SiR Specimens	90
4.16.	Change in Shape of a Water Droplet on SiR Surface treated for 5 s at (a) just after SD Treatment, (b) 10 min Later, and (c) after Hydrophobicity Recovery	91
4.17.	Change in Shape of a Water droplet on SiR Surface Treated for 25 s at (a) just after SD Treatment, (b) 10 min Later, and (c) after Hydrophobicity Recovery	92
4.18.	Contact Angle Recovery Times on Unused, 10- and 20-year-aged SiR Specimens	93
4.19.	SEM Images of an Unused SiR Specimen (a) Before an SD Treatment and (b) After an SD Treatment for 25 s	95
4.20.	ATR-FTIR Spectra of an Unused SiR Specimen before and after an SD Treatment for 25 s	96
4.21.	Peak Intensity Ratio of Chemical Bond of an Unused SiR Specimen	

	before and after an SD Treatment for 25 s	97
4.22.	Experimental Setup	100
4.23.	Frequency Spectra of SD Current Obtained through FFT Analysis	102
4.24.	Waveform due to Filamentary Discharge Obtained through a 10 MHz-HPF	103
4.25.	Uniformly Generated SD on a 150-mesh Plate of an SD Electrode	104
4.26.	Measurement Image of Surface Temperature on 150-mesh Plate	107
4.27.	Optical Emissions during an SD Treatment	110
5.1.	A Fabrication Cycle of Artificially Degraded Surface on a SiR Specimen	114
5.2.	Schematic Diagram of an Experimental Setup for Generating SD	116
5.3.	SEM Images Measured on Artificially Degraded SiR Surfaces made by (a) 1-cycle Test and (b) 2-cycle Test	120
5.4.	Variations in Contact Angle Measured on Artificially Degraded SiR Surface Made by a 1-cycle Test and a 2-cycle Test	121
5.5.	Peak Intensity Ratios on SiR Surfaces before Making Degraded Surface and Artificially Degraded SiR Surfaces Made by a 1-cycle Test and a 2-cycle Test	123
5.6.	Decreasing Rates of Peak Intensity Ratios of Aged And Artificially Degraded SiR Surfaces (a) Si-O Bond, (b) Si-CH ₃ Bond, (c) C-H Bond and (d) O-H Bond in ATH	124
5.7.	SEM Images on SiR Surfaces (a) Before and (b) After SD Treatment	127
5.8.	Temporal Variation of Contact Angles on SiR Surfaces Before Fabrication Cycle, 1-cycle Test and 2-cycle Test after SD Treatment	128
5.9.	Shape Changes of a Water droplet on SiR Surface before making Degraded Surface (a) just after SD Treatment, (b) 10 min Later, and (c) after Hydrophobicity Recovery (SD Treatment Time = 25 s)	129
5.10.	Shape Changes of a Water Droplet on Artificially Degraded SiR Surface made by a 1-cycle Test (a) just after SD Treatment, (b) 10 min Later, and (c) after Hydrophobicity Recovery (SD Treatment Time = 25 s)	130

5.11.	Shape Changes of a Water Droplet on Artificially Degraded SiR Surface made by a 2-cycle Test (a) just after SD Treatment, (b) 10 min Later, and (c) after Hydrophobicity Recovery (SD Treatment Time = 25 s).	131
5.12.	Hydrophobicity Recovery Times on SiR Surface before making Degraded Surface and Artificially Degraded SiR Surfaces made by a 1-cycle Test and a 2-cycle Test	132

LISTS OF TABLES

Table	Page
2.1. Classification Criteria for HC	12
3.1. Cycles Differ in UV Irradiation Time without Step 3	53
3.2. Cycles Differ in Heating Temperature without Step 2	53
3.3. Cycles Differ in Heating Temperature with All Steps	53
4.1. Detailed Data Used in Experimental Test	72
4.2. Surface Treatment on a 150-mesh Plate during an SD Treatment	108
4.3. Contact Angle and Hydrophobicity Recovery Time of Unused and 20-year-aged SiR Surface after an SD Treatment	109
5.1. Experimental Conditions of an SD Treatment	117

CHAPTER 1

INTRODUCTION

1.1 Background

In electrical power systems, a line post insulator plays a vital part in maintaining the system's reliability. Porcelain insulators have been widely used in overhead transmission and distribution lines due to their excellent insulation performance and weather resistance [1]-[3]. However, the porcelain insulators have poor impact resistance, and withstand voltage characteristics deteriorate if the surface is polluted. In recent years, polymer materials have been used as housing materials for insulators of electrical power lines because of their excellent mechanical strength, lightweight design, and good hydrophobic characteristics [4]-[6]. In particular, the lightweight of polymer insulators affects the economic design of towers in high-voltage transmission lines. Therefore, the transmission line voltage can be upgraded without any significant dimensional changes to supporting towers. Thermoplastic polymer materials such as polytetrafluoroethylene (PTFE), polyolefin elastomers (POE) and polyethylene high-density (HDPE) are used at a low voltage level both in outdoor and indoor electrical applications [6]. On the other hand, polymer materials such as epoxy resins (ER), ethylene vinyl acetate (EVA), ethylene propylene diene monomer (EPDM) and silicone rubber (SiR), which are classified as thermoset elastomers, are used as housing materials for high-voltage outdoor insulators. If the insulators manufactured from epoxy resins are installed outdoors at cold temperatures, their performance becomes poor and surface damage occurs, which may lead to failure [6]. SiR is popular as a housing material for outdoor insulators because of its superior hydrophobicity characteristic, excellent breakdown strength and high volume resistivity. However, it has less resistance to tracking/erosion and a weak mechanism [7] [8]. On the other hand, EPDM has better resistance to tracking/erosion and a relatively stronger mechanism. However, EPDM has low surface and volume resistivity compared with SiR [9] [10]. Considering the overall performance of polymer materials, SiR insulators have been mostly preferred in high-voltage overhead transmission and distribution lines because of their superior hydrophobicity characteristics.

SiR insulators with high hydrophobicity can reduce the leakage current in polluted environments under severe weather. Even if the hydrophobicity property temporarily decreases [11]-[14], it can be recovered by the dispersion of low molecular weight (LMW) fluid from the

bulk to the surface. The hydrophobicity loss and its recovery may repeatedly occur over time. As a result, foreign matters are taken in LMW on the SiR surface, and then a polluted surface layer is newly formed. The polluted degradation surface may lead to dry band arcing or flashover. If there is a diagnostic technique to investigate the degradation degree of the SiR surface, it contributes to the long-term maintenance of SiR insulators.

1.2 Aim and Objectives

The main aim to perform this study is to establish a diagnostic technique for the degradation degree of SiR surface used for insulators. The principal aims of this thesis are as follows:

- 1) To investigate the characteristics of aged SiR insulators in order to realize the fabrication of artificially degraded SiR surfaces,
- 2) To fabricate artificially degraded SiR surfaces, which have similar characteristics to the degraded SiR surfaces operated in outdoor. Because a lot of aged SiR specimens should be prepared to establish a diagnostic technique for the degradation degree of SiR surfaces. However, it is difficult to collect aged SiR insulators with different numbers of years in use.
- 3) To grasp the degradation degree of aged SiR surfaces using a 20-times salt-fog aging test.
- 4) To propose a novel technique, which uses the surface discharge (SD) formed on the SiR surface to evaluate the degradation degree on a SiR surface in a short time.
- 5) To characterize SD in order to interpret the decrease mechanism of hydrophobicity characteristic by an SD treatment in detail.

The objectives of this thesis are as follows:

- 1) To maintain the reliability of high-voltage overhead transmission and distribution lines with good insulation performance, and
- 2) To contribute to the long-term maintenance of SiR insulators.

1.3 Methods

1.3.1 Acceleration of Degraded SiR Surface

A considerable number of studies have been conducted on the long-term reliability of SiR insulators [15]-[19]. For example, Mohammad reza Ahmadi-veshki *et al.*, [17] investigated

the effect of pollution, humidity, and 1000 h aging on flashover voltage. Based on the experimentally obtained data, flashover probability, risk, and reliability of insulator utilization were calculated. That is, the long-term reliability was evaluated by using accelerated aging specimens. Also, K. Ning *et al.*, [18] investigated the aging process of SiR arranged in a mountainous region environment. The used specimens were cut out from aged SiR, however, they were de-energized. Thus, there seem to be few reports which evaluate degradation characteristics of SiR energized for a long period of time because it is difficult to collect aged SiR insulators used in outdoor for more than several decades.

A large number of studies show that temperature, humidity, ultraviolet (UV) radiation and other environmental parameters are the main factors affecting the aging speed of SiR. Many researchers have also carried out a lot of work on the degradation mechanisms of SiR under different aging. L. Ying *et al.*, [20] performed the aging process of SiR by UV irradiation (320-400 nm) for 1000 h. Then, the effect of different curing parameters on the UV aging resistance of SiR. Y. Deng *et al.*, [21] investigated the hydrothermal aging performance of high-temperature vulcanized (HTV) SiR and its degradation mechanism. The hydrothermal aging device included humidity, temperature and pressure, however, the UV irradiation process was not included. I. Ullah *et al.*, [22] studied the weather ability of room-temperature vulcanized (RTV) SiR under high pressure, ultraviolet radiation and temperature stress. The surface of all samples showed obvious discoloration, which may be caused by the cyclization behavior in the polymer during the process of UV irradiation, heat and high electrical stress. In addition, J. Chen *et al.*, [23] studied the influence of accelerated aging on the properties of an RTV anti-pollution flashover coating. In J. Chen *et al.*, [23], a xenon lamp weathering equipment was used to conduct the accelerated aging test. The internal structure of a xenon lamp weathering equipment was composed of the sample chamber and the xenon lamp light source chamber. An air-cooled xenon arc light source, a quartz glass filter, an automatic water spraying control device, sensors (temperature, humidity, luminous flux), and a rotatable sample table were included in the xenon lamp light source chamber. The xenon arc lamp could simulate the full sunlight spectrum to reproduce the destructive light radiation. At the same time, the quartz glass filter was used to filter the xenon lamp radiation, so that the spectral energy distribution received by the sample surface was close to the natural solar spectrum, between 295 and 800 nm. The temperature and humidity in the sample chamber were controlled by air, with an appropriate temperature and humidity entering the chamber. Considering that the samples can be used in a high-humidity

and solar irradiation environment, the four-segment light-dark cycle program mode was adopted to simulate dark, light, rain, sunlight and other cyclic environments. The aging chamber with a xenon lamp with an optical filter can effectively simulate the solar spectrum at the Earth's surface and also can set up a rain environment, with high air temperature and high humidity.

Although the test results in an ambient atmosphere are relatively reliable and the consideration of unpredictable climate changes is included, the aging speed is slow, and the controllability is poor, which is not suitable for basic scientific research and industrial production. Traditional artificial aging, which is based on an AC/DC multi-stress accelerating chamber, high-temperature annealing, a UV box, etc., can only simulate one situation in a complex real service environment. An aging test chamber with a xenon arc lamp can simulate the full sunlight spectrum to reproduce destructive light radiation in different environments such as rain, and sunlight. However, there is no consideration of the pollution on SiR surface in an aging test chamber with a xenon arc lamp. The pollution on SiR surface is also an important factor because the polluted degradation SiR surface may lead to dry band arcing or flashover. In this study, we proposed a fabrication cycle which consists of a red clay adhesion process to promote physical aging, a UV irradiation process, a surface heating process, a heat radiation process, and a surface cleaning process as rainfall. The artificially degraded SiR surface, which has similar characteristics to the actual aged SiR surface, can be made within a short time by using a proposed fabrication cycle.

1.3.2 Evaluation of Degradation Degree on SiR Surface

To widen the range of usage of SiR insulators in outdoor, the deterioration mechanism and understanding of long-term reliability of SiR are the most important issue. Many researchers have investigated the failures of SiR insulators. A. H. El-Hag *et al.*, [24] studied the influence of shed parameters on the ageing performance of polymer insulators in salt fog. It was found that insulators having larger shed diameters and protected leakage distance showed better ageing performance. R. S. Gorur *et al.*, [25] found that an insulator with a protective creepage distance maintained its initial surface hydrophobicity for a much longer time than the other designs. Also, the leakage current was much lower for the protected profiles than for the other designs. Investigating the behaviour of the leakage current waveforms in the frequency domain has been widely useful in correlating the leakage current waveforms with the dry band and tracking activities [26]-[31]. S. Kumagai and N. Yoshimura [27] proposed a simple method to evaluate

the state of the polymer surface by using the leakage current characteristics. In A. H. El-Hag *et al.*, [28], low-frequency analysis of the leakage current has been suggested as an effective tool to specify the beginning of ageing and the end of the lifetime of polymer insulators in a salt-fog chamber. In Z. Farhadinejad *et al.*, [32], it has been shown that the discharges have direct relation with the third component of leakage current harmonics. It shows that the appearance of the spikes is related to the changes in leakage current and suggests that leakage current analysis may be considered as a criterion of surface erosion. In M. A. R. M. Fernando and S. M. Gubanski [33], the arcing has been correlated to the harmonics of the leakage current. It has been shown that the third harmonics correlates with surface thermal damage. In addition, R. Ullah *et al.*, [34] analyzed hydrophobicity and performed mechanical tests, leakage current tests, an attenuated total reflectance-Fourier transform infrared spectrometer (ATR-FTIR) and scanning electron microscope (SEM) tests to study the effect of multiple stress aging [34] [35]. On the other hand, to investigate pollution dependence on the discharge behaviour and the insulation performance of heavily polluted SiR, the measurements of flashover voltage and leakage current were performed [36]-[41]. Additionally, the partial discharges, dry-band arc discharges, and flashovers were observed. In a SiR sample polluted with carbon particles of conductive material, partial discharges occur between water droplets and then form interspersed dry bands. In a SiR sample polluted with red clay of nonconductive material, leakage current induces uniform dry bands and dry-band arc discharges. The noticeable difference in flashover voltage between the polluting materials is not seen. Even if the continuous leakage current owing to partial discharges increases, higher hydrophobicity is still maintained after wiping off polluting materials. Thus, investigating the influence of pollution materials on the insulation performance of polymer materials has been focused. However, studies on a diagnostic method for grasping the degree of degradation, which is useful for evaluating the long-term reliability of polymer material, have not been performed enough. In addition, in [36]-[38], the degradation diagnostic method for SiR has been performed on specimens not arranged in actual fields.

In this study, a continuous 20-times salt-fog aging test was performed by applying AC voltage for 3 h with 16 mS/cm of salt-fog, in which an unused SiR specimen and a specimen aged 20 years from a SiR insulator operated in the coastal area. The time required for recovering hydrophobicity on specimens was measured after each test cycle of a continuous 20-times salt-fog aging test. However, the continuous 20-times salt-fog aging test requires a long time. Therefore, it is necessary to propose a novel technique for evaluating the degradation degree on

SiR surfaces in a short time. Other researchers generated the corona discharge using a needle-plate electrode system for lowering hydrophobicity of SiR surface [7][39]. The corona discharge broke the molecular structure of SiR and made obvious cracks on the surface, i.e., the corona discharge caused physical and chemical changes. In this study, we proposed a novel technique which uses the surface discharge (SD) on an unused SiR surface and aged SiR surfaces. Whether an SD treatment can cause physical or chemical damage to SiR surfaces or not can be investigated by using SEM test and ATR-FTIR, respectively, In order to interpret the decrease mechanism of hydrophobicity characteristics by an SD treatment, SD can be characterised by measuring discharge current and optical emission.

1.4 Outlines of Thesis

This thesis is composed of six chapters. The outline is as follows:

- CHAPTER 1 expresses the background, aims and objectives, methods of this research, and outlines of the thesis.
- CHAPTER 2 describes the characteristics of aged 22 kV SiR insulators arranged for 20 years on distribution lines in the coastal area performing a continuous 20-time salt-fog aging test. The characteristics of SiR and its deterioration factors are first described. The hydrophobicity class (HC) of an aged SiR insulator is presented. Then, the results of the contact angle of a water droplet, the surface morphology and the chemical structure against specimens cut out from an aged SiR insulator are discussed. Finally, the measurement of electrical characteristics during a continuous 20-time salt-fog aging test is illustrated.
- CHAPTER 3 provides a short-time fabrication technique of degraded SiR surfaces whose characteristics are similar to those of degraded SiR insulators in outdoor. The features of 10 and 20-year aged SiR insulators measured by HC, contact angle of a water droplet, surface morphology and chemical structure changes are first discussed. Then a novel fabrication technique which consists of a red clay adhesion process, a UV irradiation process, a heat radiation process and a surface heating process is proposed. Here, the roles of UV irradiation and surface heating are also described. Based on the results, the fabrication of artificially degraded SiR surfaces which have similar characteristics to degraded SiR surfaces in outdoor is discussed.

- CHAPTER 4 presents the degradation diagnostic technique of SiR used for insulators in outdoor. The performance of a continuous 20-time salt-fog aging test and its outcome results are first explained. Although a good index of the degradation diagnosis on actual aged SiR surfaces can be investigated by a continuous 20-time salt-fog aging test, it takes a long time. Hence, a novel technique to grasp the degradation degree in a short time is proposed using an SD treatment and then, the recovery characteristics of hydrophobicity and analysis of physical or chemical damages on the actual aged SiR surfaces after an SD treatment are explained. Next, the characterization of SD is discussed by measuring discharge current and optical emissions.
- CHAPTER 5 discusses an evaluation of the degradation degree of artificially degraded SiR surface using an SD treatment, which investigated in Chapter 4. Two kinds of fabrication cycles are performed based on the results obtained from Chapter 3. The physical and chemical structure changes, recovery characteristics of hydrophobicity of artificially degraded SiR surfaces after an SD treatment are discussed.
- CHAPTER 6 summarizes the conclusions of the research and recommendations for the future plan.

CHAPTER 2

CHARACTERISTICS OF AGED SILICONE RUBBER INSULATORS USED IN OUTDOORS FOR 20 YEARS

2.1 Introduction

The use of silicone rubber (SiR) [4]-[5] insulators is spreading in the world, however, it is still limited in Japan. Because the SiR insulators have several excellent properties such as mechanical strength, lightweight design, and hydrophobicity [11]-[15], there are concerns about the hydrophobicity degradation and the decrease of insulation performance by a long-time use in the Japanese climate with high temperature and high humidity. SiR insulators in outdoor are exposed to multiple stresses such as UV radiation, heat, humidity and pollution. It is well known that hydrophobicity allows the formation of discrete water droplets on the insulator surface. Even if the insulator surface loses its hydrophobicity with aging or under extreme humidification, it is recovered by the diffusion of LMW silicone fluid from the bulk. Under the multiple stresses, hydrophobicity loss and its recovery may keep repeating over time. Foreign matters may be taken in LMW over time at the surface, and then the polluted degradation surface is newly formed. The decrease of hydrophobicity results in continuous water channel formation, which may lead to dry band arcing and subsequently flashover. That is, there is a possibility that the surface degradation causes the decrease of insulation performance.

If there is a diagnostic technique to investigate the degradation degree of the SiR surface, it contributes to long-term maintenance. To establish a diagnostic technique for the degradation degree of the SiR surface, a lot of aged specimens should be prepared. However, considering the difficulty of collecting aged SiR insulators with different numbers of years in use, artificially making degraded SiR surfaces is desirable. Therefore, we attempted to artificially make the degradation surface which has similar characteristics to the degraded surface in outdoor. To realize the fabrication, the characteristics of aged SiR used in outdoor must be grasped.

In this chapter, the characteristics of SiR and deterioration factors are first explained. Then, the characteristics of aged 22 kV-SiR-line post insulator arranged for 20 years on distribution lines in the coastal area are grasped. To grasp the characteristics of aged SiR

surfaces, the hydrophobicity level, the contact angle of a water droplet, the surface morphology, the chemical structure, and the electric characteristics of aged SiR surfaces were measured.

2.2 Characteristics of SiR and Deterioration Factors

2.2.1 Chemical Structure of SiR

Figure 2.1 shows the chemical structure of SiR [42]. SiR has siloxane bonds (Si-O) with strong bonding strength as its backbone of SiR (dimethylpolysiloxane). Therefore, SiR has higher heat resistance and chemical stability, and it provides better electrical insulation. In addition, regarding surface water repellency, the methyl group (CH₃) in the side chain has the lowest critical surface tension next to the fluorocarbon group (CF_n) as an organic group. In particular, the solid material of SiR contains a liquid LMW component such as silicone oil, and this LMW component with low surface tension moves in the porous solid freely. This characteristic indicates that SiR has high elasticity, high compressibility, and excellent water repellency. Polymer materials such as SiR themselves are good insulators and have properties such as high insulation resistance and strengthened dielectric breakdown along the surface.

On the other hand, the major concern of SiR insulators is their life expectancy. If SiR insulators are installed in an outdoor environment, their dielectric, thermal and mechanical properties are partially degraded. SiR surface tracking/erosion during an operation can be caused due to electrical stress, which includes corona discharges and dry band arcing. Environmental stresses such as dry sunlight heating in arid areas, UV irradiation, moisture and acid rain contribute to the aging of SiR insulators. These environmental parameters may lead to thermal impact due to heating and radiation, the corrosion of metal-end-fittings and the flow of leakage current on the degraded surface under moist conditions. It may cause flashovers leading to permanent failure of SiR insulators. To achieve enhanced electrical, thermal and mechanical properties of SiR insulators, SiR is mixed with powders of inorganic materials such as Aluminum Tri-Hydrate (ATH) and silicon dioxide (SiO₂) as fillers. Furthermore, due to the effects of antioxidants and additives on UV resistance, excellent material properties have been achieved.

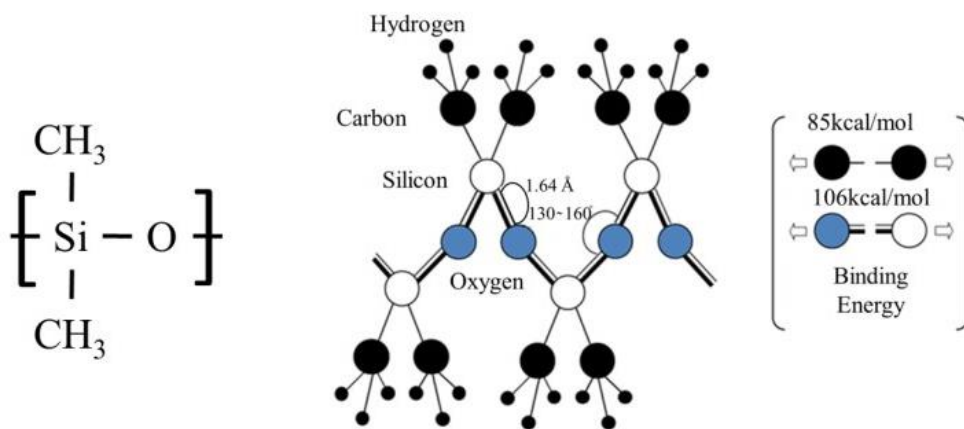


Figure 2.1. Chemical Structure of SiR Bonding Model [42].

2.2.2 Hydrophobicity Characteristics of SiR

2.2.2.1 Swedish Transmission Research Institute Method

The hydrophobicity class (HC) is used for grasping the hydrophobic state. If SiR insulators are exposed to UV rays and PDs, their hydrophobicity might be varied over time. There are seven HC (from HC 1 to HC 7) to classify the hydrophobicity of the insulator surface, which is implemented by a Swedish Transmission Research Institute (STRI) method [43] [44]. If the surface of the SiR insulator is a completely hydrophobic surface, it is defined as HC 1. If the surface of the SiR insulator is a completely hydrophilic (easily wetted) surface, it is defined as HC 7. Table 2.1 illustrates the classification criteria for HC. Figure 2.2 shows the typical examples of surfaces with HC from 1 to 6 [43].

Table 2.1. Classification Criteria for hydrophobicity class (HC) [43].

HC	Description
1	Only discrete droplets are formed. $\theta_r \approx 80^\circ$ or larger for the majority of droplets.
2	Only discrete droplets are formed. $50^\circ < \theta_r < 80^\circ$ for the majority of droplets.
3	Only discrete droplets are formed. $20^\circ < \theta_r < 50^\circ$ for the majority of droplet. Usually they are no longer circular.
4	Both discrete droplets and wetted traces from the water runnels or water film are observed (i.e. $\theta_r = 0^\circ$). Completely wetted areas $< 2 \text{ cm}^2$. Together they cover $< 90\%$ of the tested area.
5	Some completely wetted areas $> 2 \text{ cm}^2$, which cover $< 90\%$ of the tested area.
6	Wetted areas cover $> 90\%$, i.e. small unwetted areas (spots/traces) are still observed.
7	Continuous water film over the whole tested area.

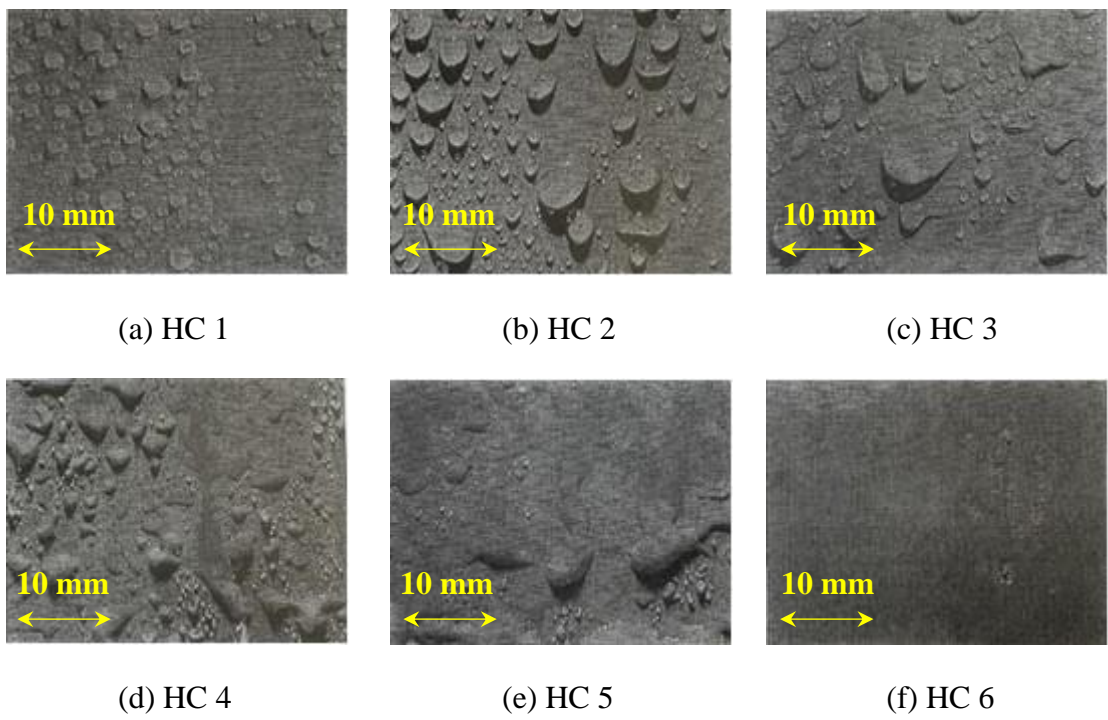


Figure 2.2. Typical Examples of Surfaces with HC from 1 to 6 [43].

2.2.2.2 Hydrophobicity Loss and Recovery of SiR

Figure 2.3 shows the water repellency recovery mechanism by surface dispersion of small molecule components or inversion of polar groups. Regarding the surface water repellency of SiR, the LMW silicone component in the material is uniformly dispersed on the surface to form a hydrophobic surface. If it is characterized by rainfall, the electric discharge occurs. After the electric discharge has occurred, the small molecule component causes losses and decrease the water repellency. However, over a certain period, the water repellency is gradually restored by seeping from the inside of the material to the surface [45]. In particular, regarding the surface dispersion of this small molecule component, it is said that it seeps out to the surface so as to wrap around the wet layer covering the surface. Regarding the time-varying characteristics of this water repellency, it has been pointed out that the siloxane group (polar group) and methyl group (non-polar group) near the surface are inverted. The correlation between the polar group behaviour and the temporal change in water repellency has not been investigated [46].

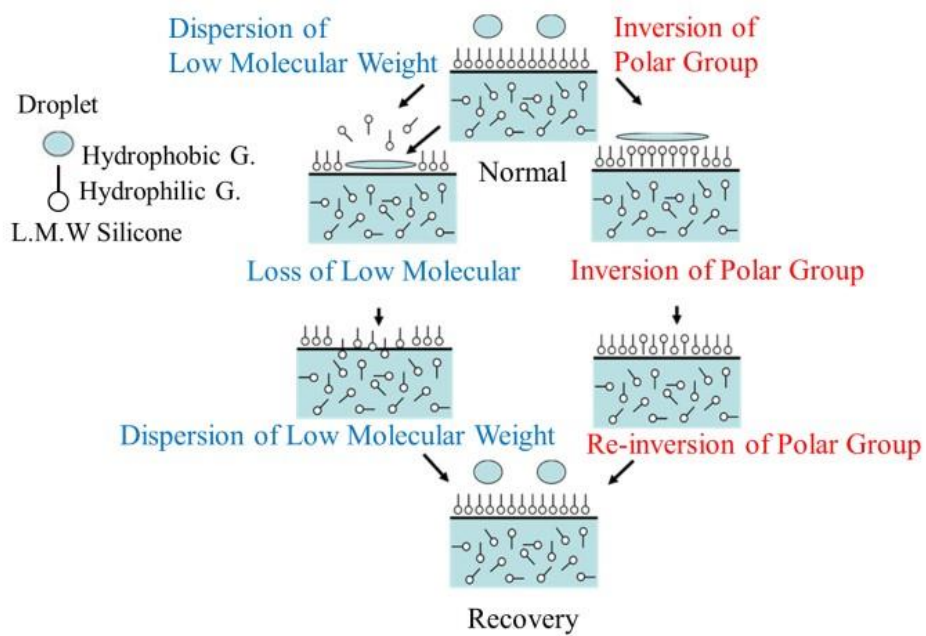


Figure 2.3. Water Repellency Recovery Mechanism.

2.3 Experimental Methods

2.3.1 Characterization of aged SiR specimen

Figure 2.4 shows a 22 kV-SiR-line post insulator arranged in the coastal area with an average yearly temperature of 16 °C and an average annual rainfall of 1600 mm. The creepage distance of the SiR insulator is 650 mm, and the number of sheds with a diameter of 150 mm is 5. SiR contains 50% of alumina trihydrate (ATH). From Figure 2.4, pollution adhesion is recognized. It is noted that Shed 1 and Body 1 were covered with an insulator cover for 20 years in operation. Also, any discharge traces were not visibly recognized on the entire surface. Six specimens cut out from body portions and five specimens from shed portions were prepared, as shown in Figure 2.5. The removal number of aged SiR insulators was one. Because the pollution state and the degradation degree might be dependent on natural stresses at a particular place, a lot of aged specimens are required to grasp the insulation performance of aged SiR insulators. However, this study aims to investigate the characteristics of aged SiR for making artificially degraded SiR surfaces. It will be possible to achieve this purpose by investigating the relationship between the characteristics of polluted surfaces and the electric characteristics. The hydrophobic state on the SiR surface was grasped using a Swedish Transmission Research Institute (STIR) method as explained in Section 2.2.3.1. The contact angle of a water droplet on the SiR surface was measured using a contact angle meter (AUTO 100, Simage) which automatically measured 7 μl of a water droplet dropped from a syringe to each SiR specimen surface. The surface microstructures of aged SiR specimens were observed by scanning electron microscope (SEM). The surface roughness was measured by using a surface roughness tester (DR 130, SATO TECH). The chemical changes were observed using an attenuated total reflection-Fourier transform infrared spectroscopy (ATR-FTIR) (FT/IR-6600ST, JASCO). The variations of Si-O in siloxane bond (1083 cm^{-1}), methyl group Si-CH₃ (1260 cm^{-1}), C-H bond in a methyl group and O-H in ATH intensity ratios of target chemical bonds of aged SiR specimens against those of an unused specimen were evaluated, that is, the peak intensities on an unused specimen are set to reference.

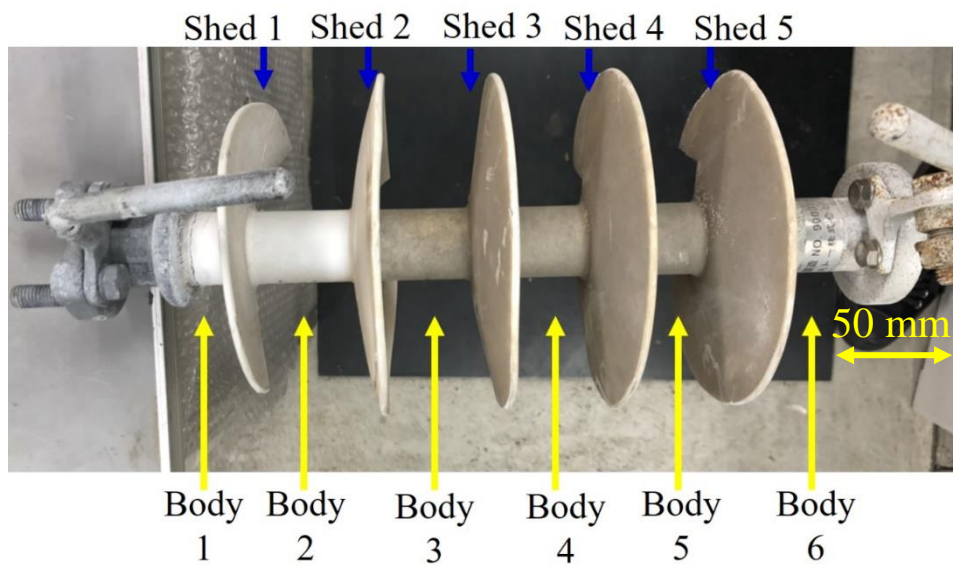


Figure 2.4. Appearance of a 22 kV-SiR Insulator Aged 20 years.

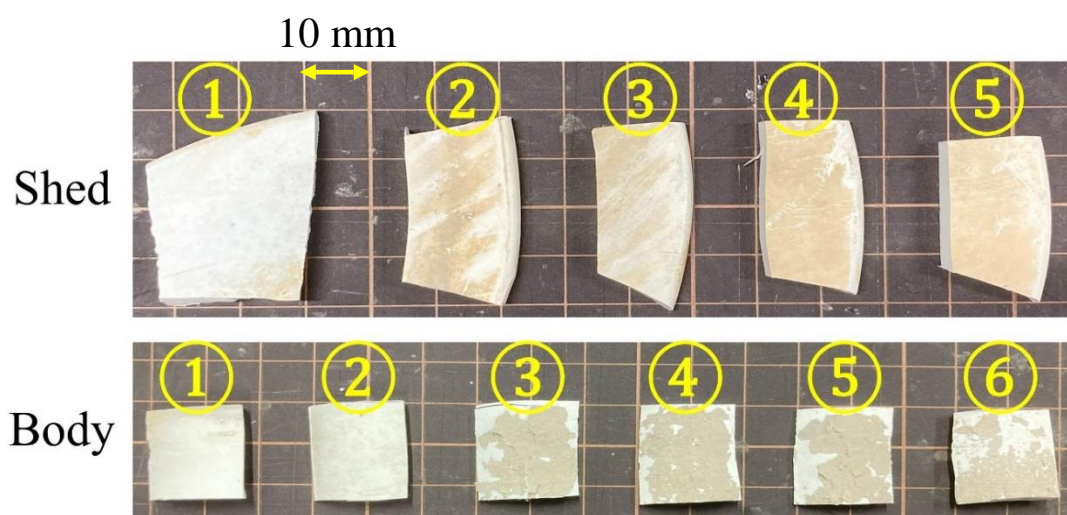


Figure 2.5. SiR Specimens Cut Out from Figure 2.4 (Before Wiping with Alcohol).

2.3.2 20-times Salt-fog Aging Test

Figure 2.6 shows the experimental setup of a 20-times salt fog aging test for measuring electric characteristics. A pair of metal electrodes was placed on a SiR specimen which was 75 mm long, 50 mm wide, and 4-7 mm thick, and the distance between two metal electrodes on the specimen was 50 mm. The thickness range was the variation in the thickness of a shed in the radial direction. Two specimens were cut out from Shed 1 and Shed 5. Because the body portion is in cylindrical shape, any specimens for the aging test could not be cut out. Therefore, a 20-times salt fog aging test was conducted on shed specimens. The shed inclination angle of a 22 kV-SiR line post insulator is 15°. Therefore, the specimen with an inclination angle of 15° was arranged in the center of a chamber with a volume of $1.5 \times 1.5 \times 1.5 \text{ m}^3$, which simulated the inclination angle of sheds of aged SiR insulator as mentioned above. A spray rate of salt fog with a diameter of 10 μm was 0.9 l/h, and its conductivity was set at 16 mS/cm [19] which simulated the condition of the coastal area and easily produced partial discharges among discrete water droplets.

A part of the test cycles in a 20-times salt fog aging test is shown in Figure 2.7. First, salt fog was applied for 2 h without applying ac voltage, which made numerous water droplets having a diameter less than 1 mm even on the surface of aged specimens, as shown in Figure 2.8(a). Next, ac voltage of 6 kV was applied for 3 h, and the leakage current was monitored on a PC through an A/D converter with a sampling rate of 2.4 kS/s. The voltage-to-ground voltage of our used 22 kV-SiR- line post insulator and the creepage distance are 13.8 kV and 650 mm, respectively.

Therefore, the average electric field is 21.2 V/mm. Because the applied average electric field in the salt fog aging test is 120 V/mm, the voltage stress in the salt fog aging test is 5.7 times larger than that in actual operation. The measurement precision was 0.1 mA. When the leakage current was measured, partial discharges among water droplets occurred as shown in Figure 2.8(b). After that, 72 h was held without applying salt fog and ac voltage. As shown in Figure 2.7, one cycle takes 77 h in total. After each test cycle, the hydrophobicity recovery time was measured.

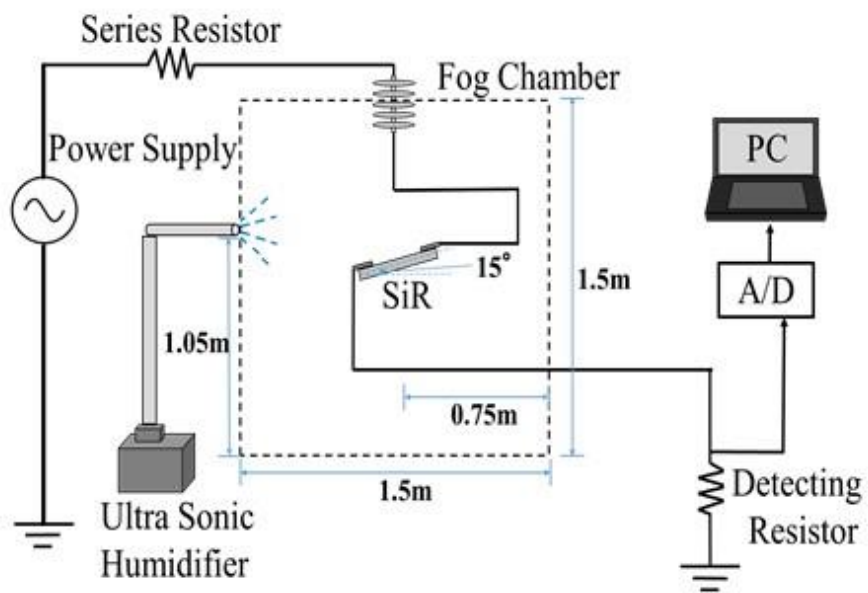


Figure 2.6. Experimental Setup of a 20-times Salt-fog Aging Test.

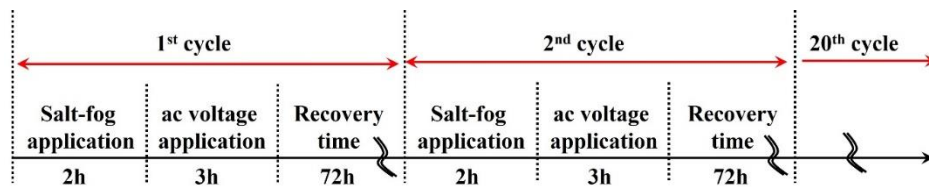
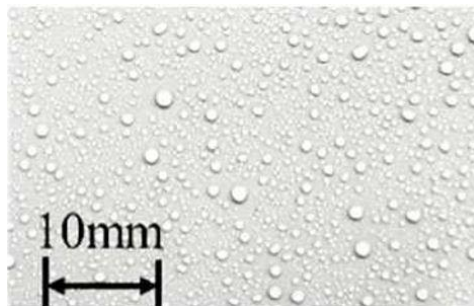
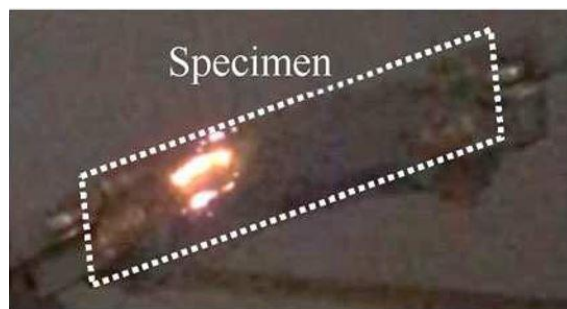


Figure 2.7. Test Cycles for Obtaining Leakage Current and Recovery Characteristics of Hydrophobicity in a 20-times Salt-fog Aging Test.



(a)



(b)

Figure 2.8. Surface State of Aged Specimen after Applying Salt-fog for 2h and Partial Discharges during a Salt-fog Aging Test (a) After Applying Salt-fog for 2 h and (b) During a Salt-fog Aging Test.

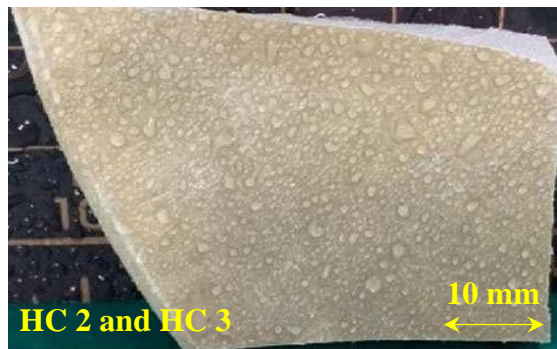
2.4 Experimental Results

2.4.1 Surface Characterization

Figure 2.9 shows example images of a sprayed aged SiR insulator before/after wiping with alcohol. HC on the entire surface of the aged insulator was in the range of HC 1-HC 2 although pollution adhesion was visibly confirmed. To investigate the reason why HC class on the polluted surface still was high, the contact angle of a water droplet on each specimen cut out from the shed or body portion of an aged SiR insulator was measured before/after wiping with alcohol. In the case of measurements of shed portions, the upper surfaces of sheds were measured. The contact angle on an unused SiR specimen was also measured. The results are shown in Figure 2.10. The number on horizontal axis indicates the measured portions shown in Figure 2.4. The contact angles on the upper shed surfaces of Sheds 1, 3, and 5 before wiping are lower than that of an unused specimen. However, by removing foreign matters capable of wiping, the low contact angles become higher than that of an unused specimen. In the case of body portion, although the contact angle of Body 1 is lower than that of an unused specimen, it becomes higher than that of an unused specimen after wiping.

Figure 2.11 shows examples of SEM images observed on Shed 5 and Body 5 before/after wiping with alcohol. Foreign matter adhesion can be seen on both surfaces of Shed 5 and Body 5 even after wiping. In Figure 2.10, the contact angles on body portions before wiping are higher than those of shed portions before wiping. Granular projections as shown in Figure 2.11(b) can be seen on body portions before wiping, which probably makes the contact angle higher. In the cases of body portions, the contact angles on Body 2-Body 6 after wiping are almost the same as those before wiping. The surface roughness on shed and body portions before/after wiping was more than $0.5\ \mu\text{m}$ while that on an unused specimen was $0.34\ \mu\text{m}$. The minute surface roughness due to foreign matter adhesion might make the contact angle larger than that of an unused specimen. However, in the cases of shed portions, the contact angles before wiping are smaller than those after wiping. For example, the surface roughness on Shed 5 before wiping was $0.78\ \mu\text{m}$ which was larger than that on the unused surface, however, the contact angle was smaller than that on the unused surface. Incidentally, the sticking quantity of massive foreign matters capable of wiping on the upper surface of Shed 5 was larger than that of Body 5. The water absorptivity of the massive foreign matters capable of wiping on Shed 5 is considered to be high, which made the contact angles before wiping low. The contact angle after removing foreign matters with high water absorptivity becomes higher than that of an

unused specimen because of the minute surface roughness due to remained foreign matter adhesion.

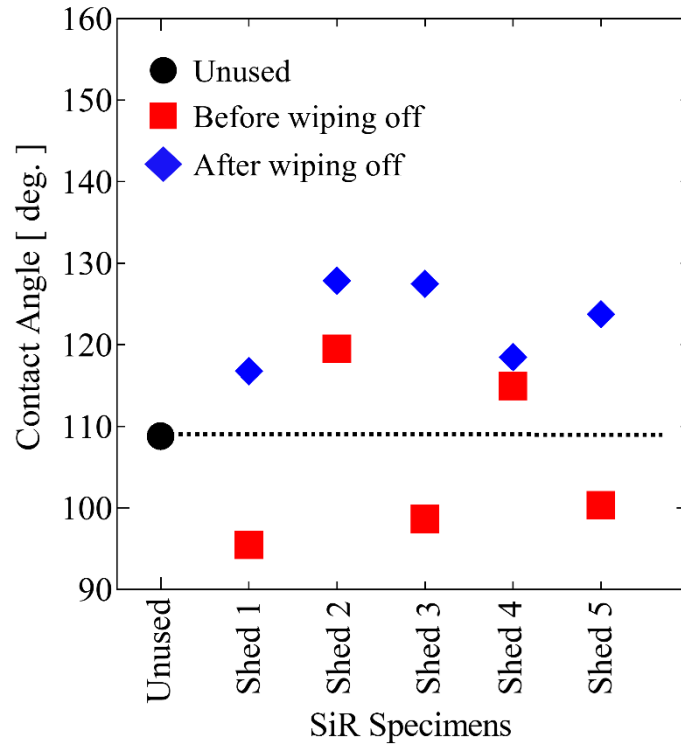


(a)

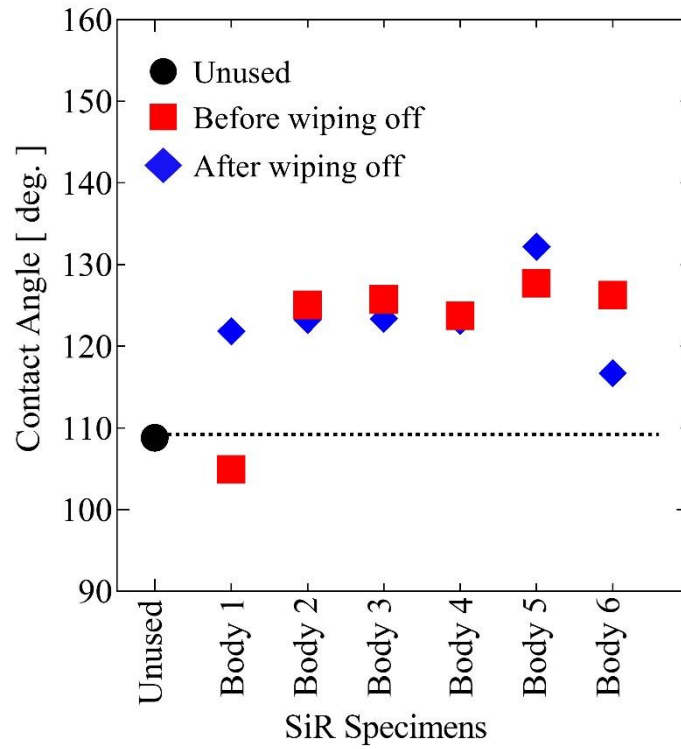


(b)

Figure 2.9. Images of a Sprayed SiR Insulator for Investigating Hydrophobicity Class Before/After Wiping with Alcohol (a) Before Wiping and (b) After Wiping.

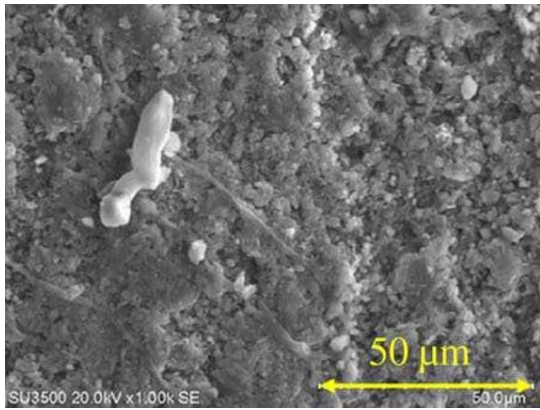


(a)

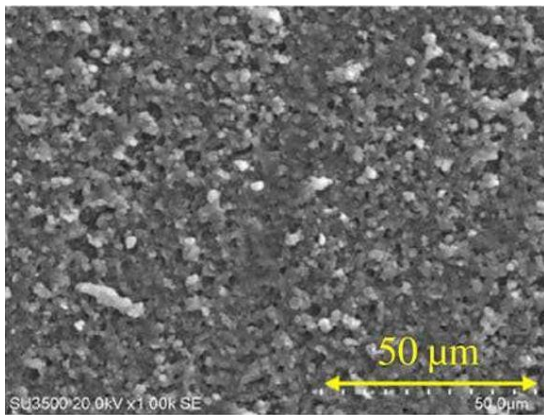


(b)

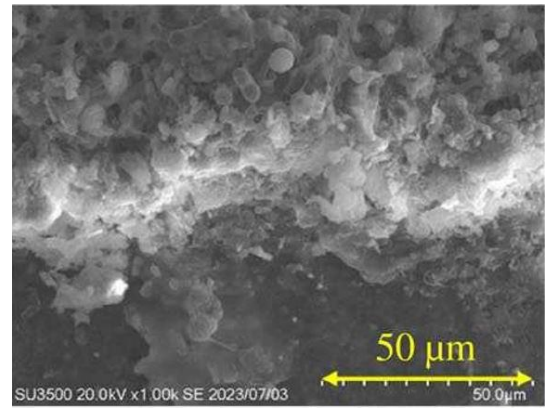
Figure 2.10. Contact Angle of Upper Surfaces of Sheds and Surfaces of Body Portions before/after Wiping (a) Upper Surface of Shed and (b) Body.



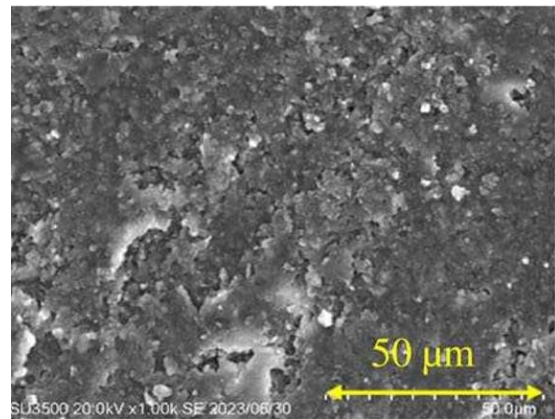
↓ After Wiping off



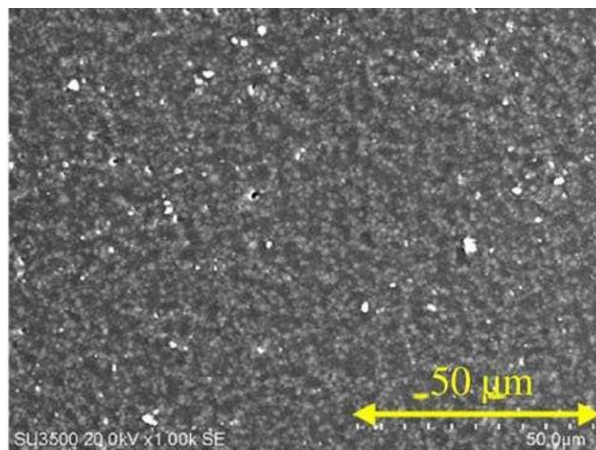
(a)



↓ After Wiping off



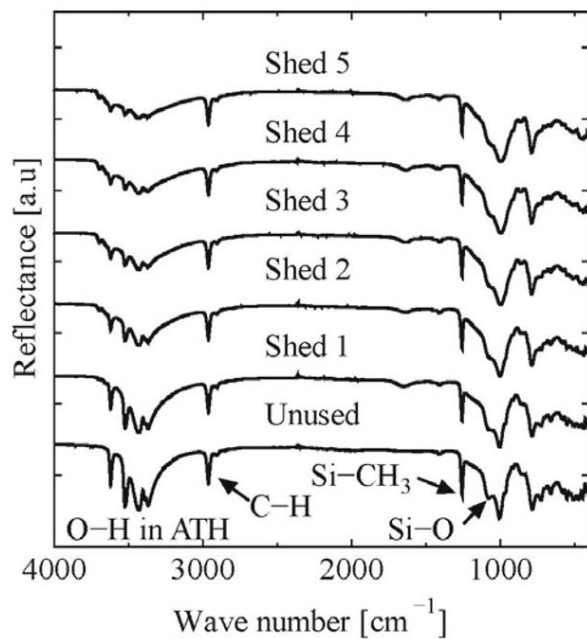
(b)



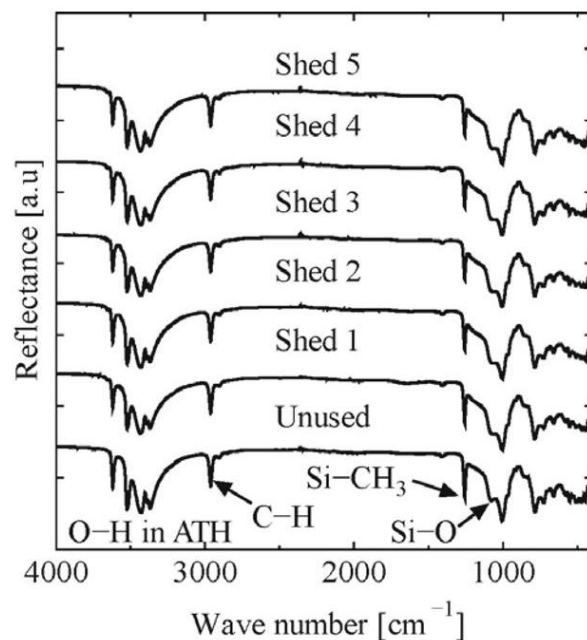
(c)

Figure 2.11. SEM Images of (a) Upper Surface of Shed 5, (b) Body 5, and (c) Unused Surface.

Typical ATR-FTIR spectra obtained from an unused SiR specimen and aged SiR specimens before/after wiping with alcohol are shown in Figure 2.12. It is difficult to grasp the obvious change in the spectral shape, however, peak intensities due to chemical bonds of Si-O, Si-CH₃, C-H, and O-H are different. Then, the peak intensity ratios of chemical bonds of the aged SiR specimen against those of an unused SiR specimen were evaluated. The results obtained before/after wiping with alcohol are shown in Figures 2.13, 2.14, 2.15 and 2.16. Peak intensity ratios corresponding to the Si-CH₃ bond, C-H bond and O-H bond of shed specimens aged 20 years are lower than that of an unused specimen even after wiping. The decrease rates of body specimens are larger than those of shed specimens. Also, the decrease rates at Sheds 3-5 and Bodies 3-6 are larger than those at Shed 1 and Body 1 because Shed 1 and Body 1 were covered with an insulator cover. Additionally, the peak intensity ratio of the O-H bond is extremely low. This indicates that the dispersed LMW and foreign matters cover the original SiR surface. By the way, a peak intensity ratio corresponding to the Si-O bond is higher than that of an unused specimen, which may reflect foreign matters such as silicon dioxide in the polluted surface. Thus, it was found that the chemical structure state is changed by multiple stresses such as UV rays and foreign matter adhesion.

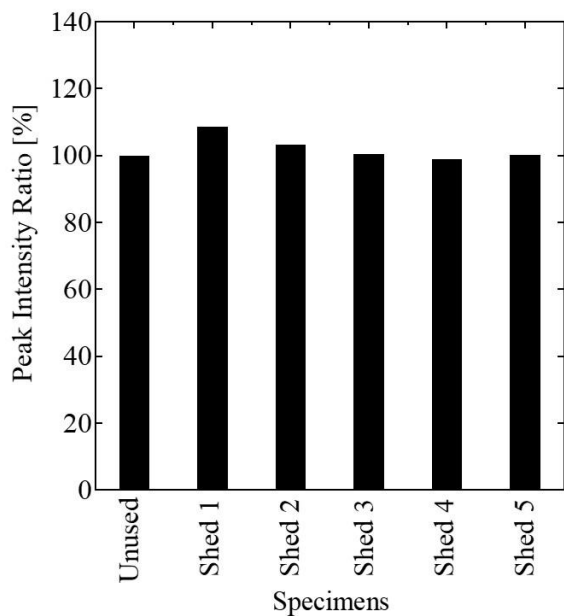


(a)

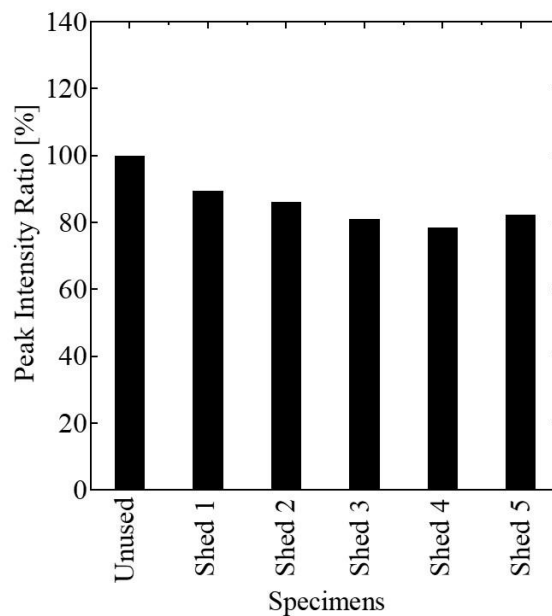


(b)

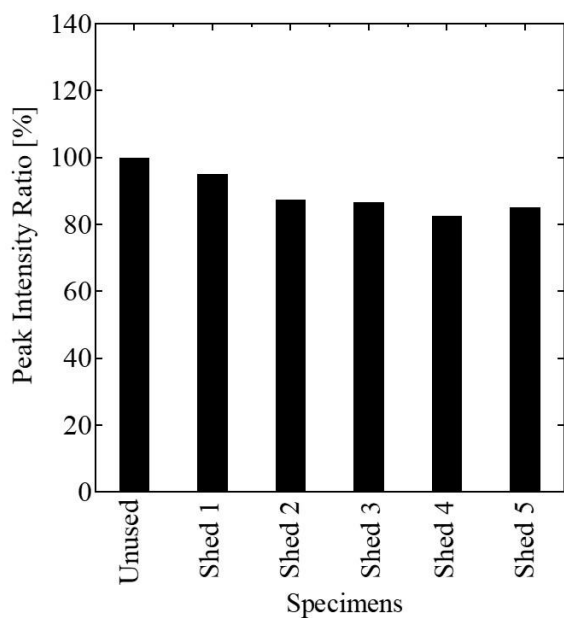
Figure 2.12. Typical ATR-FTIR Spectra Obtained on Shed and Unused Specimens
(a) Before Wiping off and (b) After Wiping off.



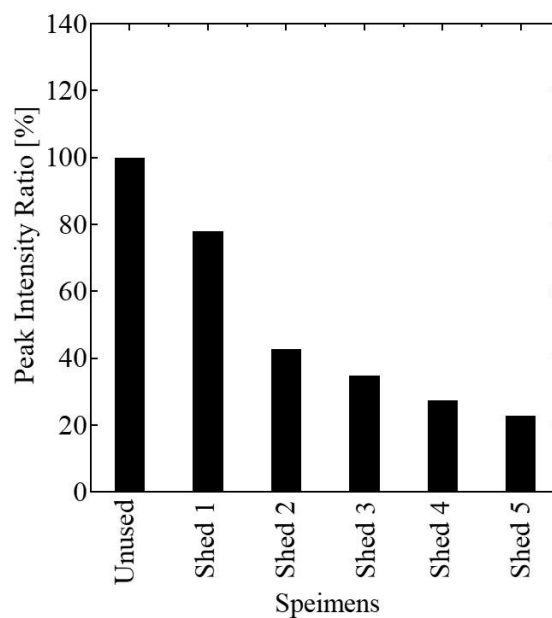
Si-O (1083 cm^{-1})



Si-CH₃ (1260 cm^{-1})

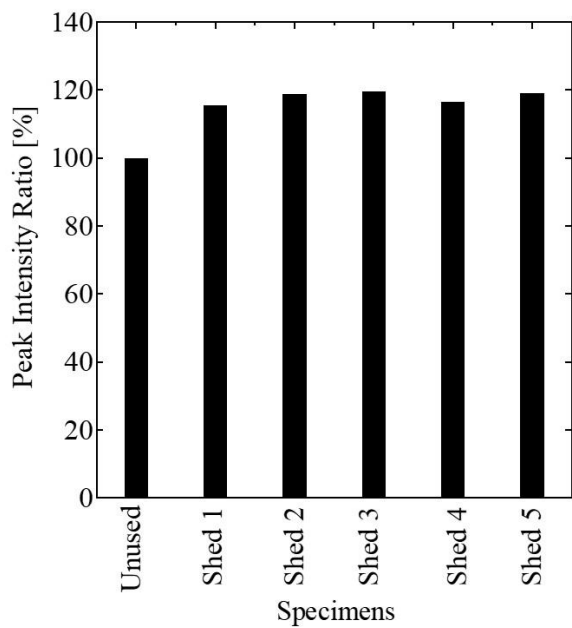


C-H (2963 cm^{-1})

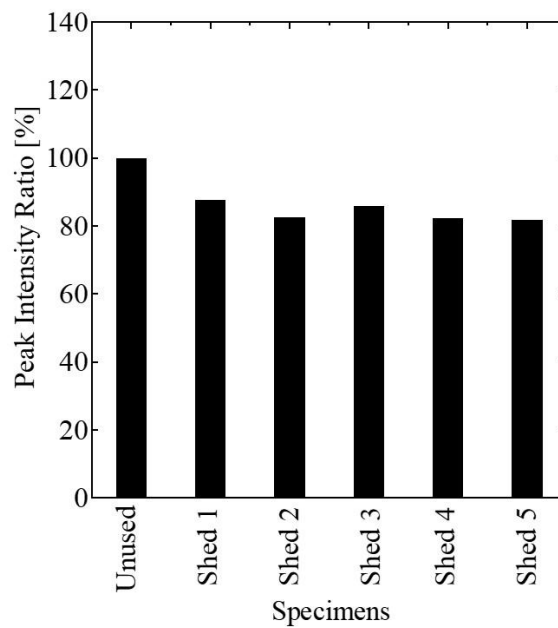


O-H in ATH (3434 cm^{-1})

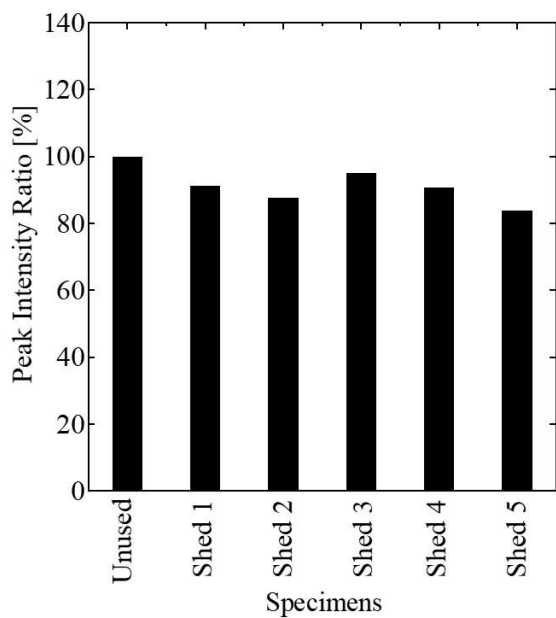
Figure 2.13. Peak Intensity Ratios of Chemical Bonds on Shed Portions before Wiping off.



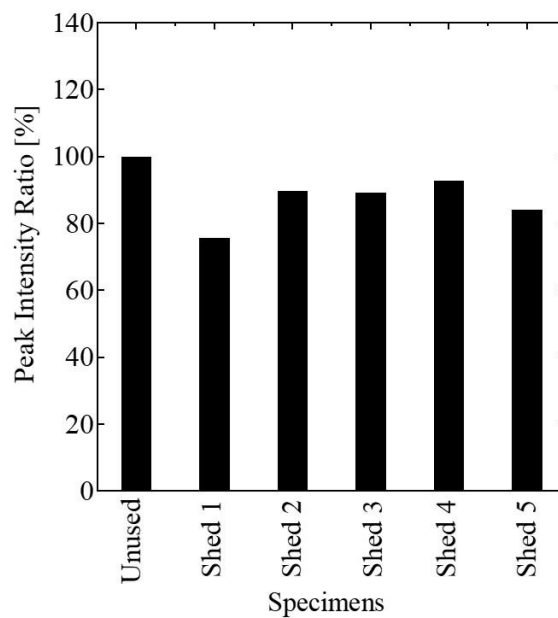
Si-O (1083 cm^{-1})



Si-CH₃ (1260 cm^{-1})

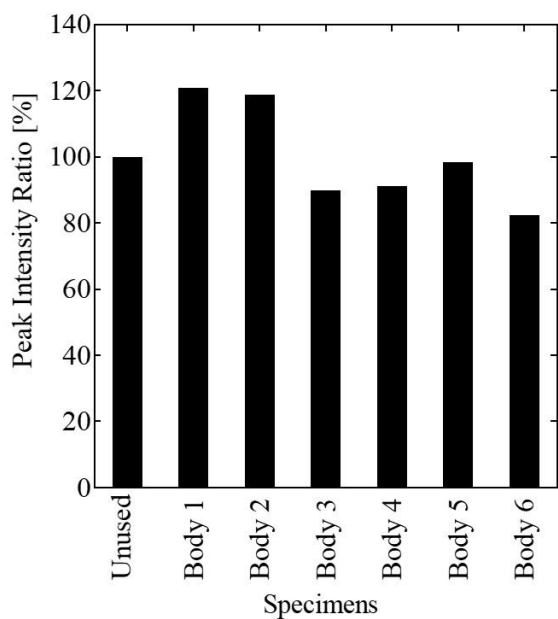


C-H (2963 cm^{-1})

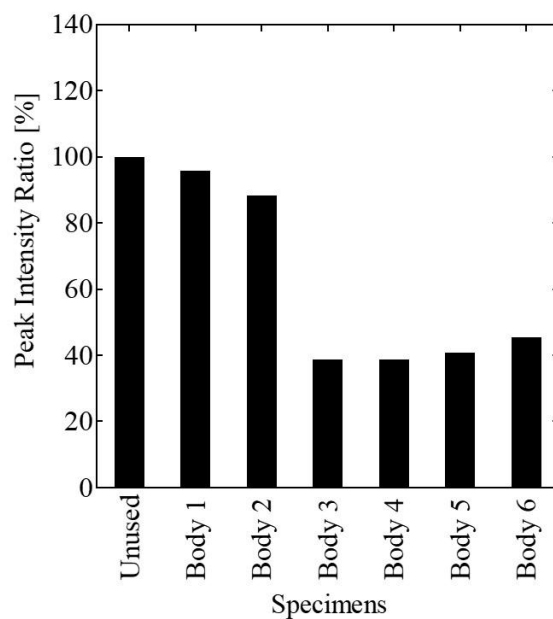


O-H in ATH (3434 cm^{-1})

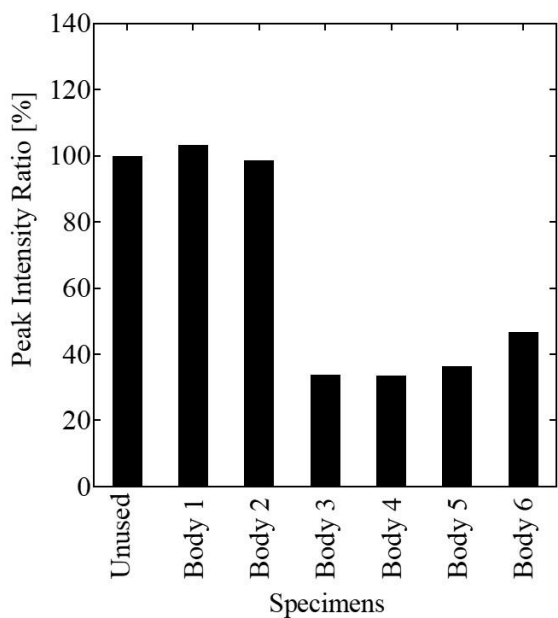
Figure 2.14. Peak Intensity Ratios of Chemical Bonds on Shed Portions after Wiping off.



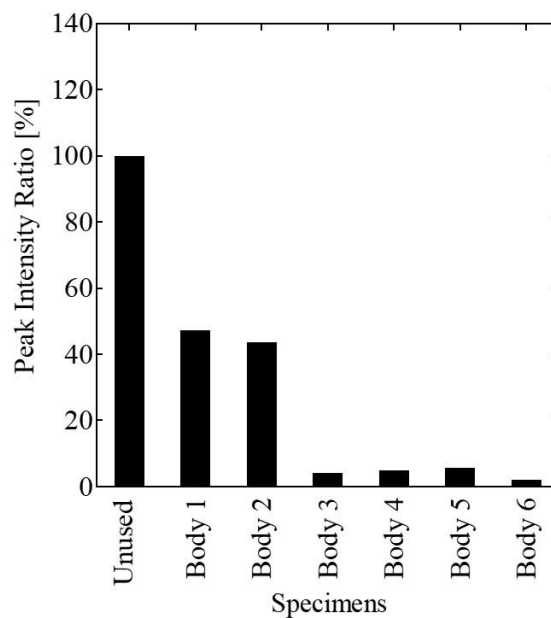
Si-O (1083 cm⁻¹)



Si-CH₃ (1260 cm⁻¹)

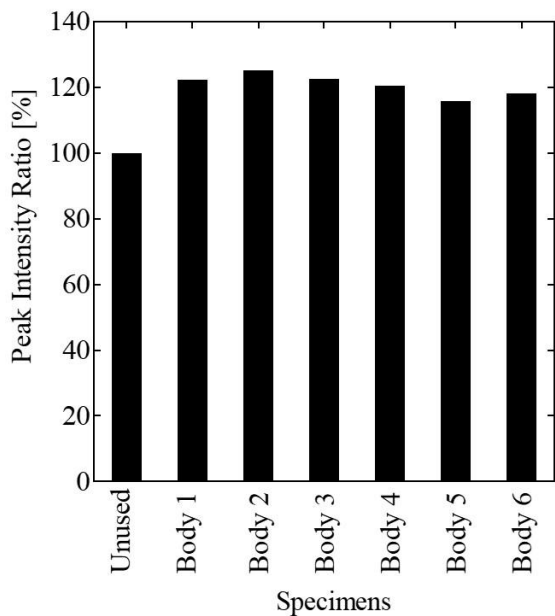


C-H (2963 cm⁻¹)

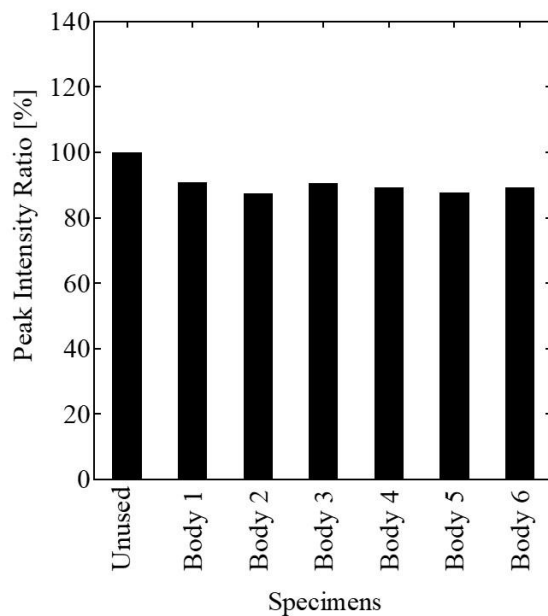


O-H in ATH (3434 cm⁻¹)

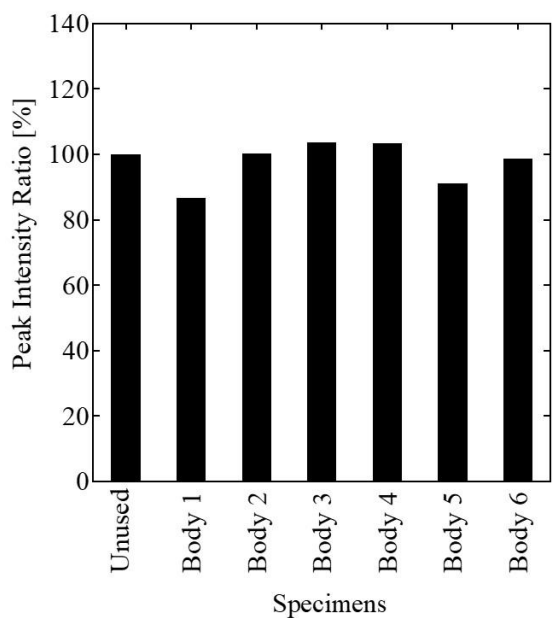
Figure 2.15. Peak Intensity Ratios of Chemical Bonds on Body Portions before Wiping off.



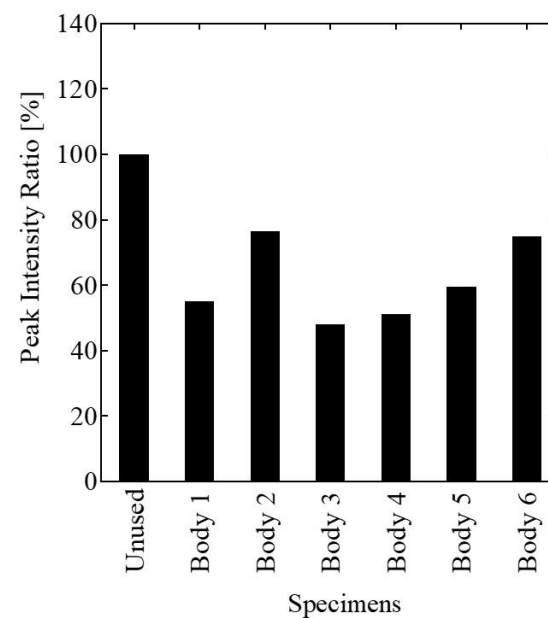
Si-O (1083 cm⁻¹)



Si-CH₃ (1260 cm⁻¹)



C-H (2963 cm⁻¹)

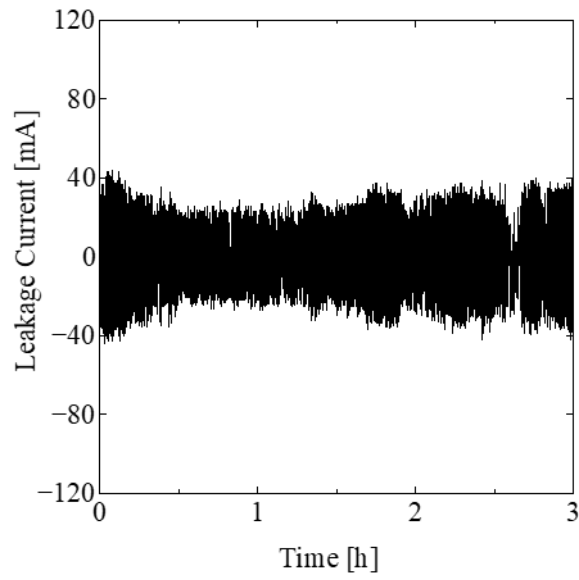


O-H in ATH (3434 cm⁻¹)

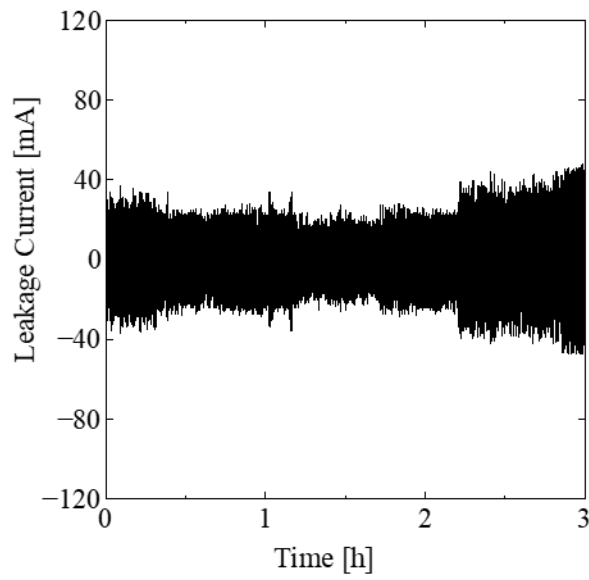
Figure 2.16. Peak Intensity Ratios of Chemical Bonds on Body Portions after Wiping off.

2.4.2 Electric Characteristics

A 20-times salt fog aging test was conducted on specimens cut out from Sheds 1 and 5. Considering the actual dry band arcing occurred on the polluted surface, the surfaces of aged SiR specimens were not wiped off in this test. Figure 2.17 shows a typical variation in leakage current obtained at the 1st and 20th cycle in a 20-times salt fog aging test. The leakage current owing to partial discharges among water droplets on the SiR surface was continuously measured. Then, the cumulative charge by integrating the leakage current in each cycle was calculated. Figure 2.18 shows the cumulative charge against the cycle number. The difference in the cumulative charge between an unused, Shed 1 and Shed 5 is not large. As shown in Figure 2.10, foreign matters made the contact angle higher. In each salt fog aging test, the foreign matters capable of wiping might be easily removed by partial discharges generated among water droplets. Further, the partial discharges might make the surface having minute roughness. It is thought that the difference in the cumulative charge did not become large because there is no large difference in the surface states between the surface influenced by the partial discharges and the unused surface.



(a)



(b)

Figure 2.17. Temporal Variations in Leakage Current (a) 1st Cycle and (b) 20th Cycle in a 20-times Salt-fog Aging Test.

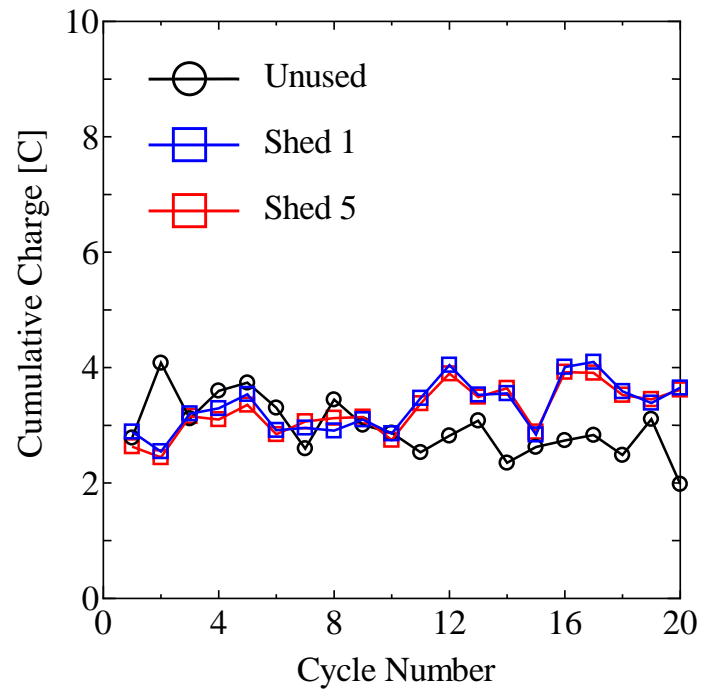
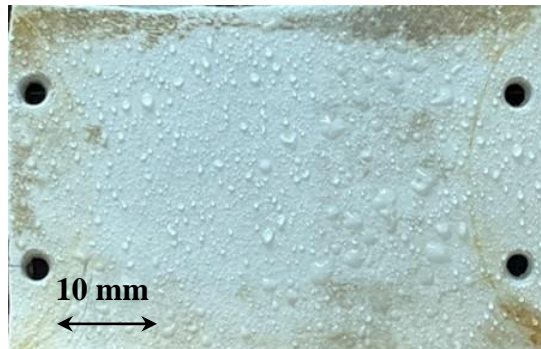


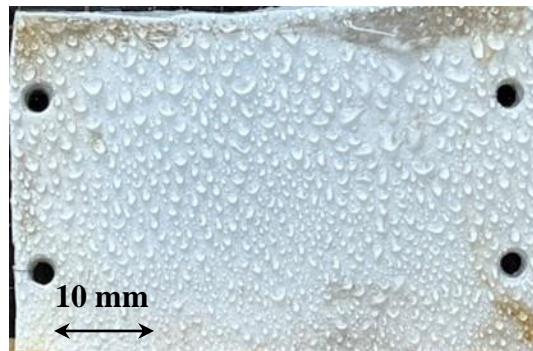
Figure 2.18. Cumulative Charge in Each Cycle.

2.4.3 Hydrophobicity Recovery Time

Figure 2.19 shows the surface states just after a 20-times salt fog aging test on specimens cut out from Shed 5 and after hydrophobicity recovery. Just after a 20-times salt fog aging test, the hydrophobicity level was HC 4. After an elapse of 20 min, the surface state returned to the initial state, that is, HC 1. This 20 min is hydrophobicity recovery time. Figure 2.20 shows the hydrophobicity recovery times of an unused specimen and specimens cut out from Sheds 1 and 5 after each cycle in a 20-times salt fog aging test. The hydrophobicity recovery times of Sheds 1 and 5 are longer than that of an unused specimen. The dispersion of LMW in the aged SiR specimen is disturbed by the polluted layer while that in the unused SiR specimen is active. Additionally, the hydrophobicity recovery time of Shed 1 is a little longer than that of Shed 5. This indicates that the formation of a pollution layer which disturbs the dispersion of LMW on the surface of Shed 1 is more progressing than that of Shed 5.



(a)



(b)

Figure 2.19. Surface States (a) just after a 20-times Salt-fog Aging Test on Specimens Cut Out from Shed 5 and (b) after Hydrophobicity Recovery.

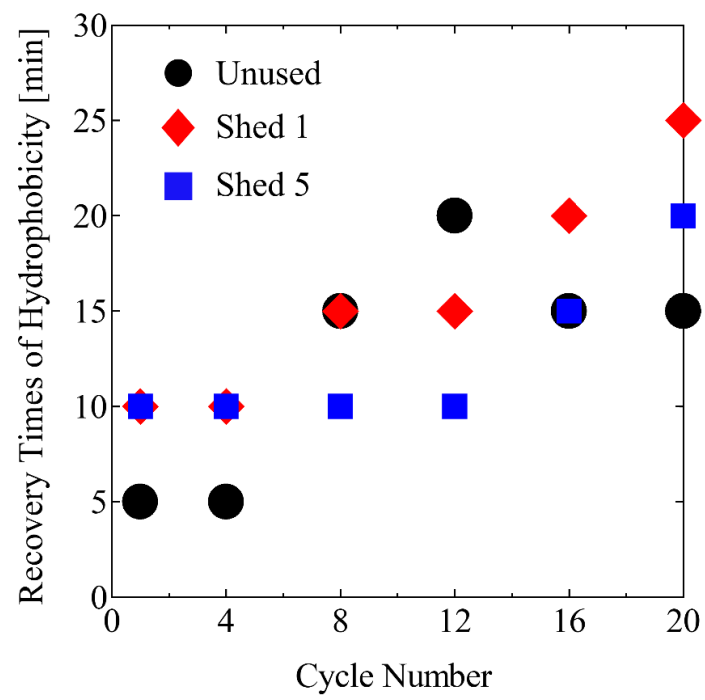


Figure 2.20. Hydrophobicity Recovery Times of Aged Shed Specimen and Unused SiR specimen.

2.5 Discussions

Contact angles on shed specimens before wiping with alcohol were lower than those on an unused specimen. However, the contact angles became higher than that on an unused specimen by removing massive foreign matter capable of wiping. Even after wiping, foreign matters remained and might be taken in LMW over time at the surface. Such polluted degradation surface with the minute surface roughness made the contact angle larger. Additionally, granular projections on the surface of the body portion made the contact angle higher. That is, high hydrophobicity is sustained by foreign matter adhesion having minute surface roughness. To artificially fabricate the SiR surface having a minute surface roughness, it is necessary to introduce fine particles such as red clay into the surface. The particle diameter of red clay is several hundred micrometres. It is thought that the red clay as foreign matter can be easily taken in LMW.

By the way, affected by foreign matter adhesion, the peak intensity ratios due to Si-CH₃, C-H, and O-H on aged SiR specimens decreased in comparison with those on an unused SiR specimen. Extremely, the decrease of O-H is larger than those of Si-CH₃ and C-H. This indicates that ATH was left behind the polluted layer while foreign matters were taken to the surface by the dispersion of LMW over time. Because Shed 1 and Body 1 were covered with an insulator cover for 20 years, the sticking quantity of foreign matter might be less than those at other portions. Therefore, the decrease of O-H at portion 1 (Shed 1 and Body 1) before wiping is small. However, after removing foreign matters capable of wiping, the decrease of O-H at portion 1 is larger than that at portion 5. As shown in Figure 2.8, foreign matters existed even after wiping. There is another polluted layer under the foreign matter capable of wiping. Concerning another polluted layer having a minute surface roughness, Shed 5 is easily affected by UV and heat, which leads to LMW dispersion accompanied by a little ATH. Then, it is considered that the decrease of O-H on uncovered portions tends to become larger than that on the covered portion. Thus, to introduce foreign matters to the surface, it is necessary to control the dispersion of LMW. Because the dispersion of LMW is activated by UV irradiation and surface heating [47], the introduction of fine particles into the surface will be promoted in a short time under UV irradiation and surface heating.

2.6 Conclusions

To establish a fabrication technique for artificially degraded SiR surfaces whose characteristics are similar to those of degraded SiR insulators in outdoors, the characteristics of aged SiR were first investigated. The used specimens were cut out from an aged 22 kV-SiR-line post insulator arranged for 20 years in the coastal area, and the hydrophobicity, contact angle of a water droplet, surface morphology, chemical structure, and electric characteristics were measured.

Major results can be summarized as follows:

- 1) The contact angle after removing foreign matters capable of wiping become higher than that of an unused specimen because of the minute surface roughness due to foreign matter adhesion.
- 2) The chemical structure state of aged SiR is changed by multiple stresses such as UV rays and foreign matter adhesion. Peak intensity ratios corresponding to the Si-CH₃ bond, C-H bond and O-H bond of shed specimens aged 20 years were lower than that of an unused specimen even after wiping.
- 3) The difference in the cumulative charge between unused and shed specimens in a 20-times salt fog aging test is not large. However, it was found that the formation of a pollution layer which disturbs the dispersion of LMW on the shed surface covered with an insulator cover is more progressing than that on the uncovered shed surface.
- 4) To artificially fabricate the SiR surface having the minute surface roughness, it is necessary to introduce fine particles such as red clay into the surface. Additionally, it is necessary to activate the dispersion of LMW by controlling UV irradiation and surface heating.

CHAPTER 3

SHORT-TIME FABRICATION OF DEGRADED SURFACE ON SILICONE RUBBER

3.1 Introduction

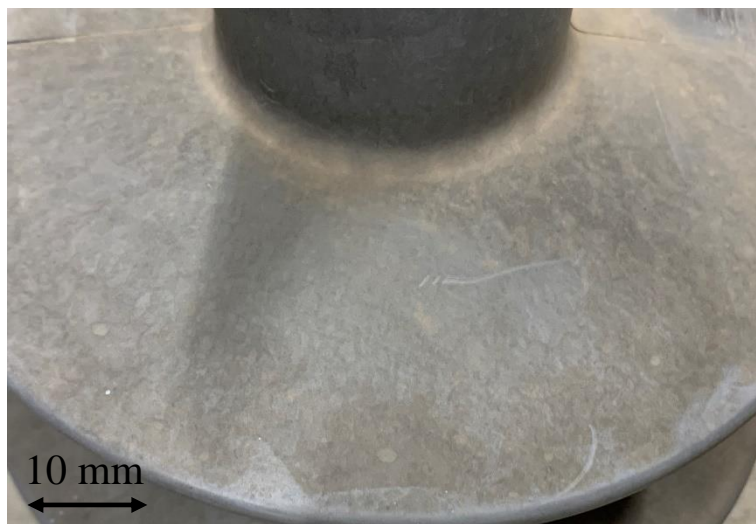
Considering the difficulty of collecting aged SiR insulators with different numbers of years in use, to artificially make degraded SiR surfaces is desirable. Therefore, artificially degraded surfaces which have similar characteristics to the degraded surfaces in outdoor will be fabricated. In Chapter 1, characteristics of 20-year-aged SiR insulators has been investigated. In this chapter, characteristics of both 10-year-aged and 20-year-aged SiR insulators are first investigated by measuring HC, contact angle of a water droplet, surface morphology, and chemical structure change. To artificially reproduce the degraded SiR surface, a novel fabrication technique which consists of a red clay adhesion process, a UV irradiation process, a heat radiation process, and a surface heating process is proposed. The roles of UV irradiation and surface heating are investigated. Based on the results, the degraded SiR surface whose characteristics are similar to those of aged SiR insulator is fabricated.

3.2 Features of Aged SiR

Aged insulators arranged for 10 and 20 years on distribution lines were used. Figure 3.1 shows 22kV-SiR-line post insulators arranged in coastal areas with an average yearly temperature of 18°C and an average annual rainfall of 2300 mm. The creepage distance of the SiR insulator is 950 mm, and the number of sheds with a diameter of 150 mm is 7. SiR contains 50% of ATH. From Figure 3.1, pollution adhesion is recognized. However, any discharge traces weren't recognized on the entire surface. The features of actually aged SiR insulators were compared with that of unused SiR. The removal numbers of aged SiR insulators were 2. Because the pollution state and the degradation degree might be dependent on natural stresses at a particular place. However, the aim of this study is to make the artificial degradation surface, i.e., to artificially reproduce the degradation surface whose characteristics are similar to those of a SiR insulator aged in outdoor.



(a)



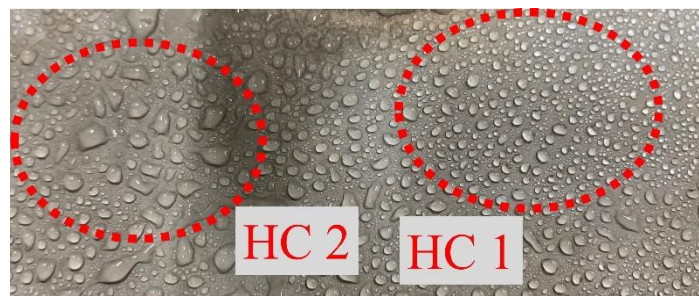
(b)

Figure 3.1. Appearance of 22 kV-SiR Insulators (a) Aged 10 Years and (b) Aged 20 Years.

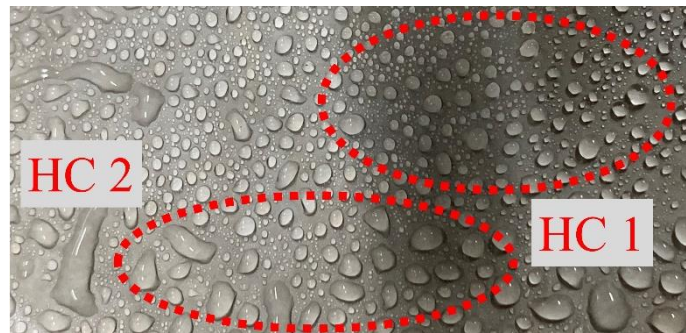
3.2.1 Surface Morphology of Aged SiR

HC of SiR insulator was classified by an STRI method explained in Section 2.2.3.1. HC on portions of SiR aged 10 and 20 years with heavily polluted surfaces are HC 1 from the shape and the distribution of discrete water droplets while those of portions with lightly polluted surfaces are HC 2 as shown in Figure 3.2.

In order to investigate the reason why HC class on the heavily polluted surface becomes higher, the contact angle of a water droplet on the SiR surface was measured using a contact angle meter which was automatically measured. To measure contact angles, five SiR specimens were cut out; one specimen from an unused SiR insulator, two specimens from a SiR insulator aged 10 years (Figure 3.1(a)) and two specimens from a SiR insulator aged 20 years (Figure 3.1(b)). Then, 7 μ L of a water droplet was dropped from a syringe to each specimen surface. The average contact angle on an unused specimen was 110.2° while those at the portion with HC 1 of specimens aged 10 and 20 years were 129.1° and 128.3°, respectively. Additionally, the contact angles on specimens aged 10 and 20 years with HC 2 are 121.3° and 119.8°, respectively. On the other hand, the contact angles on specimens aged 10 and 20 years after wiping off the surface with alcohol are 114.8° and 113.9°, respectively. Anyway, the contact angles on specimens aged 10 and 20 years become larger than that of an unused specimen. It can clearly be seen in Figure 3.3. Aged SiR insulators are exposed to multiple stresses. Foreign matters may be taken in LMW at the surface over time, and then the polluted degradation surface is formed. The surface state may be changed from the initial one, resulting in larger contact angles. Then, the surface microstructures of aged SiR specimens by SEM were first observed. SEM images of unused and aged specimens are shown in Figure 3.4. SEM images obtained on aged 10 and 20 years specimens are slightly different from that on an unused specimen, and foreign matters can be seen on the surfaces of aged 10 and 20 years specimens as shown in Figures 3.4(b) and 3.4(c). On the other hand, even after wiping off the surface with alcohol, the surface morphologies of aged SiR specimens are relatively different from those of an unused one. This may indicate that the physical surface state is changed by multiple stresses. Because there were no visible discharge traces and surface tracking on the surface of SiR insulators, the foreign matter adhesion may have a major influence on the change in the physical surface state.



(a)



(b)

Figure 3.2. Images of Sprayed SiR Insulators for Investigating Hydrophobicity Class

(a) Aged 10 Years and (b) Aged 20 Years.

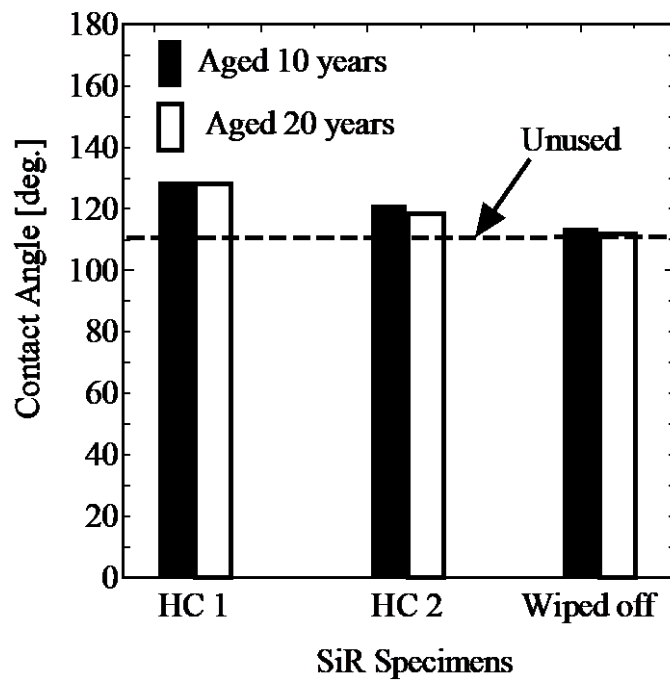
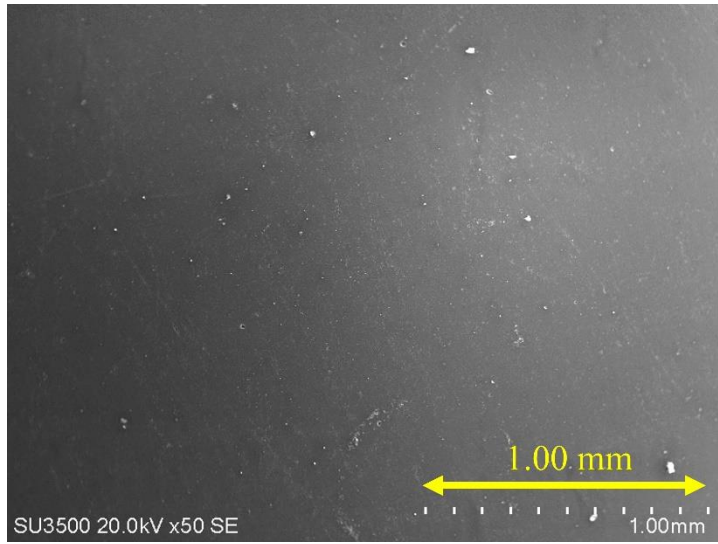
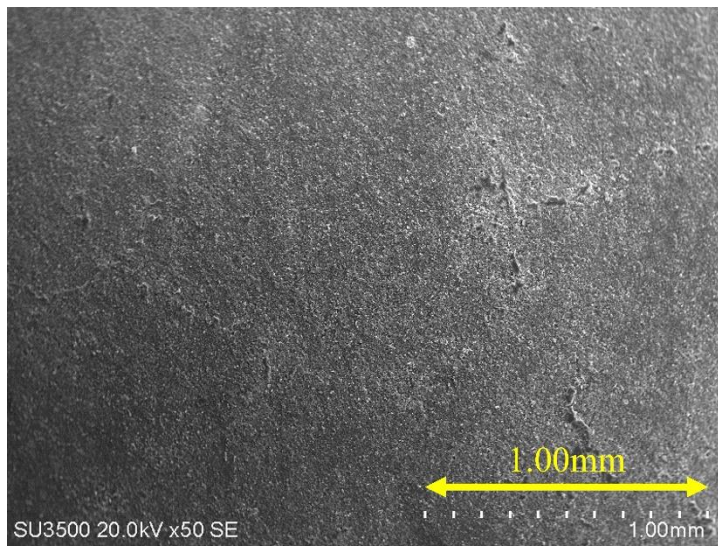


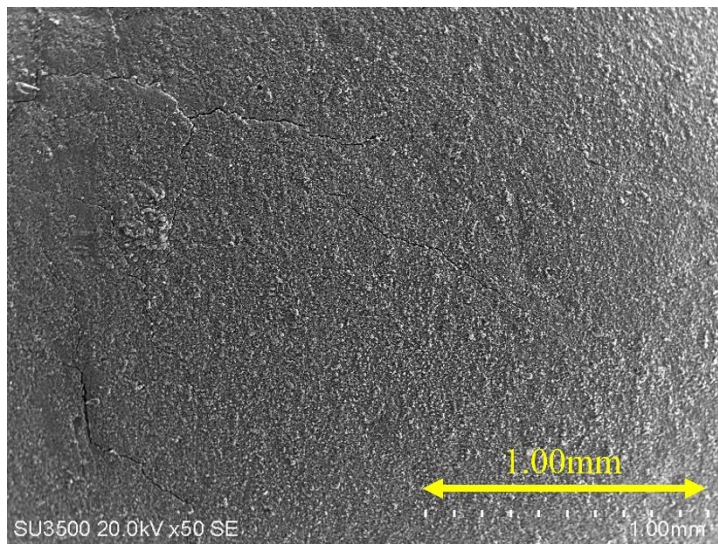
Figure 3.3. Contact Angles on Unused and Aged SiR Specimens.



(a)



(a)



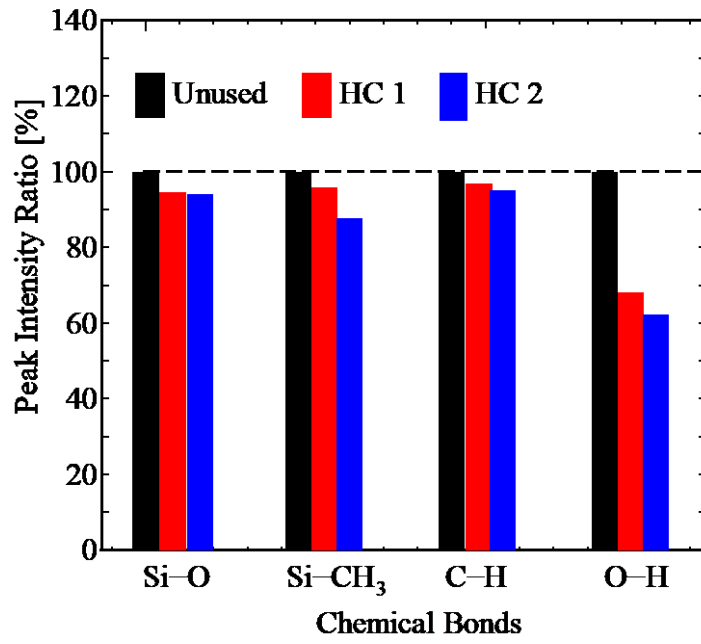
(c)

Figure 3.4. SEM Images of (a) Unused, (b) Aged 10 Years and (c) Aged 20 Years.

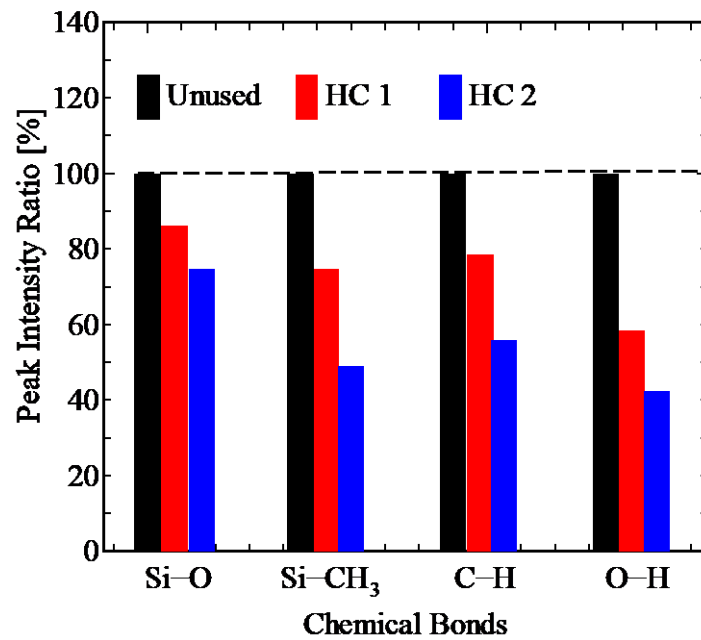
Then, a measurement of the surface roughness was carried out by using a surface roughness tester. The surface roughness at the portion with HC 1 of specimens aged 10 and 20 years were 0.59 μm and 0.62 μm , respectively while that on an unused specimen was 0.34 μm . Additionally, the surface roughness on specimens aged 10 and 20 years with HC 2 are 0.43 μm and 0.47 μm , respectively. Thus, it was found that the surface roughness owing to foreign matter adhesion on the surfaces of aged insulators made the contact angle larger.

3.2.2 Chemical Changes of Aged SiR

The molecular structure of SiR was explained in Section 2.2.1. The chemical changes of aged SiR were observed using an ATR-FTIR spectrometer. The variations of Si-O in siloxane bond (1083 cm^{-1}), methyl group Si-CH₃ (1260 cm^{-1}), C-H bond in a methyl group (2963 cm^{-1}) and O-H bond in ATH (3434 cm^{-1}) was focused [48]. The peak intensity ratios of target chemical bonds of aged SiR specimens against those of an unused specimen were evaluated, i.e., the peak intensities on an unused specimen are set to reference. The obtained results are shown in Figure 3.5. Peak intensity ratios corresponding to the Si-O bond, Si-CH₃ bond, C-H bond and O-H bond of specimens aged 10 and 20 years decrease. Owing to multiple stresses, the molecular structure of SiR is broken. Thus, it was found that the chemical structure state is changed by multiple stresses such as UV rays and foreign matter adhesion.



(a)



(b)

Figure 3.5. Peak Intensity Ratios of Chemical Bonds of (a) Aged 10 Years and (b) Aged 20 Years.

3.3 Short-Time Fabrication of Degraded Surface

In Section 3.2, it was confirmed that the surface states characterized by the physical surface roughness and the chemical composition were changed from the initial ones. Considering the results indicated in Section 3.2 and natural stresses, the degradation surface was fabricated by red clay adhesion, UV irradiation, and surface heating. The average particle diameter of red clay is approximately 1000 times smaller than that of sand. Red clay consists of silica (SiO_2) and a mixture of other minerals such as carbonate, aluminium oxides and iron oxide. The red clay can act as glue, attracting soil particles together, and therefore it can be useful for adhering to the surface of SiR specimen. In this study, red clay was a contaminant/adherent substance to promote physical aging, i.e., the red clay makes the surface roughness larger. It is noted that the adhesion of red clay on the surface of SiR specimens cannot promote chemical aging. To promote chemical aging, we carried out surface heating and UV irradiation. A small incubator (IC-150MA, AS ONE) with a length of 180 mm, a width of 240 mm, and a height of 220 mm was used for surface heating. SiR specimens with red clay adhesion were kept in an incubator. The setting temperature was in the range of 20°C - 80°C , which was controlled by a microcomputer with a thermocouple sensor. Also, the heat radiation was carried out at 25°C for 0.5 h in the incubator. A UV light source was a Xe short arc lamp (XEF-152S, Kenko Tokina) with wavelengths emitted from 375 nm to 1000 nm. The emitted light was collected and outputted. The intensity of the UV region at a position with a spot diameter of 10 mm was 19 mW/cm^2 which is 7 times larger than that of actual sunlight. SiR specimens contained 50% of ATH, and they were the same housing material for insulators. The size of the SiR specimen was $30 \text{ mm} \times 30 \text{ mm}$, and its thickness was 4 mm. The region of 10 mm in diameter on the specimen surface was irradiated with a UV light.

As shown in Figure 3.6, a fabrication cycle to artificially make the degraded surface consisted of 5 steps and one cycle required a day (24 h). First, 0.1 g of red clay was mixed with 20 mL of ionized water. 0.1 mL of the mixed liquid water was dropped on the surface of the SiR specimen. The diameter of the dropped liquid was about 10 mm. The dropped liquid was naturally dried in the atmosphere (Step 1). Next, the dried red clay region was irradiated by UV light (Step 2). Third, the SiR specimen was heated in an incubator (Step 3). Fourth, the heat radiation at 25°C for 0.5 h was secured (Step 4). Finally, the specimen surface was wiped off by using a writing brush and ionized water for 3 min and was dried for 27 min (Step 5). If visible red clay remained, it was wiped off by using alcohol and disposable wipers for another

3 min. After step 5, the contact angle was measured every 10 min until 120 min. Additionally, the surface morphology and the chemical structure of the artificially degraded SiR surface were evaluated.

By the way, the appropriate time of UV irradiation (Step 2) was unknown. Therefore, to investigate the effect of UV rays on the degradation of the SiR surface, UV irradiation with irradiation times of 2 h, 4 h, 6 h, or 8 h was performed against each specimen as shown in Table 3.1. Apart from that, heating at temperatures (T) of 20°C, 40°C, 60°C or 80°C for 4 h was carried out as shown in Table 3.2 because the appropriate heating temperature was unknown. The heating duration of 4 h was determined from the result of the appropriate UV irradiation time, which coincided with the one-cycle duration time of 24 h.

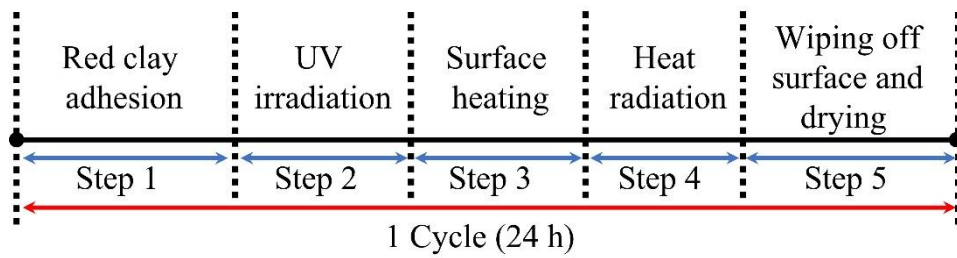


Figure 3.6. A Cycle Consisting of Red Clay Adhesion, UV Ray Irradiation and Surface Heating for Artificially Making Degraded Surface.

Table 3.1

Cycles Differ in UV Irradiation Time without Step 3

Case		UV 2 h	UV 4 h	UV 6 h	UV 8 h
Duration time (h)	Step 1	21	19	17	15
	Step 2	2	4	6	8
	Step 3	-	-	-	-
	Step 4	0.5	0.5	0.5	0.5
	Step 5	0.5	0.5	0.5	0.5

Table 3.2

Cycles Differ in Heating Temperature without Step 2

Case		20°C	40°C	60°C	80°C
Duration time (h)	Step 1	19	19	19	19
	Step 2	-	-	-	-
	Step 3	4	4	4	4
	Step 4	0.5	0.5	0.5	0.5
	Step 5	0.5	0.5	0.5	0.5

Table 3.3

Cycles Differ in Heating Temperature with All Steps

Case		UV+ 20°C	UV+ 40°C	UV+ 60°C	UV+ 80°C
Duration time (h)	Step 1	13	13	13	13
	Step 2	6	6	6	6
	Step 3	4	4	4	4
	Step 4	0.5	0.5	0.5	0.5
	Step 5	0.5	0.5	0.5	0.5

3.4 Results and Discussions

3.4.1 UV Irradiation Effect

To evaluate the appropriate time of UV irradiation for artificially making the degraded SiR surface, the experiments on 5 cases were performed as shown in Table 3.1. Specimen heating (Step 3) wasn't carried out.

The average contact angle of a water droplet on the SiR surface before UV irradiation was 102.8°. After each experiment, the cleaning by using a writing brush and ionized water couldn't remove visible substances adhering to the SiR surface. This indicates that UV irradiation makes red clay adhesion stronger. Following cleaning by using a writing brush and ionized water for 3 min, cleaning by using alcohol and disposable wipers was performed for 3 min. The visible red clay was removed by this work. The averaged contact angles measured after removing visible red clay in the cases of UV2h, UV4h, UV6h, and UV8h were 101.07°, 100.1°, 98.07°, and 97.4°, respectively. They are smaller than the initial value. Due to UV irradiation, the molecular structure of SiR is broken and its contact angle decreases. The contact angle recovery rates against an initial value in 5 cases are shown in Figure 3.7. The contact angles recover to an initial value within 30 min. LMW components disperse in SiR and it makes a new containment layer on the surface of SiR. From the viewpoint of making the degraded surface in a short time, it is desirable that the new containment layer is formed in a short time. The UV irradiation for 8 h largely decreased the contact angle. However, the recovery time was the longest. Then, the appropriate time of UV irradiation was set at 6 h in this study.

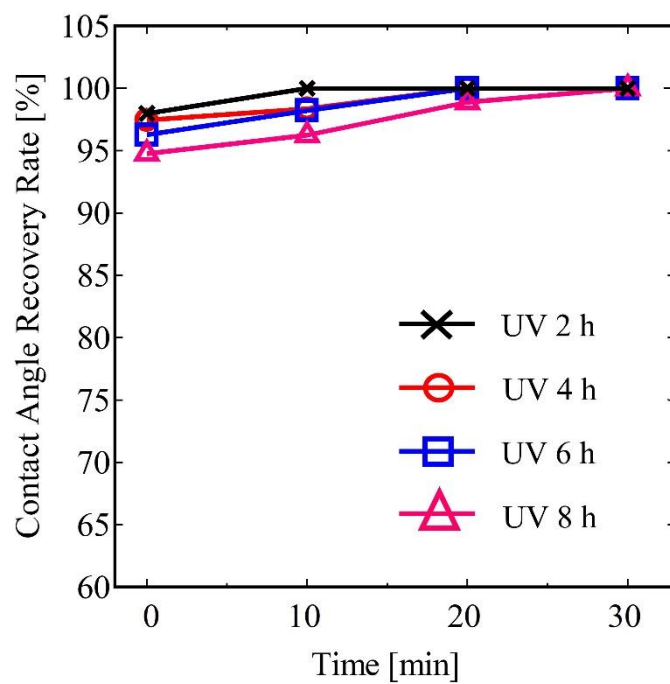


Figure 3.7. Contact Angle Recovery Rates under Various UV Irradiation Times without Step 3.

3.4.2 Heating Effect

To investigate the heating effect on artificially making degraded SiR surfaces, the experiments on 5 cases shown in Table 3.2 were performed. Here, UV irradiation on each specimen (Step 2) wasn't carried out. The averaged contact angles were measured after removing visible red clay. It should be noted that red clay on the SiR surface was easily removed by using a writing brush and ionized water. The averaged contact angles measured after removing visible red clay in the cases of $T = 20^{\circ}\text{C}$, 40°C , 60°C , and 80°C were 100.8° , 99.2° , 97.7° , and 94.2° , respectively. The contact angles are lower than an initial value of 102.8° . Additionally, as mentioned in Section 3.4.1, the contact angle in the case of UV irradiation for 4 h is 100.1° . The effect of the surface heating at 40°C to lower the contact angle is almost equivalent to UV irradiation for 4 h, i.e., the surface heating over 40°C can promote the lowering of the contact angle. The contact angle recovery rates against an initial value are shown in Figure 3.8.

The required recovery time at 40°C is 20 min and it is the same as that in the case of UV4h. The surface free energy of the SiR surface is reflected in the hydrophobic character. Due to surface heating, LMW fluid from the bulk to the surface is promoted and an LMW-enriched surface is formed. As a result, the surface free energy on the LMW surface becomes larger and then the contact angle becomes smaller [49]. Therefore, the contact angle after surface heating decreases from the initial value. After that, the surface free energy becomes smaller due to the volatilization of LMW siloxane with the lapse of time [50], which restores the contact angle to an initial contact angle. Thus, although the surface heating over 40°C can make the contact angle smaller, the red clay on the surface is easily removed and the contact angle recovers to an initial value in a short time, i.e., the surface heating process is not enough to artificially make the degraded surface which has similar characteristics to the degraded surface in outdoor. Therefore, it was considered that a combination of UV irradiation for breaking molecular structure and surface heating for promoting LMW dispersion can make the artificially degraded SiR surface in a short time.

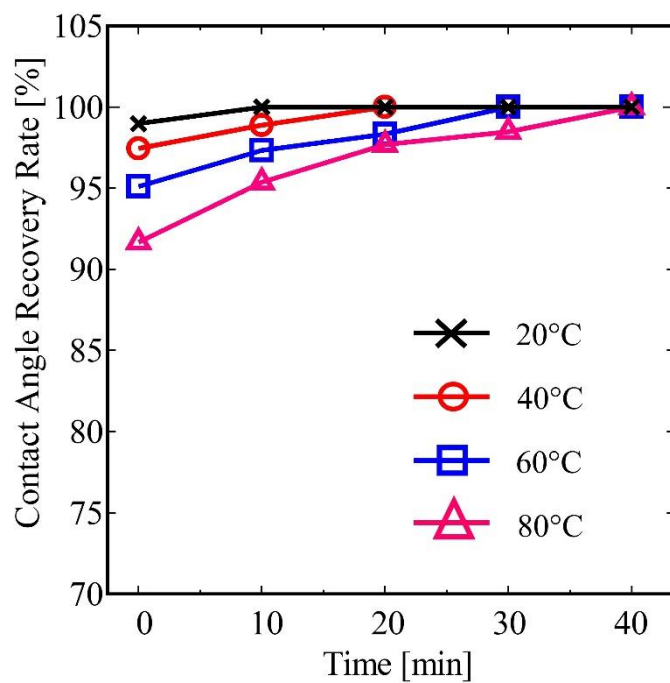


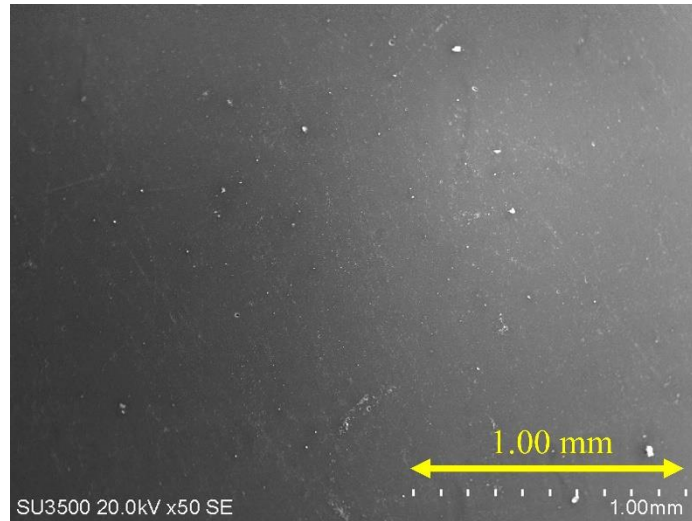
Figure 3.8. Contact Angle Recovery Rates under Various Heating Temperatures without Step 2.

3.4.3 Fabrication by Red Clay Adhesion, UV Ray Irradiation and Surface Heating

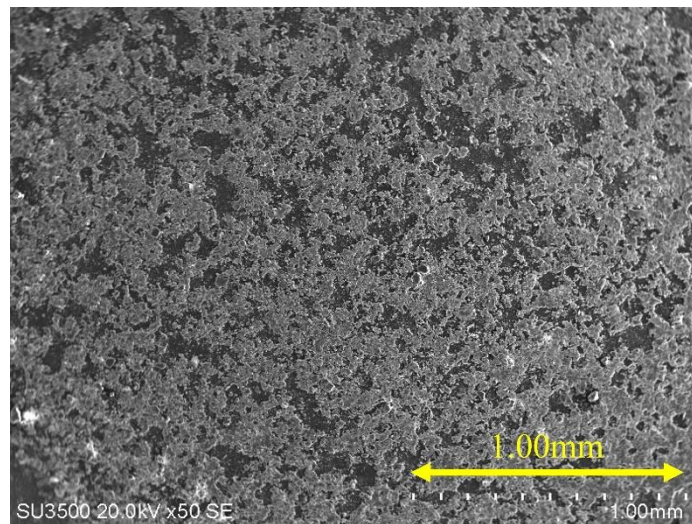
Based on the results in Section 3.4.1 and Section 3.4.2, the experimental conditions were set as shown in Table 3.3. UV irradiation time was set at 6 h. Because the appropriate temperature wasn't fixed while the role of the surface heating could be understood, the heating temperature was set at 20°C, 40°C, 60°C, and 80°C.

After step 4, the red clay adhesion on the SiR surface was wiped off by using a writing brush and ionized water, which is equivalent to a fact of being washed by rainfall. Because the SiR surface was irradiated by UV rays, the visible red clay on the surface wasn't removed. The averaged contact angles were measured after wiping off by using a writing brush and ionized water in the cases of $T = 20^\circ\text{C}$, 40°C , 60°C , and 80°C were 122.05° , 122.8° , 122.6° , and 123.3° , respectively. The presence of red clay on the SiR surface makes the contact angle larger than the initial value. The contact angles measured on aged 10 years and 20 years SiR specimens with pollution adhesion were also larger than that of an untreated one, and they are similar to that on a specimen aged 10 years with HC 2. A UV irradiation process and a surface heating process promote the formation of a new contaminated layer in the presence of foreign matter like red clay. The contact angle is dependent on the surface structure of the SiR specimen [49], and the contact angle becomes larger due to the roughness of the contaminated layer, which can be clearly known seeing Figure 3.9. The surface roughness of an untreated SiR specimen shown in Figure 3.9(a) was $0.20\ \mu\text{m}$. Figure 3.9(b) shows an SEM image of fabricated SiR specimens after wiping off with ionized water and its surface roughness was $0.37\ \mu\text{m}$. Even after wiping it off with alcohol, a small amount of red clay still remained as shown in Figure 3.9(c) and its surface roughness was $0.25\ \mu\text{m}$.

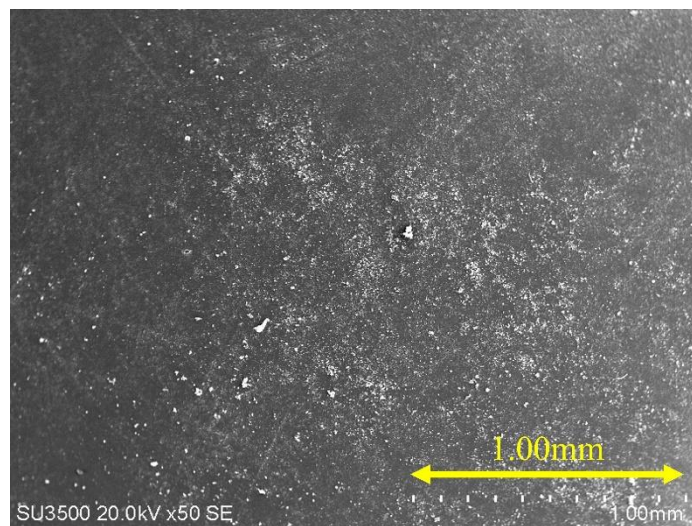
Figure 3.10 shows the comparison of contact angles after wiping off with ionized water or alcohol. Red clay adhesion which makes the contact angle larger is obviously seen. After the visible red clay was wiped off with alcohol, the contact angles became smaller with the increase in the heating temperature. Figure 3.11 shows the contact angle recovery rates against an initial value of 102.8° . The required recovery times in the cases of UV+60°C and UV+80°C don't recover to the initial value at 120 min, i.e., the required recovery times become longer with the increase of the heating temperature. Additionally, in comparison with the results in Figure 3.8, the required recovery times become longer. A combination of UV irradiation for breaking SiR molecular structure and surface heating for promoting dispersion of LMW significantly introduces red clay into SiR, which affects the formation of degraded SiR surface.



(a)



(b)



(c)

Figure 3.9. SEM Images of (a) Untreated, (b) After Wiping off with Ionized Water, and (c) After Wiping off with Alcohol.

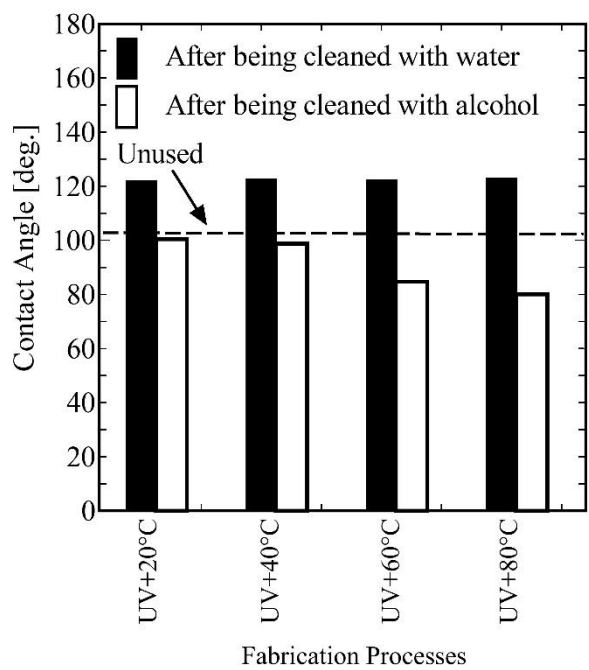


Figure 3.10. Comparison of Contact Angles of Fabricated SiR Surface after Wiping off with Ionized Water and Alcohol.

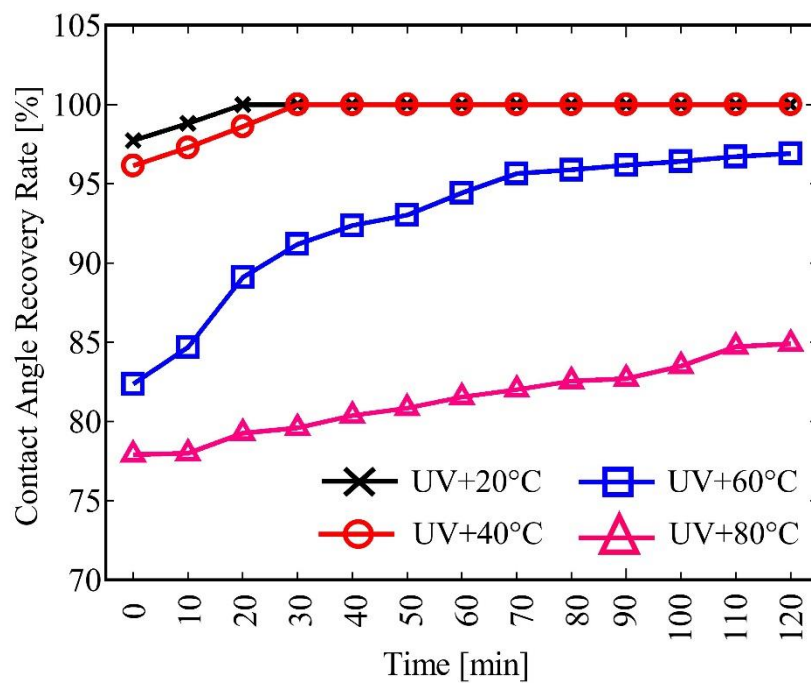


Figure 3.11. Contact Angle Recovery Rates on SiR Surfaces Fabricated with UV Ray Irradiation and Surface Heating.

Figure 3.12 shows the ATR-FTIR peak intensity ratios of fabricated SiR surface, in which peak intensities on an untreated SiR surface are set to reference. The peak intensity ratios corresponding to Si-O, Si-CH₃, C-H, and O-H bonds of fabricated SiR surfaces are smaller than those of an untreated specimen. Especially, C-H bonds significantly decrease at $T = 60^{\circ}\text{C}$ and 80°C . Due to UV irradiation and surface heating, the molecular structure of SiR can be damaged. Not only the ATH structure but also the side chains as C-H and Si-CH₃ are broken, and then free radicals such as H• and CH₃ are formed [18][47]. At the same time, surface heating can split the Si-O-Si group into free radicals of Si-O and Si [51]. Therefore, the cross-linking reactions change the original SiR surface into the degraded surface. Under this surface state, red clay is easily introduced into SiR through LMW dispersion promoted by surface heating. Finally, by comparing the results shown in Figures 3.5 and 3.12, it is found that the peak intensity ratios obtained in the cases of UV+20°C and UV+40°C are similar to those on a specimen aged 10 years with HC 2.

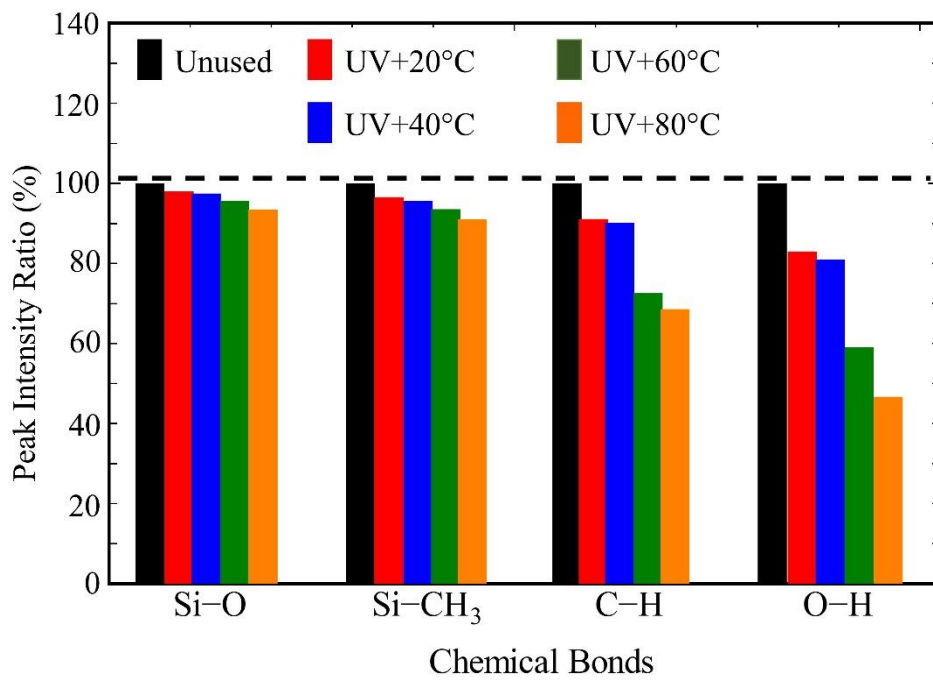


Figure 3.12. Peak Intensity Ratios of Targeted Chemical Bonds of Fabricated SiR Surface.

3.5 Conclusions

The degraded SiR surface whose characteristics are similar to those of degraded surfaces in outdoor attempted to fabricate. To grasp the characteristics of the degraded SiR surface, the hydrophobicity, surface morphology, and chemical structure changes of SiR insulators aged 10 and 20 years in outdoor were first investigated. Although foreign matters on aged SiR specimens existed on their surfaces, hydrophobicity was still high. Additionally, the partial contact angles of the aged specimens were larger than those of an unused SiR specimen. It was found that the minute surface roughness due to foreign matter adhesion makes the contact angle larger. The chemical surface structure of aged SiR specimens was also varied from that of an unused SiR specimen. Si-O, Si-CH₃, C-H, and O-H bonds decreased.

To fabricate the artificially degraded SiR surface, a 24 h-fabrication cycle which consists of a red clay adhesion process, a UV irradiation process, a surface heating process, a heat radiation process, and a surface cleaning process was proposed. The appropriate time of UV irradiation was first evaluated by omitting a surface heating process. The UV irradiation for 8 h largely decreased the contact angle. However, the appropriate time of UV irradiation was set at 6 h in this study from the viewpoint of realizing a short-time fabrication. Next, the surface heating effect was investigated by omitting a UV irradiation process. The surface heating promoted the dispersion of LMW, and the surface heating over 40°C made the contact angle smaller. However, the red clay on the surface was easily removed and the contact angle recovered to an initial value in a short time. Therefore, it was found that the surface heating process is not enough to artificially make the degraded surface and that a combination of UV irradiation for breaking molecular structure and surface heating for promoting LMW dispersion is necessary. Based on the results, the artificially degraded SiR surface was fabricated with the presence of red clay at different surface heating temperatures. The contact angle and the chemical structure on the artificially degraded SiR surface, which was fabricated by UV irradiation for 6 h and surface heating at 20°C or 40°C, were similar to those of a SiR specimen aged 10 years with HC 2.

UV irradiation time and the amount of red clay in a fabrication cycle were constant in this study, and they still have room for improvement. It is considered that various degraded SiR surfaces can be made by changing such conditions.

CHAPTER 4

DEGRADATION DIAGNOSTIC TECHNIQUE OF SILICONE RUBBER

4.1 Introduction

In this Chapter, the degradation diagnostic technique of SiR was evaluated to contribute to the long-term maintenance of SiR insulators outdoors. A continuous 20-times salt-fog aging test was first performed by applying AC voltage for 3 h with 16 mS/cm of salt-fog, in which an unused SiR specimen and a specimen aged 20 years from a SiR insulator operated in the coastal area. The time required for recovering hydrophobicity on specimens was measured after each test cycle of a continuous 20-times salt-fog aging test. The hydrophobicity recovery time of SiR specimens becomes longer with the increase in the number of test cycles. In addition, the hydrophobicity recovery time on a SiR specimen aged 20 years was much longer than that on an unused SiR specimen. During a continuous 20-time salt-fog aging test, the polluted surface was slightly eroded by PDs which were generated among discrete water droplets formed by the salt-fog supply. The surface erosion may promote the diffusion of LMW in SiR specimens, and then the hydrophobicity of the SiR specimen can be recovered. Thus, it was found that the hydrophobicity recovery time in the continuous 20-times salt-fog aging test is a good index to evaluate the degradation degree of SiR. Due to the difference in degradation degrees, the required time for recovering hydrophobicity might be varied. However, the continuous 20-times salt-fog aging test requires a long time. There are countless water drops on the SiR surface and their locations are temporally varied by PDs. That is, the required time to expose a particular spot of the SiR surface to PDs is long.

In contrast, to measure the degradation degree of polymer insulators in a short time, SD, which was generated by using a quartz glass electrode, was applied to a particular spot on the surface of the polymer specimen. The hydrophobicity recovery times of an unused SiR specimen and a 20-year-aged SiR specimen were evaluated after SD treatment. Additionally, whether SD treatment can cause physical or chemical damage to the surface of polymer specimens or not was investigated by using SEM and an ATR-FTIR spectrometer (ATR-FTIR), respectively. It was found that the degradation degree of the SiR specimen can be investigated with no physical or chemical damage after SD treatment. However, the decrease mechanism of the hydrophobicity characteristic by SD treatment wasn't interpreted in detail.

Therefore, SD was characterized by measuring discharge current and optical emissions. The discharge current of SD, generated by applying high-frequency voltage, was measured by using a high-frequency current transformer (HFCT) sensor. In addition, the characteristic of discharge current in the frequency domain was analyzed using the Fast Fourier Transform (FFT) and a high pass filter (HPF). Finally, to investigate the reason why the SDs cause the hydrophobicity loss, the surface temperature on the mesh plate of an electrode and optical emissions were observed by using an infrared thermography camera and a fiber optical spectrometer, respectively.

4.2 Degradation Monitoring of SiR Used for Insulators

4.2.1 Methodology

4.2.1.1 Test Method of Chemical Structure Analysis

Figure 4.1 shows a SiR line post insulator for a 22kV distribution system. The SiR insulator was arranged for 20 years in the coastal area, where the average yearly temperature at the installation place is 15°C. The filler content of ATH in the SiR insulator is about 50%. In the experiment, 6 specimens cut out from the body and 5 specimens from the shed were prepared. The portions of 1 and 2 were covered with an insulator cover during the installation for 20 years in the actual system. Additionally, “Sample A” was prepared as unused and non-deteriorated SiR. Figure 4.2 shows the appearance of the specimen A. Then, 12 specimens were used for measurements of ATR-FTIR and salt fog aging tests.

FTIR doesn't irradiate the sample with the infrared rays by changing the wavelength. However, it irradiates the sample with continuous light and Fourier transforms the interference pattern to obtain the absorption spectrum. It is a method to obtain information on the atomic group. Since it is possible to simultaneously measure the incident light in the entire wavenumber range due to continuous light, the high sensitivity measurement is possible in a short time. The FTIR analysis measures the absorption of light in the infrared region. There are several methods to obtain this absorption spectrum, and they are used properly according to the purpose of application. ATR is one the most used technologies for FTIR to introduce light onto a sample in order to obtain structural and compositional information. Therefore, the ATR method was adopted in this experiment, and the reflected light spectrum due to the structure of infrared light was measured.

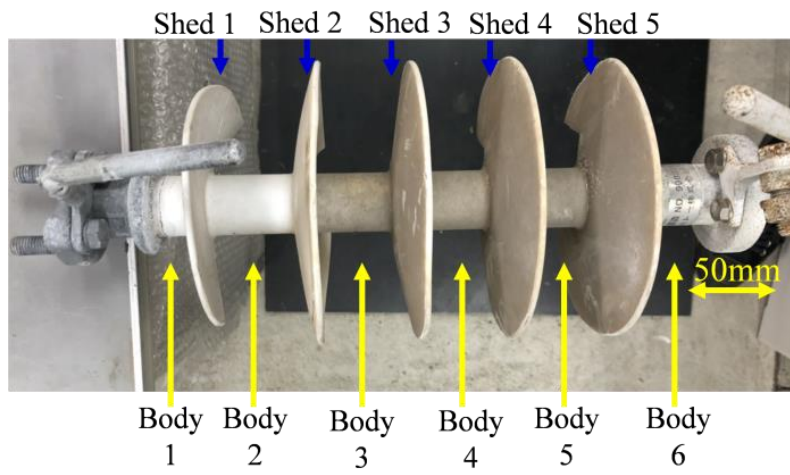


Figure 4.1. 20 Years Aged SiR Insulator Used in Actual System.

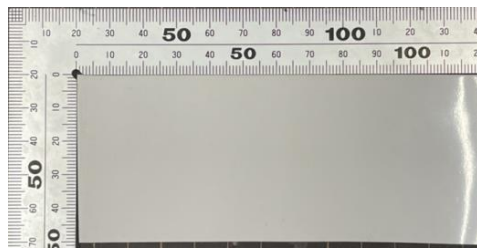


Figure 4.2. Specimen Size of SiR.

4.2.1.2 Experimental Setup of Salt-fog Aging Test

Figure 4.3 shows the experimental setup of salt fog aging test used in this experiment. In Figure 4.3, a pair of metal electrodes was placed on a SiR specimen cut from the 20 years aged insulator (Figure 4.1) and an unused one. The length distance of two metal electrodes was 25 mm, and the sample size of a SiR specimen is $50 \text{ mm} \times 50 \text{ mm} \times t 2 \text{ mm}$. In the salt fog aging test, a spray rate of 0.9 (L/h) spray the conductivity of 16 (mS/cm) to simulate the condition of coastal area. Then, ac voltage (3 kV) was applied for 3 h. The detailed conditions are shown in Table 4.1.

In the experiment, the salt fog aging test was repeatedly performed until 20th cycle as shown in Figure 4.4. Firstly, a hydrophobicity level is identified as HC1 by using a STRI method. HC1 is preferred as the condition that the discrete droplets are only formed. After that, the leakage current and hydrophobicity recovery time were measured in each cycle. Then, the leakage current and hydrophobicity recovery time of a 20 years aged specimen were compared with those of an unused specimen. Finally, a good index was mentioned for degradation monitoring of the actual aging polymeric insulator.

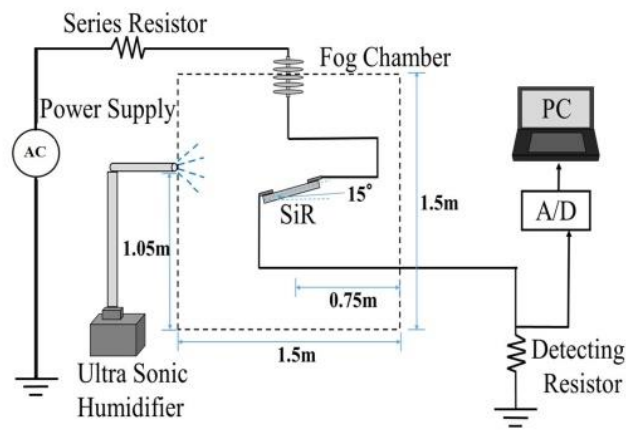


Figure 4.3. Experimental Setup of Salt-fog Aging Test.

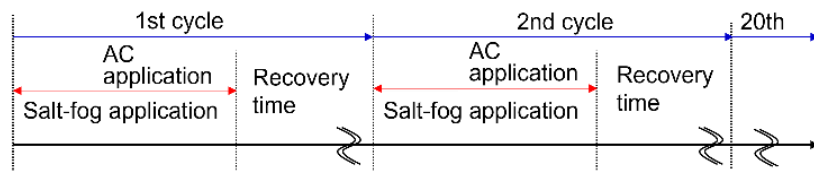


Figure 4.4. Test Cycles for Obtaining Leakage Current and Recovery Characteristics of Hydrophobicity.

Table 4.1. Detailed Data Used in Experimental Test.

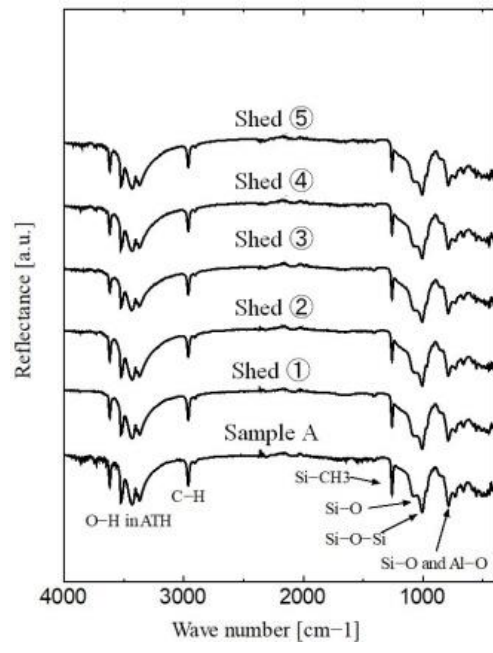
Series Resistor [k Ω]	100
Applied Voltage[kV]	AC 3
Specimen	SiR
Spray Rate [L/h]	0.9
Conductivity [mS/cm]	16

4.2.2 Results and Discussions

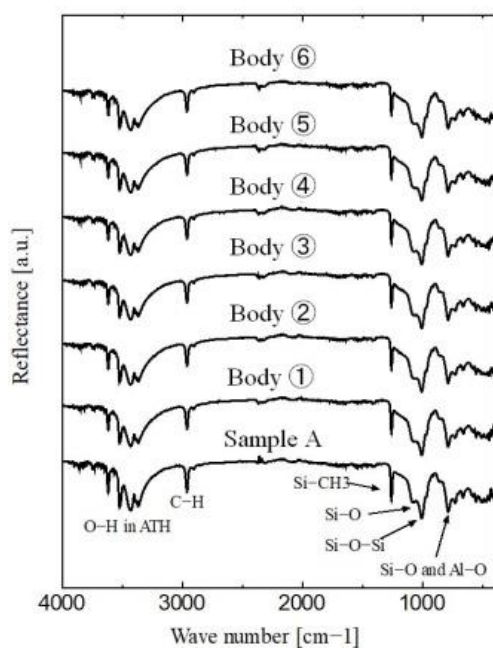
4.2.2.1 Chemical Structure Analysis

Figure 4.5 shows the analysis results at shed and bodies. Figures 4.6 and 4.7 show peak intensity ratios at wavenumbers 1083cm^{-1} , 1260 cm^{-1} , 2963 cm^{-1} , and 3434 cm^{-1} of shed and body positions, respectively. In both figures, the peak intensity of specimen A is 1. From Figures 4.6 and 4.7, it can be confirmed that the FTIR spectrum of the 20 years aged methyl group (Si-CH₃) and the C-H bond in the methyl group are decreasing. However, the siloxane bond (Si-O) is increasing. It is considered that the siloxane bond of the polar group increased on the SiR surface and the methyl group of the non-polar group decreased due to the oxidation with aging. In addition, from Figure 4.6 (b), it can be seen that the range of decrease in the spectrum is relatively large for the shed positions of 2, 3, 4 and 5. From Figure 4.1, it can be seen that the insulators are relatively severely soiled in positions of 2, 3, 4, and 5. Since the shed positions of 2, 3, 4 and 5 were easily affected by environmental factors such as UV rays, rain, wind, and dust. Therefore, the LMW components became polluted due to the breakage of the side chains, the loss of LMW components, and the accumulation of pollutants.

In addition, from Figure 4.6(d), an increase can be confirmed in the peak intensity ratio of the OH group. From this, it is considered that ATH precipitation occurs on the SiR surface. The changes in the FTIR spectrum of body positions are similar to those of shed position. It is clearly seen in Figure 4.5 (b) and Figure 4.7. Therefore, the 20 years aged insulator has deteriorated in performance as an insulator due to changes in the chemical structure of the outer cover material SiR, such as surface contamination and side chain breakage due to the UV rays. Although chemical structure changes on surface of specimen were found, the differences were not remarkable. Thus, the chemical analysis is not enough to measure the degradation degree of SiR insulator.

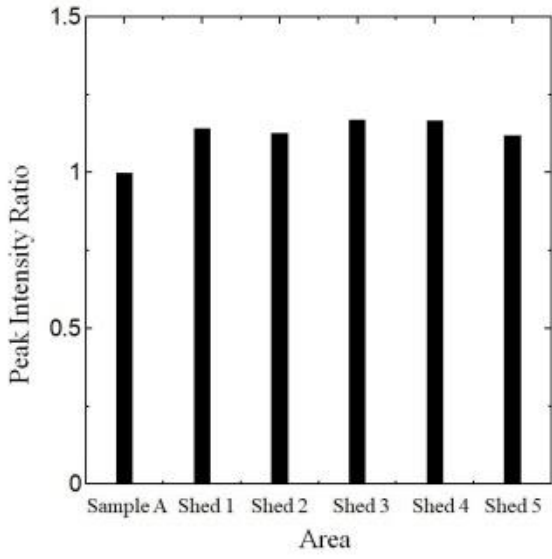


(a)

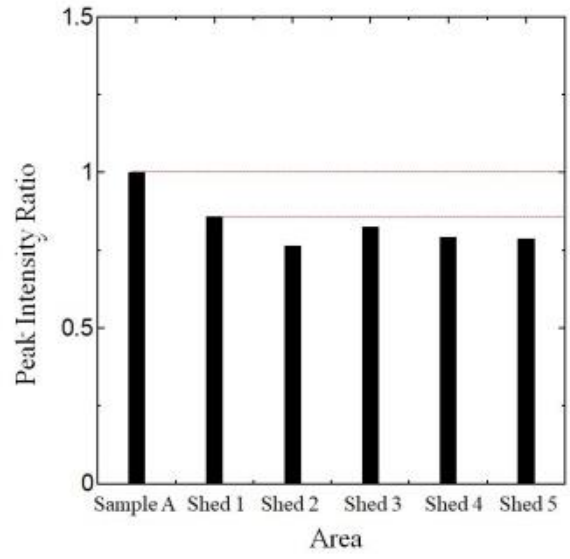


(b)

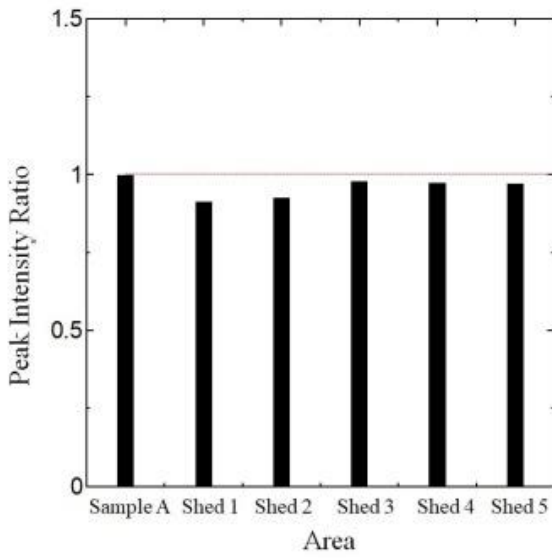
Figure 4.5. ATR-FTIR Spectrum by ATR Method.



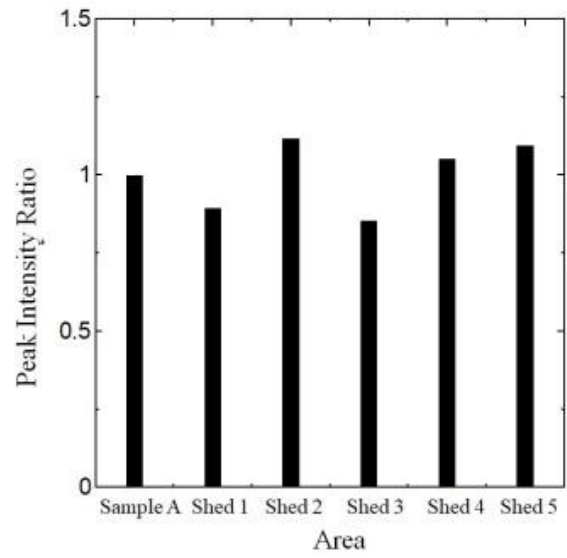
(a) Si-O (1083 cm^{-1})



(b) Si-CH₃ (1260 cm^{-1})

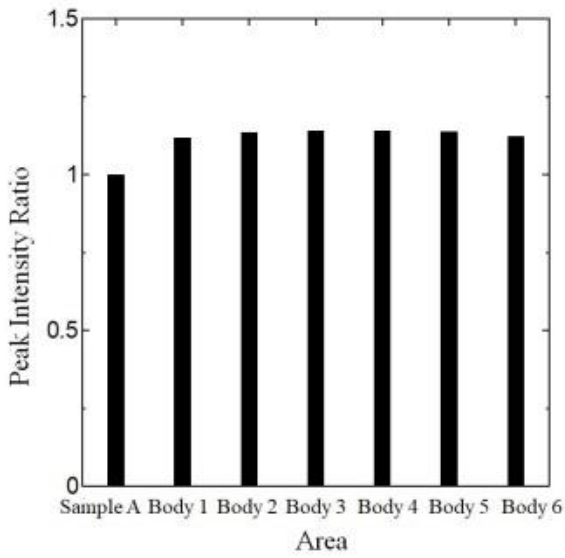


(c) C-H (2963 cm^{-1})

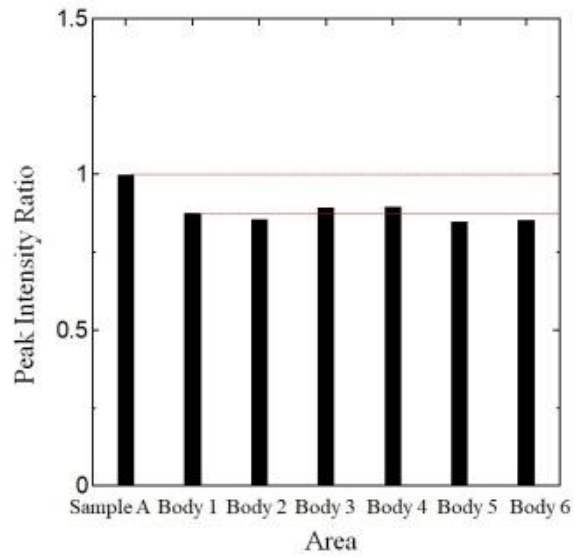


(d) O-H in ATH (3434 cm^{-1})

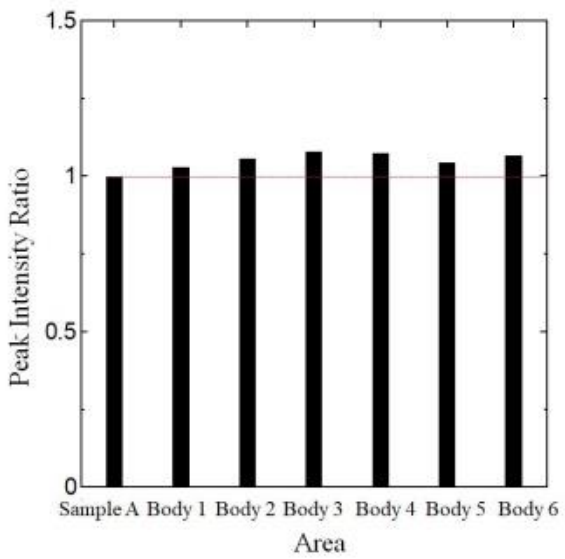
Figure 4.6. Peak Intensity Ratio (Specimen A and Shed).



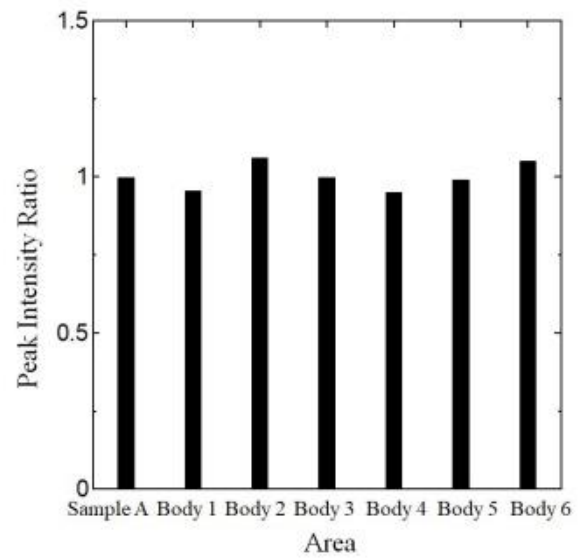
(a) Si-O (1083 cm^{-1})



(b) Si-CH₃ (1260 cm^{-1})



(c) C-H (2963 cm^{-1})



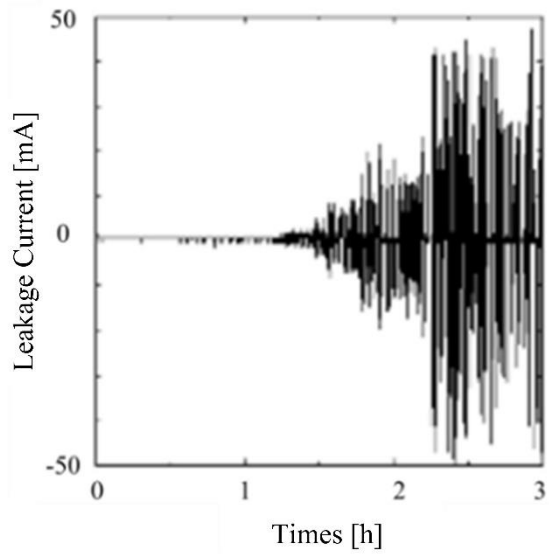
(d) O-H in ATH (3434 cm^{-1})

Figure 4.7. Peak Intensity Ratio (Specimen A and Body).

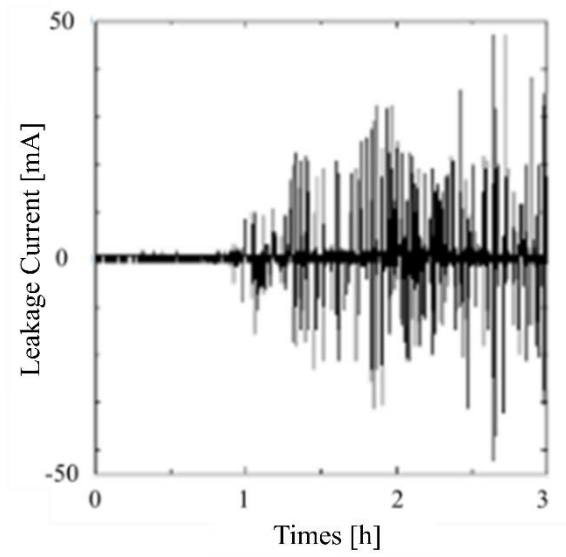
4.2.2.2 Salt-fog Aging Test

Figures 4.8 and 4.9 show the temporal variations in leakage current of an unused and a 20 years aged SiR specimen, obtained at 1st cycle, 5th cycle, 10th and 20th cycle. Comparing with Figures 4.8 and 4.9, there are differences in the discharge ignition time (required time until the leakage current is detectable from the voltage application) at 1st and 5th cycle. The discharge ignition time of an unused specimen is significantly longer than that of 20 years aged specimen. However, there are no significant differences in the discharge ignition time at 10th and 20th cycle in Figures 4.8(c), 4.8(d), 4.9(c), and 4.9(d). On the other hand, the maximum leakage current of an unused specimen is about 45 mA in Figure 4.8(b), and that of 20 years aged specimen is about 50 mA. The difference between two specimens is less, and therefore the comparison of electrical property isn't enough to measure the degradation degree of SiR insulator.

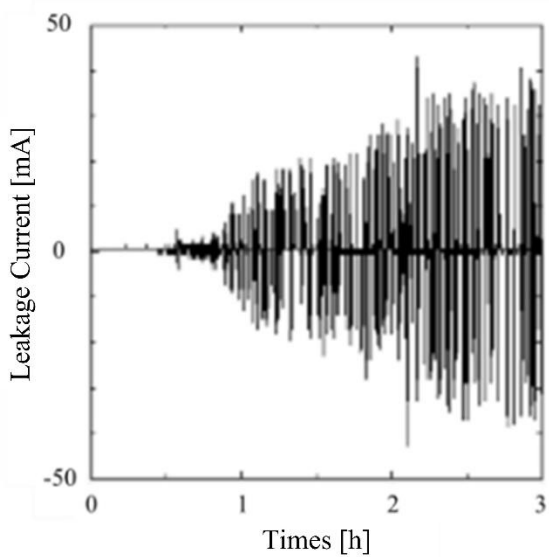
Figure 4.10 shows the required time for hydrophobicity recovery in minutes of an unused specimen and 20 years aged specimen. In Figure 4.10, the blue rectangular shape is represented by hydrophobicity recovery time of 20 years aged specimen and the red circle shape is represented by the hydrophobicity recovery time of an unused specimen. It is clearly seen that the hydrophobicity recovery time of 20 years aged specimen is significantly longer than that of an unused specimen.



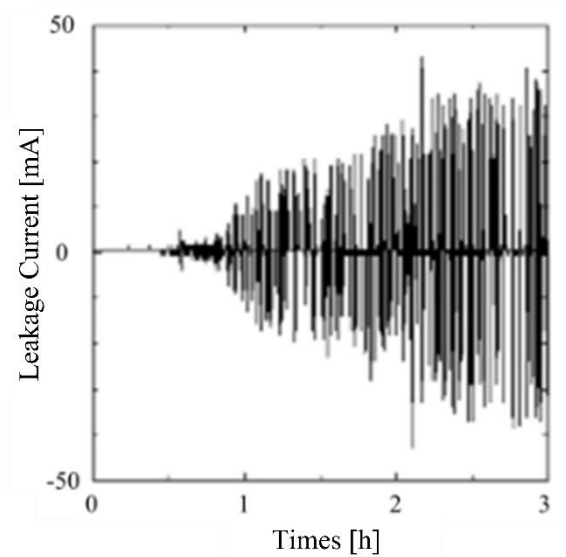
(a) 1st cycle



(b) 5th cycle

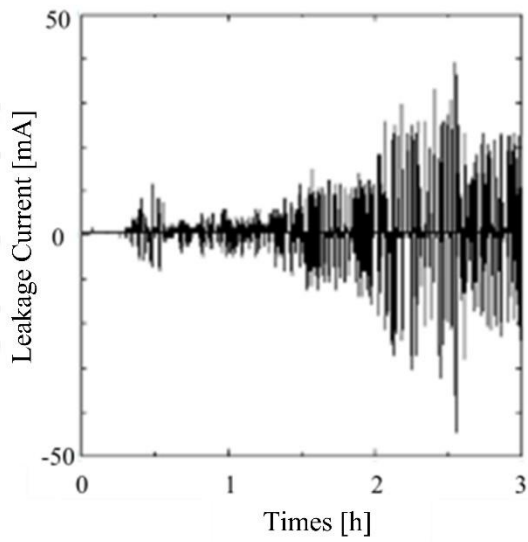


(c) 10th cycle

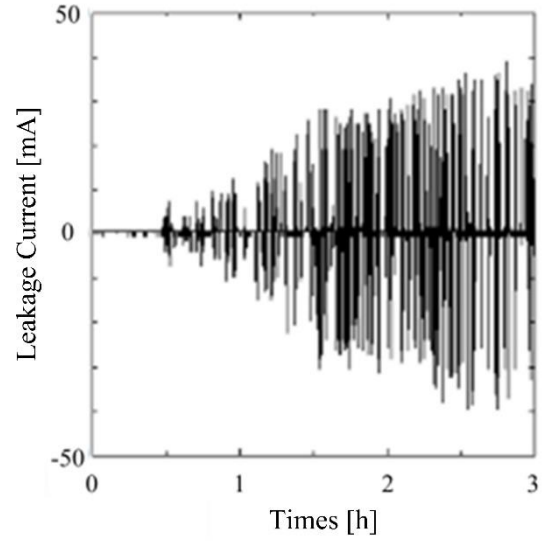


(d) 20th cycle

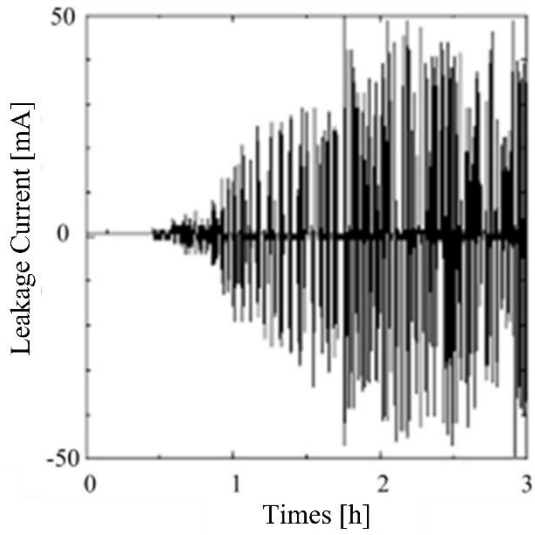
Figure 4.8. Leakage Current of an Unused Specimen.



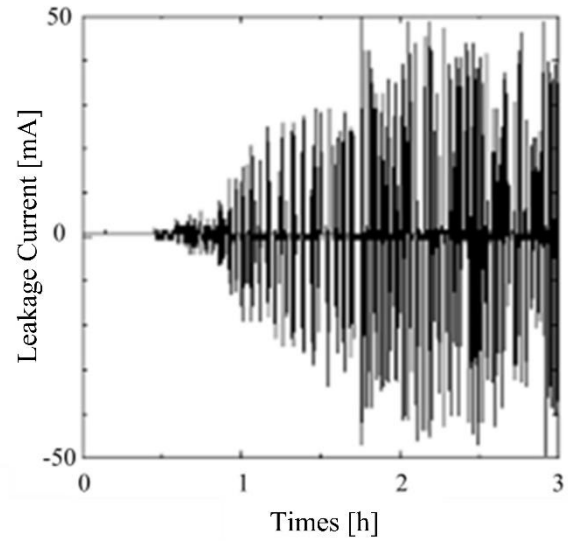
(a) 1st cycle



(b) 5th cycle



(c) 10th cycle



(d) 20th cycle

Figure 4.9. Leakage Current of 20 Years Aged Specimen.

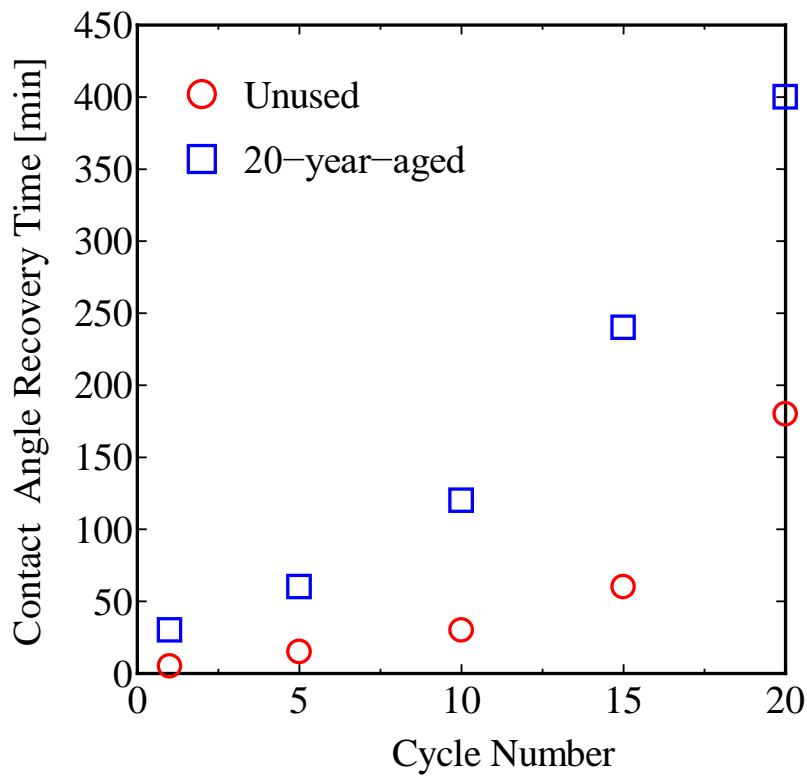


Figure 4.10. Difference of Hydrophobicity Recovery Time between 20 Years Aged Specimen and an Unused Specimen.

4.2.3 Conclusions of Degradation Monitoring of SiR Used for Insulators

A chemical structure analysis was performed against specimens cut out from a 20 years aged SiR insulator by using ATR-FTIR. In comparison with the result obtained from an unused SiR specimen, the spectral intensity changes in Si-CH₃, C-H bond and O-H bond were observed. However, the observed difference was not remarkable. A continuous salt fog aging test was also carried out. The maximum leakage currents between a 20 years aged specimen and an unused specimen were the almost same. The discharge ignition times at 1st and 5th cycle were different between the two specimens. However, the difference wasn't observed with the increase of the salt fog aging test. Then, the evaluation of electrical property isn't enough to monitor the degradation degree.

On the other hand, the required times for recovering hydrophobicity of 20 years aged specimen clearly became longer with the increase of the salt fog aging test, and the difference from the required times of an unused specimen was large. Thus, it can be concluded that hydrophobicity recovery time for our continuous salt fog aging test is a good index to monitor the degradation of silicone rubber used for insulators.

4.3 Evaluation of Degradation Degree of SiR using Surface Discharge

4.3.1 Experimental Setup

To effectively expose PD to a particular spot of the SiR surface, an SD electrode, which was expected to generate uniform SDs on the surface of the SiR specimen was made. The electrode configuration is shown in Figure 4.11, which consists of a glass plate with a thickness of 0.5 mm, aluminium (Al) tape with a thickness of 0.1 mm and a 150-mesh - SUS wire mesh plate. The mesh had a 0.1 mm hole size and 0.06 mm thick wire. The glass plate having 75 mm long and 25 mm wide was sandwiched by the Al tape and the 150-mesh plate. Al tape and 150-mesh plate were 80 mm long and 20 mm wide. The Al tape and the 150-mesh plate were fixed with adhesive, and the size of an overlapped area between the Al tape and the 150-mesh plate on the glass plate was 20 mm by 30 mm. 8 kV with a frequency of 10 kHz was applied to the 150-mesh plate while the Al tape was earthed. The surface of SiR specimen, which was facing to the 150-mesh plate, was treated by the SD. The applied voltage and the discharge current were measured by a H. V. probe (EP-50K, Nisshin Pulse Electronics) and a CT sensor, (I-125-1 HF, Prodyn) respectively. A digital oscilloscope (DLM2054, Yokogawa) with a sampling frequency of 1.25 GHz was used for recording waveform data. The schematic diagram of an

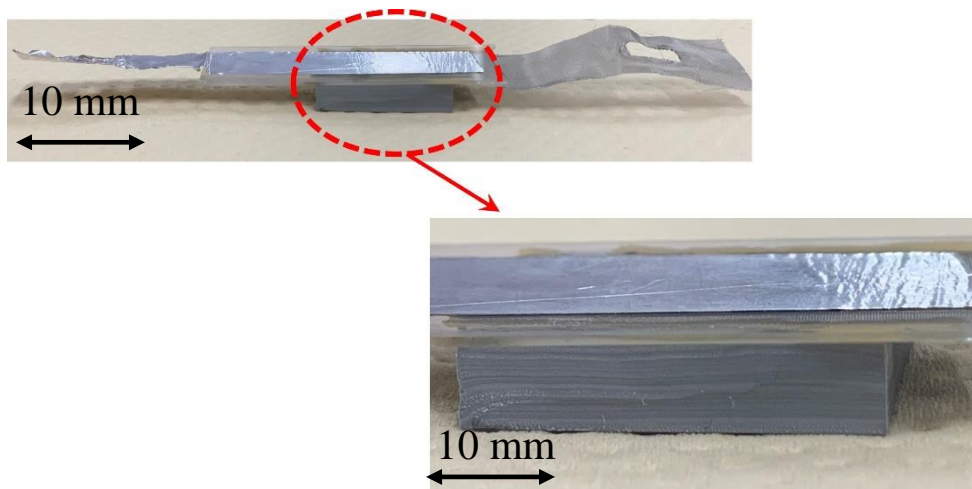
experimental setup for SD treatment is shown in Figure 4.12. The surface treatment time was set at 5, 10, 15, 20 and 25 s. The recovery characteristics of hydrophobicity on SiR specimens were evaluated by measuring the contact angle of a water droplet on the SiR surface. After each SD treatment, 7 μ L of a water droplet was dropped from a syringe to the SiR surface. The contact angle of the water droplet was measured by using a contact angle meter which was automatically measured. Additionally, SEM and ATR-FTIR measurements were performed whether physical or chemical damages were caused by a SD treatment, or not.



(a) Top View (From Al Tap)



(b) Top View (From Mesh Plate)



(c) Side View (With SiR Specimen)

Figure 4.11. Electrode Configuration for Generating SD.

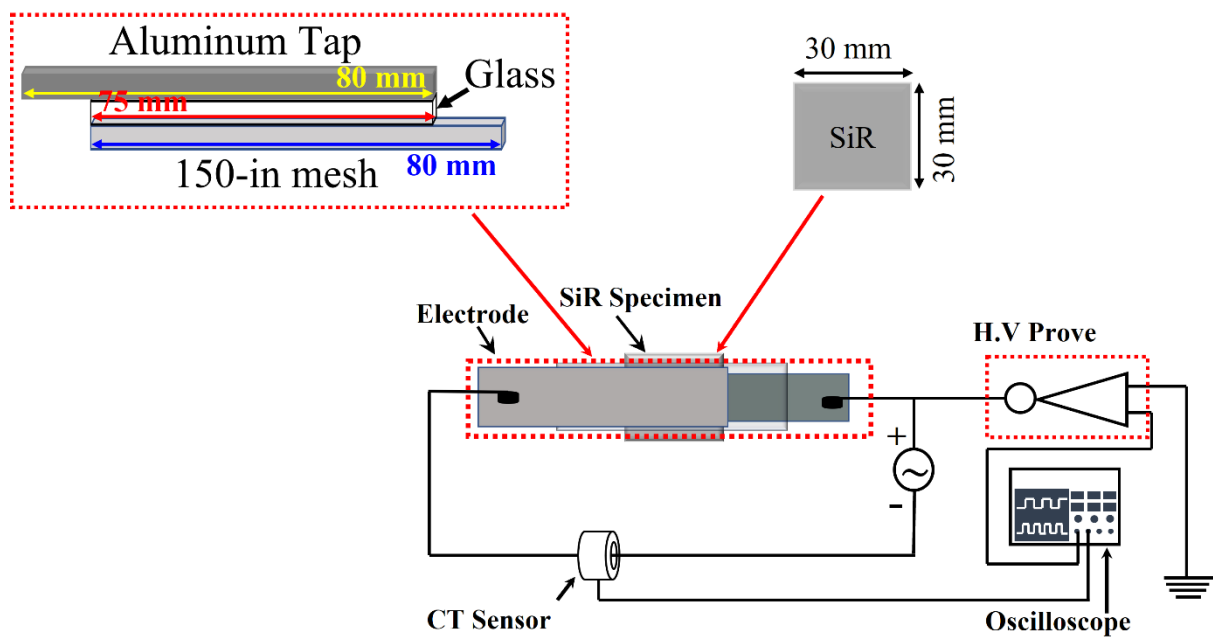


Figure 4.12. Schematic Diagram of an Experimental Setup for SD Treatment.

4.3.2 Results and Discussions

4.3.2.1 Characteristics of Surface Discharge

Examples of detected waveforms of the applied voltage and the discharge current are shown in Figure 4.13. It should be noted that the discharge current includes the displacement current due to the capacitance component of an SD electrode system. The applied voltage has vibration-damping characteristics, and the full width at half maximum of each voltage pulse is about 1 μ s. The sharp voltage rising promotes the ionization of molecules, and therefore the prescribed surface treatment by SD might be accomplished within a short time. In addition, the value of the discharge current during an SD treatment was about 60 mA while that during a 20-cycle salt-fog aging test was about 45 mA mentioned in Section 4.2.2.2. The detected discharge current did not significantly differ from that obtained during a 20-cycle salt-fog aging test.

In Figure 4.14, SD is uniformly generated on a 150-mesh plate. As mentioned above, the size of an overlapped area between an Al tape and a 150-mesh plate on a glass plate was 20 mm by 30 mm. To uniformly treat the SiR surface, the center area of the SiR surface with $20 \times 20 \text{ mm}^2$ was arranged on the SD area with $10 \times 10 \text{ mm}^2$ indicated by a dotted black line.

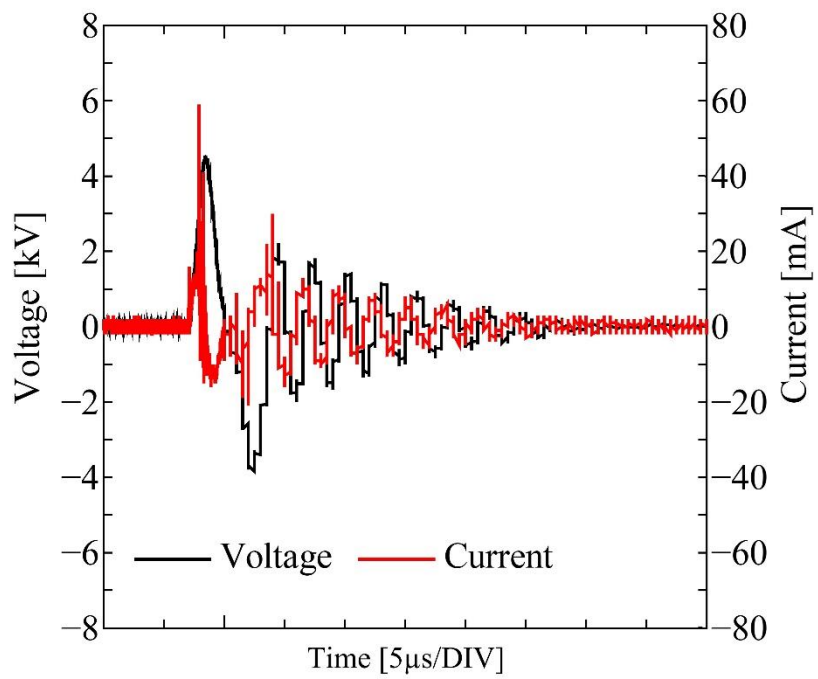


Figure 4.13. Waveforms of Applied Voltage and Discharge Current in an SD Treatment.

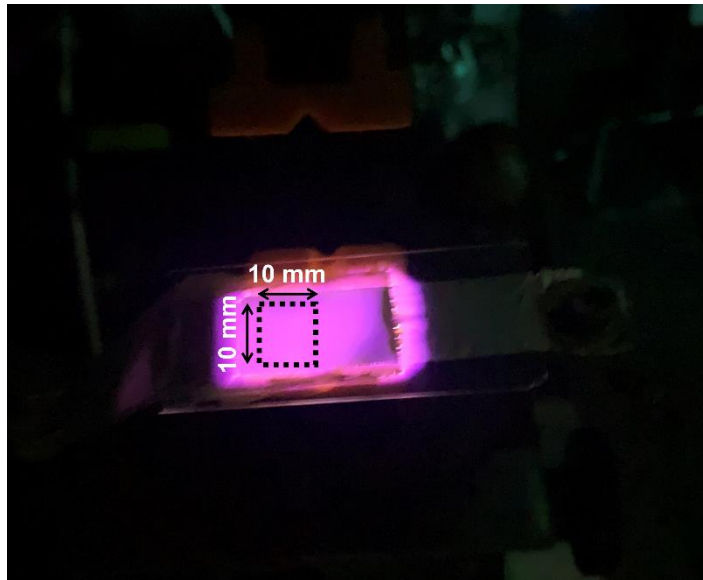


Figure 4.14. Appearance of Uniformly Formed SD on a 150-mesh Plate.

4.3.2.2 Recovery Characteristics of Hydrophobicity

The temporal variations of contact angle on SiR specimens after SD treatments are shown in Figure 4.15. The contact angle on an unused SiR specimen before SD treatment was 109.9° while those on 10 and 20-year-aged SiR specimens were 117.4° and 115.3° , respectively. After the SD treatment for 5 s, the contact angles on unused, 10 and 20-year-aged SiR specimens decreased to 104.9° , 113.1° , and 110.0° , respectively.

In addition, after an SD treatment for 25 s, the contact angles on unused, 10 and 20-year-aged SiR specimens decreased to 93.4° , 95.3° , and 94.2° , respectively. Thus, the SD treatment within 25 s can lower the contact angle, and the contact angle decreases with the increase of the treatment time. The molecular structure of SiR consists of a siloxane bond (Si-O) and the side chain of methyl groups (CH_3) in the dimethylpolysiloxane bond. The binding energy of C-H in CH_3 is 4.25eV while that of the Si-O bond is 4.60eV [52][53]. Because the SD is generated on a glass plate by applying high-frequency voltage, it becomes a non-equilibrium atmospheric pressure plasma [7]. It is well known that electron temperature following electron energy distribution function is in the range of 1 – 10 eV. Therefore, direct energy transfer from energetic particles with higher energy than binding energies mentioned above to the SiR surface can easily change chemical characteristics, and then the contact angle on the SiR surface decreases.

The decreased contact angles by SD treatments gradually recovered as shown in Figures 4.16 and 4.17, which demonstrate hydrophobicity recovery due to LMW silicone fluid diffusing from the bulk. The contact angle measurement was continuously performed at intervals of 10 min. Contact angle recovery time was defined as the required time necessary for returning the contact angle to the initial value, i.e., hydrophobicity recovery time. Figure 4.18 shows the contact angle recovery time on unused, 10 and 20-year-aged SiR specimens. In the case of SD treatments for 25 s, the contact angle recovery times on 10 and 20-year-aged SiR specimens were 140 min and 160 min, respectively while that on an unused SiR specimen was 110 min. Thus, the contact angle recovery times on 10 and 20-year-aged SiR specimens were much longer than those on an unused SiR specimen. SD modifies characteristics on the SiR surface, and then it promotes the dispersion of LMW fluid. As a result, the surface hydrophobicity can be nearly recovered to the initial state [54]. The surface states of aged SiR specimens are different from those of unused SiR specimens, and foreign matters are also re-confirmed. The dispersion of LMW in the aged SiR specimen could be disturbed by the

degradation layer while that in the unused SiR specimen is active. The disturbance of LMW by the degradation layer reflects the longer hydrophobicity recovery tendency. That is, the contact angle recovery time after the SD treatment may be useful for investigating the degradation degree.

By the way, the contact angle recovery time increases with the increase of SD treatment time. We have already performed a continuous 20-times salt-fog aging test applying AC voltage in order to investigate the hydrophobicity recovery time, as shown in Figure 4.10. The hydrophobicity recovery time on a SiR specimen aged 20 years was much longer compared with that on an unused SiR specimen. Although the contact angle recovery times in an SD treatment technique are different from those in a continuous 20-times salt-fog aging test, their recovery tendencies are the same, i.e., the hydrophobicity recovery time becomes longer with the increase of the number of salt-fog aging tests or the SD treatment time.

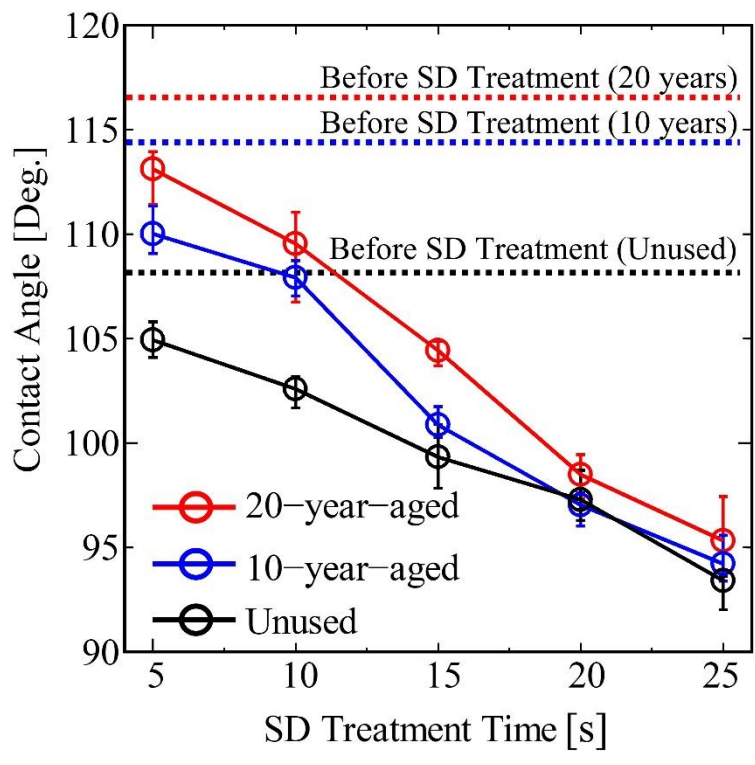
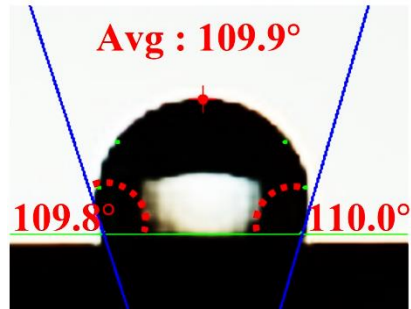
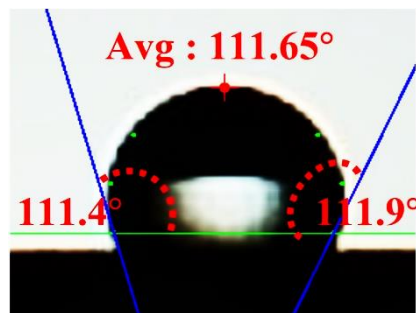


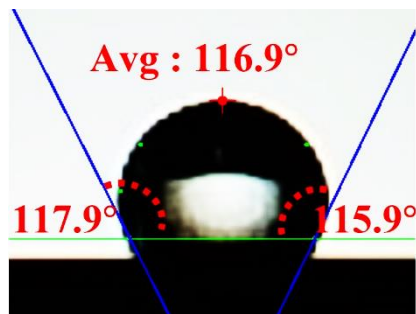
Figure 4.15. Variations of Contact Angles on Unused, 10 and 20-year-aged SiR Specimens.



(a)

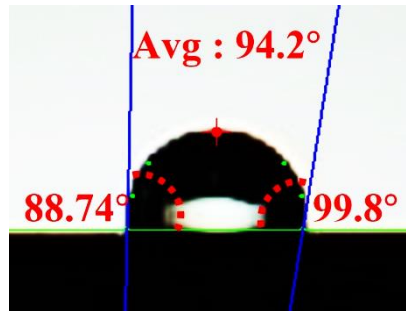


(b)

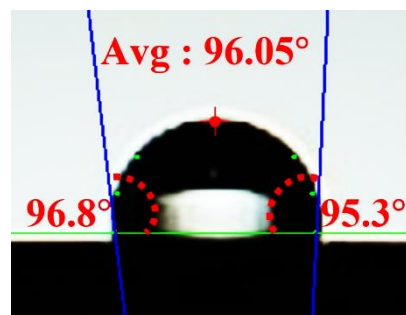


(c)

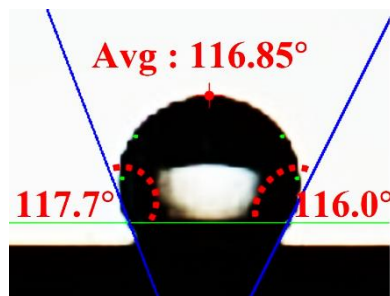
Figure 4.16. Change in Shape of a Water Droplet on SiR Surface treated for 5 s at (a) just after SD Treatment, (b) 10 min Later, and (c) after Hydrophobicity Recovery.



(a)



(b)



(c)

Figure 4.17. Change in Shape of a Water droplet on SiR Surface Treated for 25 s at (a) just after SD Treatment, (b) 10 min Later, and (c) after Hydrophobicity Recovery.

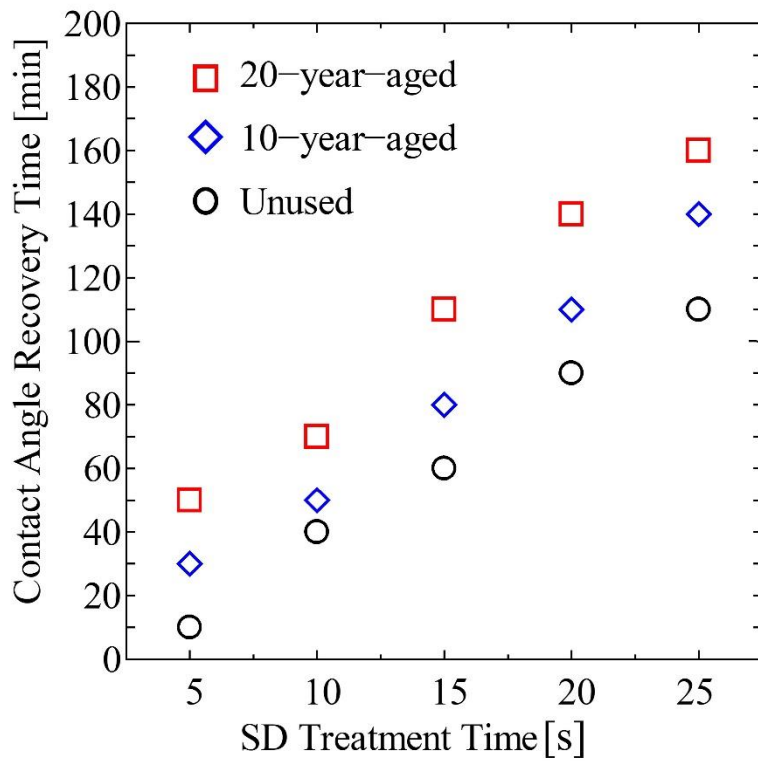
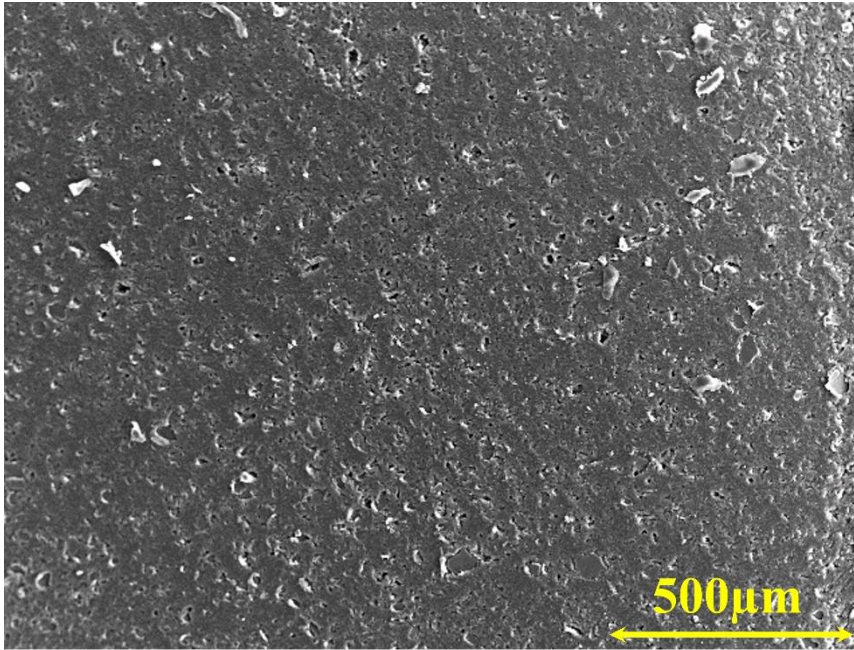


Figure 4.18. Contact Angle Recovery Times on Unused, 10- and 20-year-aged SiR Specimens.

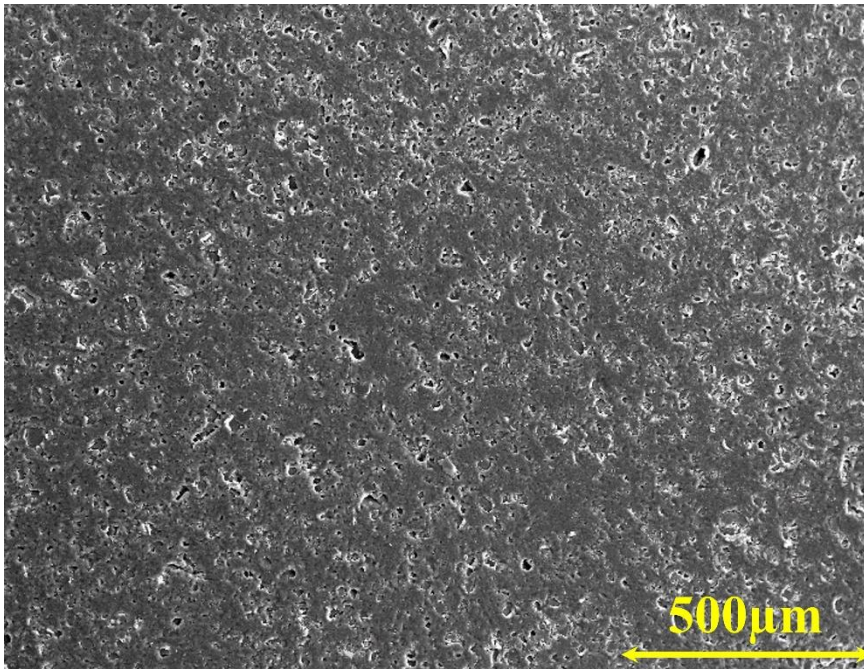
4.3.2.3 Analysis of Physical or Chemical Damages on SiR Specimens after SD Treatment

For lowering hydrophobicity, other researchers generated the corona discharge using a needle-plate electrode system [7]. The corona discharge broke the molecular structure of SiR and made obvious cracks on the surface, i.e., the corona discharge caused physical and chemical changes. SD is used for grasping the degradation degree, and it must not give damages which may lower the insulation performance.

In order to observe the treated SiR surface, SEM image evaluation was performed. SEM images on an unused SiR specimen before and after an SD treatment for 25 s are represented in Figure 4.19. The obvious cracks or other physical damages cannot be seen after the SD treatment. Next, the ATR-FTIR spectra of an unused SiR specimen were measured to analyse chemical damages. Figure 4.20 shows the ATR-FTIR spectra of an unused SiR specimen before and after the SD treatment for 25 s. The obvious spectral changes in the spectra before and after the SD treatment cannot be seen. Additionally, the peak intensity ratios of chemical bonds such as Si-O, Si-CH₃, C-H and O-H in ATH before and after the SD treatment were evaluated, and the result is shown in Figure 4.21. The ratios of Si-O, Si-CH₃, and C-H after the SD treatment slightly decrease in comparison to those before the SD treatment, however, the difference is less. It is considered that the SD treatment doesn't cause physical or chemical damage to the surface of the SiR specimen.



(a)



(b)

Figure 4.19. SEM Images of an Unused SiR Specimen (a) Before an SD Treatment and (b) After an SD Treatment for 25 s.

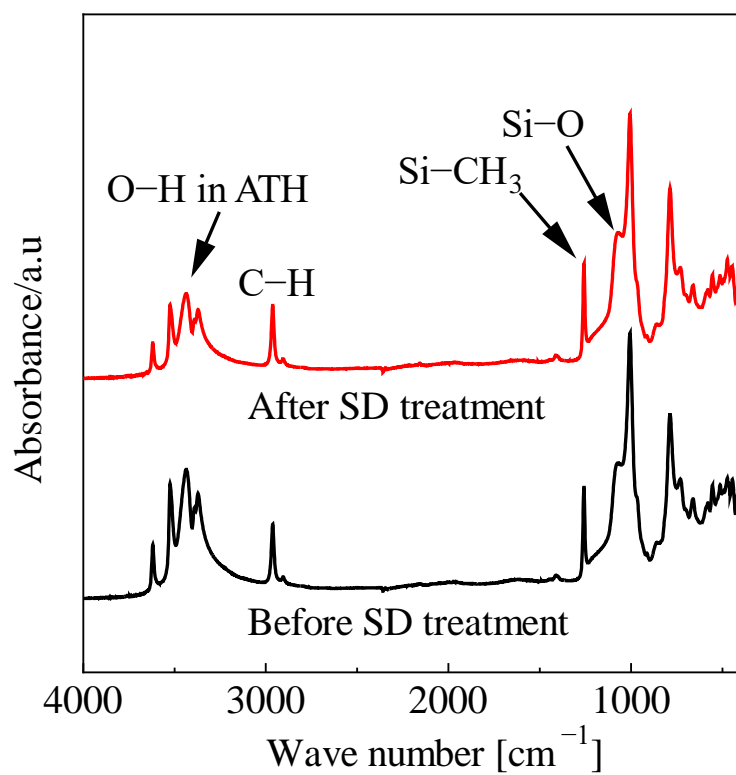


Figure 4.20. ATR-FTIR Spectra of an Unused SiR Specimen before and after an SD Treatment for 25 s.

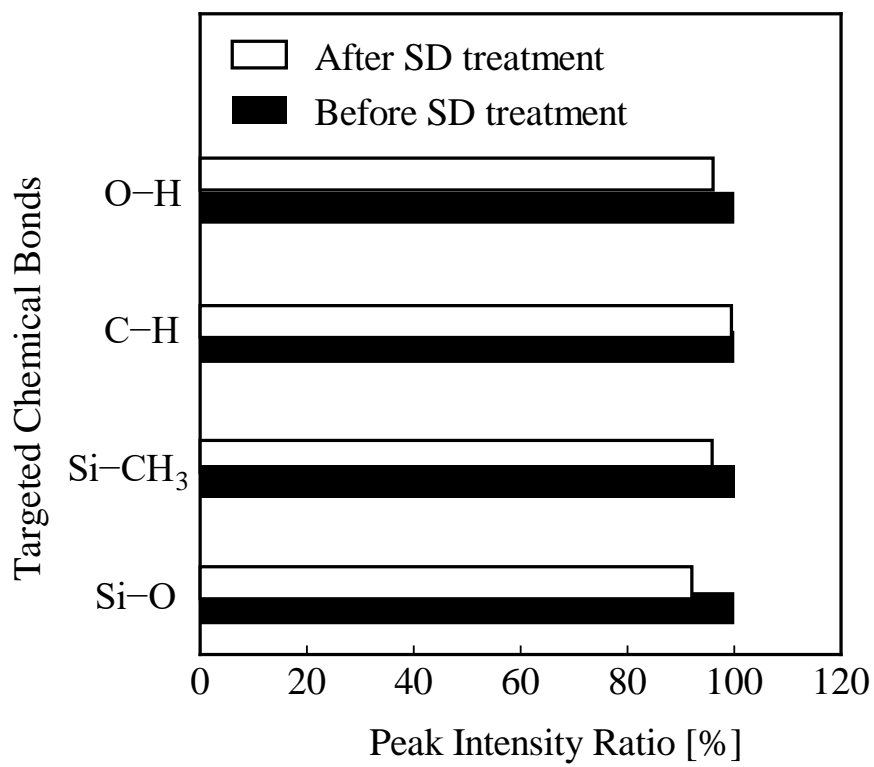


Figure 4.21. Peak Intensity Ratio of Chemical Bond of an Unused SiR Specimen before and after an SD Treatment for 25 s.

4.3.3 Conclusions of Evaluation of Degradation Degree of SiR using Surface Discharge

In order to grasp the degradation degree of SiR, a novel technique using SDs with a mesh plate as a high-voltage electrode was proposed. The mesh plate was closely arranged on the surface of the SiR specimen. The surfaces of SiR specimens cut out from unused, 10 and 20-year-aged insulators were treated for 5, 10, 15, 20 and 25 s. After the SD treatment, the contact angle of each SiR specimen was measured at intervals of 10 min. Then, the contact angle recovery time was investigated in order to evaluate the degradation degree. Additionally, SEM and ATR-FTIR measurements were performed to confirm whether the SD treatment causes physical and chemical damages to the SiR surfaces or not. The major results can be summarized as follows:

- 1) An SD electrode can generate uniform discharge plasma for lowering hydrophobicity characteristics. The detected discharge current did not significantly differ from that obtained during the salt fog aging test.
- 2) An SD treatment accelerates hydrophobicity loss on the SiR surface. The contact angle decreases with the increase of the SD treatment time. The contact angle recovery times on 10 and 20-year-aged SiR specimens are much longer as compared to that on an unused SiR specimen. The dispersion of LMW in the aged SiR specimen might be disturbed by the degradation layer while that in the unused SiR specimen is active. The disturbance of LMW by the degradation layer reflects the longer hydrophobicity recovery tendency. Thus, the contact angle recovery time after the SD treatment may be useful for investigating the degradation degree.
- 3) An SD treatment cannot cause not only physical but also chemical damages to the surface of the SiR specimen.

The proposed technique has the possibility which investigate the degradation degree of SiR specimen without causing any physical or chemical damage. Additionally, applications in outdoors are also possible after developing a portable high-voltage source and an SD electrode system. However, the decrease mechanism of the hydrophobicity characteristic by SD treatment wasn't interpreted in detail. In Section 4.4, the characterization of SD used for measuring the degradation degree of SiR insulators will be discussed.

4.4 Characterization of SD used for Measuring Degradation Degree of SiR Insulator

4.4.1 Experimental Setup

A schematic diagram of an experimental setup is shown in Figure 4.22. An H.V. probe was connected to a mesh plate for applying voltage while an Al tape was earthed. An HFCT sensor was used to measure the SD current. The applied voltage and the SD current were recorded by a digital oscilloscope with a sampling frequency of 1.25 GHz. In the experiments, 8 kV with the high frequency of 10 kHz was applied and the applied SD treatment time was set from 5 s to 25 s. The SD current was analyzed by fast Fourier transform (FFT) and applied a high pass filter (HPF). To investigate the reason why the SDs cause the hydrophobicity loss, the surface temperature on the mesh plate during an SD treatment was measured by using an infrared thermography camera (FLIR C3, FLIR Systems AB). In addition, to observe the optical emission spectra, a fiber optical spectrometer (USB4000, Ocean Optic) was faced about 30 mm from the surface of an SD electrode.

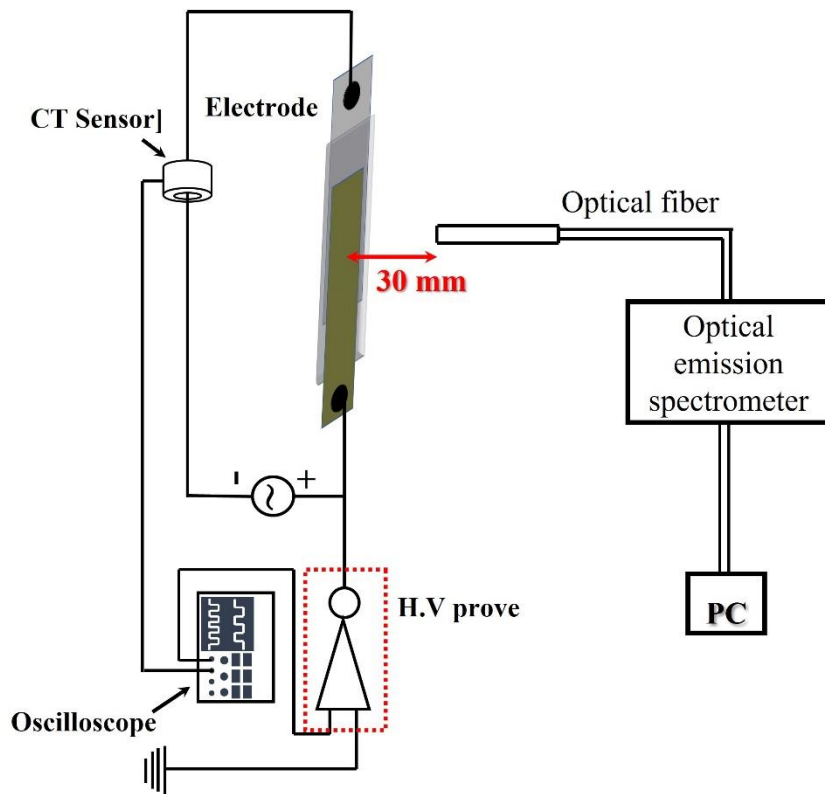


Figure 4.22. Experimental Setup.

4.4.2 Results and Discussions

4.4.2.1 Characterization of SD

According to Section 4.2 and Section 4.3, the value of the discharge current during an SD treatment was about 60 mA while that during a 20-cycle salt-fog aging test was about 45 mA. The detected discharge current did not significantly differ from that obtained during a 20-cycle salt-fog aging test. In addition, any visible erosions couldn't be seen on the SiR surface after an SD treatment.

On the other hand, the displacement current due to the capacitance component of an SD electrode system is included in the detected current. Therefore, the discharge current was analyzed with FFT. Figure 4.23 shows the frequency spectra of discharge current obtained by FFT. The main frequency components are 25 MHz and 30 MHz. Because the frequency of applied voltage is 10 kHz, the frequency components of 25 MHz (40 ns) and 30 MHz (33.3 ns) are due to SDs. Based on the result, we applied an HPF of 10 MHz to the detected SD current. The filtered waveform is shown in Figure 4.24. Pulsive current is clearly seen, and therefore it is considered that the SDs consist of filamentary discharges. Figure 4.25 shows uniformly generated SD on the 150-mesh plate of an SD electrode. The image was taken by a digital camera, and the exposure time was much longer in comparison with the detected current pulse duration, i.e., the observed image is the integrated SDs which consist of a lot of filamentary discharges.

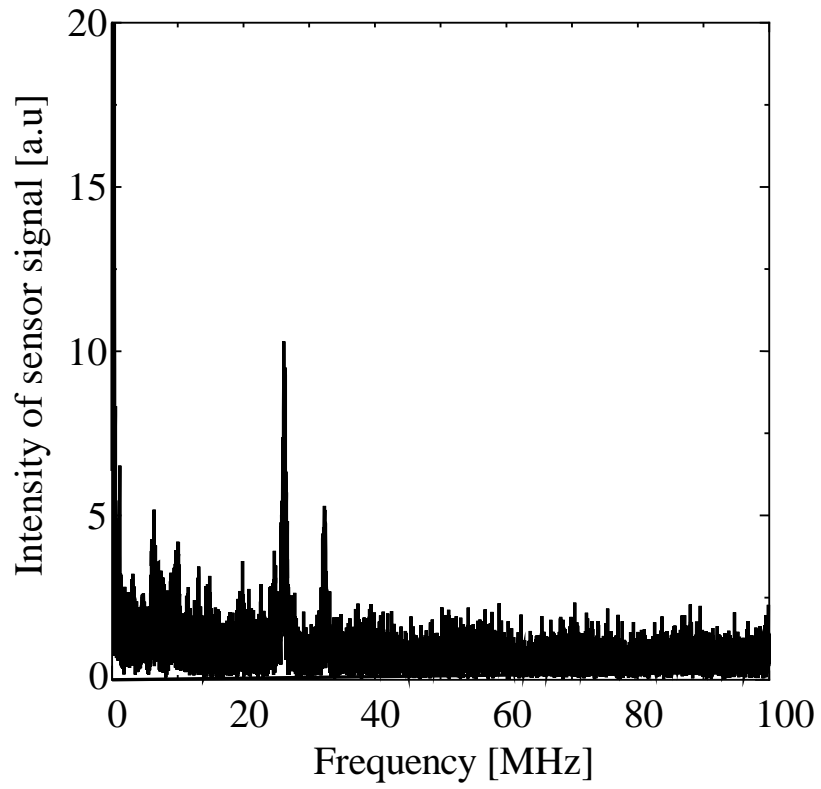


Figure 4.23. Frequency Spectra of SD Current Obtained through FFT Analysis.

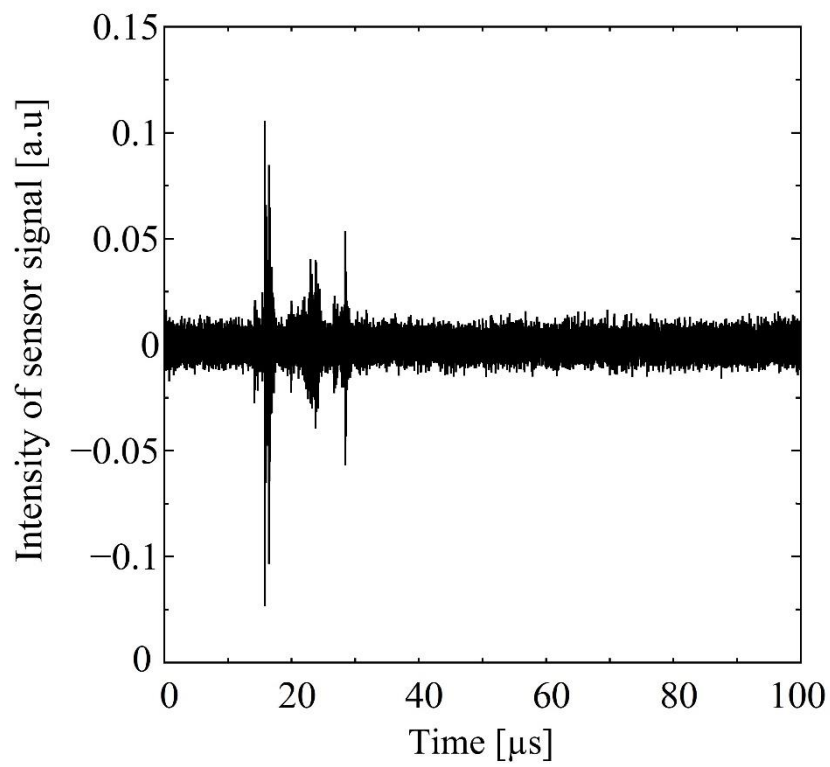


Figure 4.24. Waveform due to Filamentary Discharge Obtained through a 10 MHz-HPF.

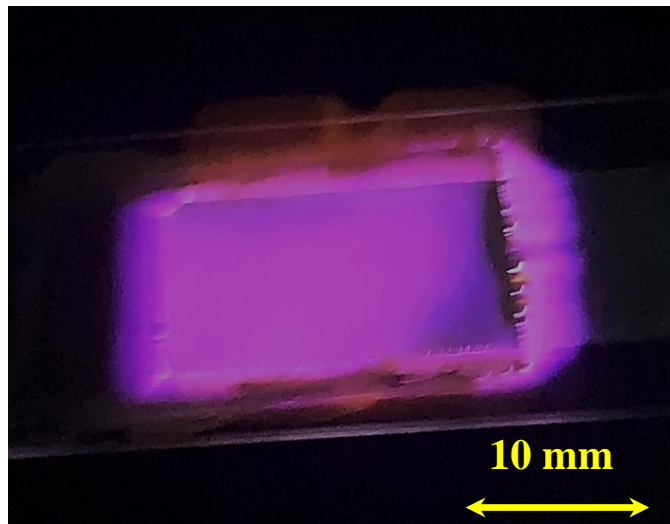


Figure 4.25. Uniformly Generated SD on a 150-mesh Plate of an SD Electrode.

4.4.2.2 Surface Temperature and Optical Emission of an SD electrode

The surface temperature of an SD electrode was measured under a room temperature of 14.7° C and a humidity of 36% before and during an SD treatment. Before an SD treatment, the surface temperature of the 150-mesh plate was 13.3 ° C. After 5 s of an SD treatment, the surface temperature of the 150-mesh plate was 28.4°C. Figure 4.26 is the measurement image of surface temperature on the 150-mesh plate in 5 s of an SD measurement. The surface temperature of the 150-mesh plate significantly increased to 73° C after 25 s of an SD treatment. Table 4.2 illustrates the surface temperature of the 150-mesh plate during an SD treatment. The surface temperature increases as the elapsed time becomes long.

The investigated hydrophobicity recovery time, which is obtained by measuring the contact angle of unused and 20-year-aged SiR specimens after 5, 10, 15, 20, and 25 s of SD treatment times is shown in Table 4.3. The hydrophobicity recovery times of unused and 20-year-aged polymer specimens after 5 s of an SD treatment time were 10 and 50 min, respectively. It was found that the difference in hydrophobicity recovery time of unused and 20-year-aged.

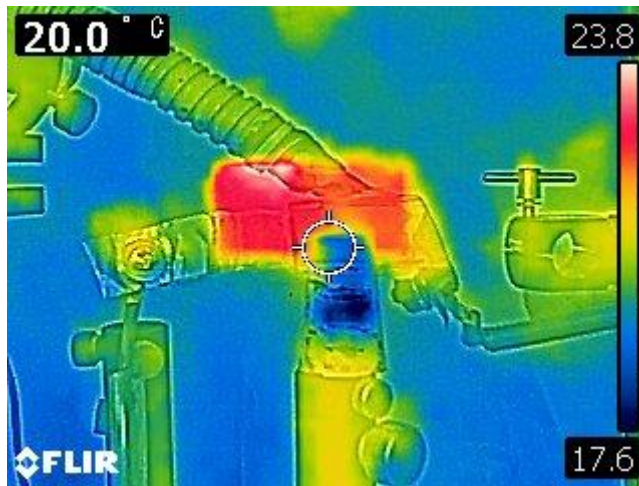
SiR specimens can be significantly diagnosed even if the treatment time of an SD was 5 s. The hydrophobicity recovery of the polymer surface is reflected by the dispersion of low molecular weight (LMW) fluid from the bulk to the surface [54]. On the other hand, LMW dispersion in the polymer surface can be promoted by surface high-temperature treatment [49] [50]. The prescribed SD electrode generated surface temperature on the 150-mesh plate during an SD treatment. However, it should be noted that several minutes for heating on the SiR surface are required to promote LMW dispersion. An SD was applied to the SiR surface within 5s to 25s in an SD treatment. Therefore, the contact angle loss and hydrophobicity recovery on the SiR surface cannot be caused by the surface temperature during an SD treatment because the application time of an SD treatment is not enough to promote LMW.

The molecular structure of the SiR specimen is composed of a siloxane bond (Si-O) and methyl groups (CH₃) in the dimethylpolysiloxane bond as the side chain. The hydrophobicity characteristic of SiR is corresponding to the side chain of CH₃. SD emits light between a wavelength of 300 and 400 nm as shown in Figure 4.27. If SD emits light with a wavelength of less than 291 nm, C-H can be cut by an SD treatment. However, such intense light emissions were not detected, and therefore, the C-H bond in the side chain of SiR cannot be cut due to the light emissions of SD. On the other hand, SD generates a non-equilibrium atmospheric

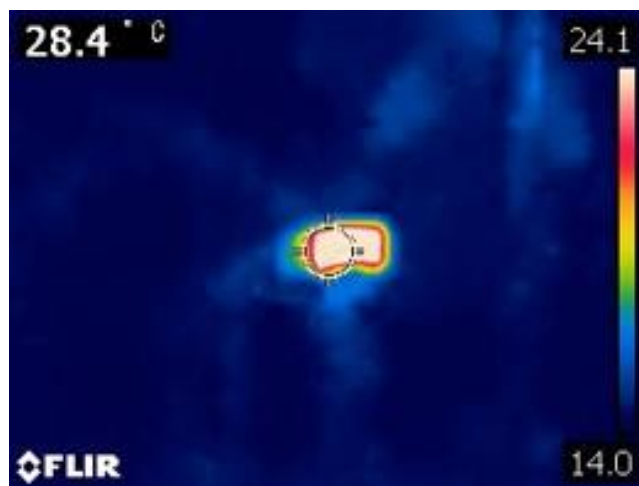
pressure plasma because the high-frequency voltage was applied [7]. The plasma generated from SD is composed of nitrogen, oxygen and other gas. The discharge of nitrogen and oxygen generates the filamentary discharge. It is well known that the electron temperature following the electron energy distribution function is in the range of 1-10 eV [52]. The binding energy of C-H in the side chain is 4.25 eV [53]. The direct energy transfer from energetic particles of the SD is higher than the binding energy of C-H in the side chain. Therefore, SD can easily change the chemical characteristics of SiR, and then, the contact angle on the polymer surface can decrease.



(a) Image without infrared radiation (IR)



(b) Before an SD Treatment



(c) During an SD Treatment (5 s)

Figure 4.26. Measurement Image of Surface Temperature on 150-mesh Plate

Table 4.2. Surface Treatment on a 150-mesh Plate during an SD Treatment.

Elapsed Time [s]	Surface Temperature [Deg.]
0	13.3
5	28.4
10	40
15	59
20	68
25	73

Table 4.3. Contact Angle and Hydrophobicity Recovery Time of Unused and 20-year-aged SiR Surface after an SD Treatment.

Specimen	SD Treatment Time [s]	Contact Angle [deg.]	Hydrophobicity Recovery Time [min]
Unused SiR	5	104.9	10
	10	102.5	40
	15	99.3	60
	20	97.2	90
	25	93.4	110
20-year-aged SiR	5	110.0	50
	10	107.9	70
	15	100.8	110
	20	97.0	140
	25	94.2	160

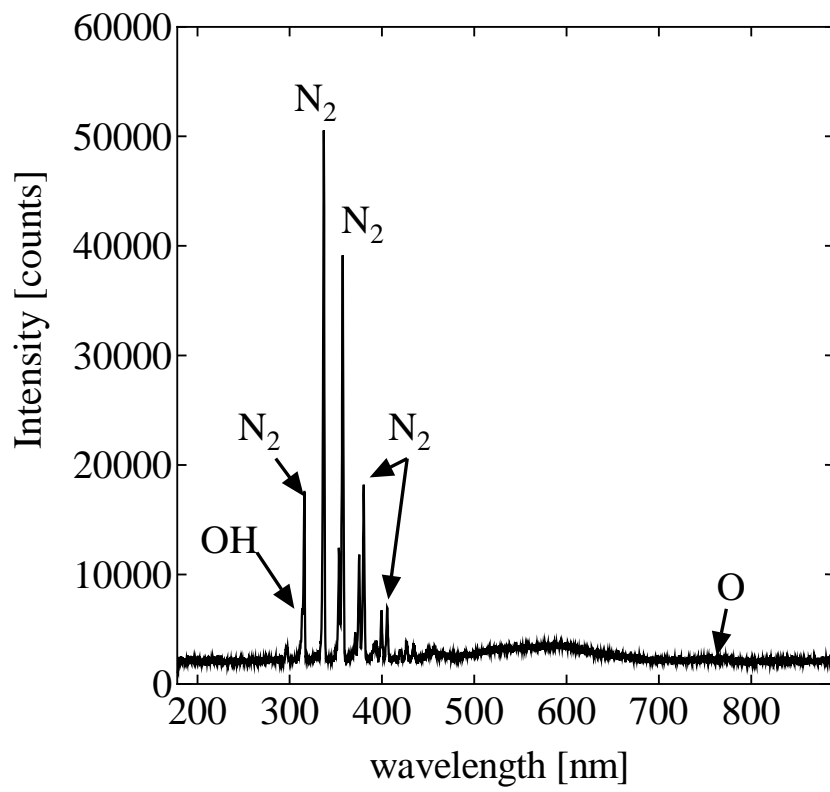


Figure 4.27. Optical Emissions during an SD Treatment.

4.4.3 Conclusions of Characterization of SD Used for Measuring Degradation Degree of SiR Insulator

To characterise the SD used for measuring the degradation degree of the polymer insulator, the SD current was measured by using an HFCT sensor. In addition, the surface temperature on the 150-mesh plate during an SD treatment and the optical emissions were observed by using an infrared thermography camera and a Fiber optical spectrometer, respectively. The major results are concluded as follows:

- 1) The detected SD current during an SD treatment did not significantly differ from that obtained during the 20-cycle-salt-fog aging test. Moreover, it could be confirmed that the SD has filamentary discharges.
- 2) The surface temperature on the 150-mesh plate during an SD treatment cannot promote the decrease of the contact angle on the SiR surface because the treatment time of an SD is short.
- 3) Optical emissions with wavelengths of less than 291 nm which can cut the C-H bond of SiR weren't observed. Therefore, it is thought that the direct energy transfer from energetic particles with higher energy than the binding energy of C-H changes chemical characteristics and decreases the contact angle on the SiR surface.

CHAPTER 5

EVALUATION OF DEGRADATION DEGREE OF ARTIFICIALLY DEGRADED SiR SURFACE USING SURFACE DISCHARGE

5.1 Introduction

In Chapter 3, the artificially degraded SiR surface can be fabricated. However, we performed only one fabrication cycle. In addition, we grasped the degradation degree of aged SiR surface using both a salt-fog aging test and an SD treatment in Chapter 4. The degradation degree on artificially degraded SiR surfaces has not yet been evaluated.

In this Chapter, the degradation degree of the artificially degraded SiR surfaces was evaluated using an SD treatment. The artificially degraded SiR surface fabrication consisted of 5 steps and a 1-cycle test required 24 h, as explained in Chapter 3. In this Chapter, the degraded SiR surfaces were fabricated by a 1-cycle and a 2-cycle test. Next, the artificially degraded SiR surface was exposed to surface discharge (SD), as explained in Chapter 4.

5.2 Experimental Method

5.2.1 Surface Morphology of Aged SiR

Figure 5.1 shows a fabrication cycle for making an artificially degraded surface on a SiR specimen. The fabrication cycle consists of 5 steps and one cycle requires 24 h. In this experiment, one fabrication cycle (1-cycle test) of 24 h and two fabrication cycles (2-cycle test) of 48 h were performed. A SiR specimen with a surface roughness of $0.13\mu\text{m}$ contains 50% of ATH. The size of SiR specimens was $30\text{ mm} \times 30\text{ mm}$ and its thickness was 4 mm. The average particle diameter of red clay as a pollution material is approximately 1000 times smaller than that of sand. In step 1, red clay was used as a contaminant or adherent substance to promote physical aging. 0.1 g of red clay was mixed with 20 mL of ionized water, and 0.14 mL of the mixed liquid water was dropped on the surface of the SiR specimen. The dropped water has a diameter of 10 mm and it required 13 h to be naturally dried in the atmosphere. A Xe short arc lamp was used as a UV light source in step 2, which emits light having a wavelength of 375 nm to 1000 nm. The UV output power is 19 mW/cm^2 , which is 7 times larger than that in the sunlight. The dried red clay region on the SiR surface was exposed to UV light for 6 h. Next, the UV light-irradiated SiR surface with red clay adhesion was kept inside a small incubator at

40°C. An incubator is 180 mm in length, 240 mm in width and 220 mm in height, and the setting temperature is controlled by a microcomputer with a thermocouple sensor. The duration for the surface heating process was 4 h. In step 4, each SiR specimen was placed at 25°C for 0.5 h to perform the heat radiation process. In the final step, a writing brush, ionized water and alcohol were used to clean the SiR surface. The SiR surface with red clay adhesion was first cleaned using a writing brush and ionized water for 3 min, and 12 min was required for drying the surfaces. However, there was still visible red clay on the surfaces. Therefore, the SiR surface was cleaned using a writing brush and alcohol for another 3 min, and 12 min was required for drying. After the artificially degraded SiR surface has been fabricated, the contact angles were measured. 7 μ L of a water droplet was dropped from a syringe to the SiR surface and the contact angle of the dropped water droplet was automatically measured by using a contact angle meter every 10 min. Next, a surface roughness tester and SEM microscopy were used for measurements of surface roughness and surface morphology, respectively. Chemical structure change on the artificially degraded SiR surface was measured by ATR-FTIR spectroscopy. Based on the results, the difference between the artificially degraded SiR surface and the SiR insulator surface aged in outdoor was investigated.

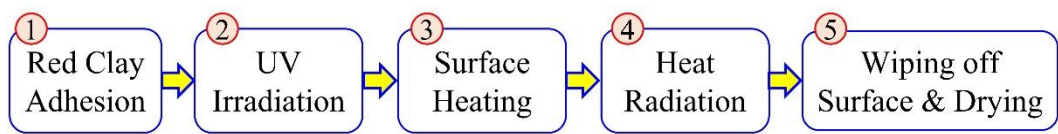


Figure 5.1. A Fabrication Cycle of Artificially Degraded Surface on a SiR Specimen.

5.2.2 Surface Discharge Treatment

An SD electrode consists of a quartz glass plate, an aluminium (Al) tape and a 150-mesh-SUS wire mesh plate. The length and the width of the quartz glass plate are 75 mm and 25 mm, respectively, and the thickness is 0.5 mm. The 150-mesh plate is 80 mm in length and 15 mm in width. The hole size and thickness are 0.1 mm and 0.06 mm, respectively. The size of the Al tape is 80 mm in length and 20 mm in width and the thickness is 0.1 mm. A quartz glass plate is sandwiched between the Al tape and the 150-mesh-SUS wire mesh plate. The overlapped region of the Al tape and the 150-mesh-SUS wire mesh plate on the quartz glass is 15 mm × 30 mm in which SD is formed. Figure 5.2 shows a schematic diagram of an experimental setup for generating SD. An H.V. probe and a CT sensor were used to measure the applied voltage and the discharge current, respectively. The 150-mesh-SUS wire mesh plate was connected to an H.V. source while the Al tape was earthed. To record waveform data, a digital oscilloscope with a sampling frequency of 1.25 GHz was used. SD treatments were performed under certain conditions in Table 5.1. Before each SD treatment, the artificially degraded SiR surface, which was fabricated following via 5 steps in Section 5.2.1, was cleaned with alcohol, i.e., there is no visible red clay and any silicon oil on the SiR surface. Then, the artificially degraded SiR surface was faced with a 150-mesh-SUS wire mesh plate in the SD treatment. After each SD treatment, the contact angle of the artificially degraded SiR surface was measured every 10 min until it was restored to an original contact angle.

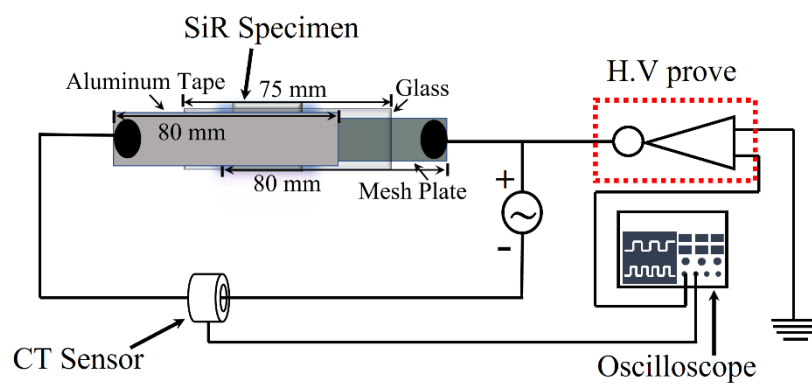


Figure 5.2. Schematic Diagram of an Experimental Setup for Generating SD.

Table 5.1. Experimental Conditions of SD Treatments.

Voltage [kV]	8
Frequency [kHz]	10
SD treatment time [s]	5, 10, 15, 20, 25

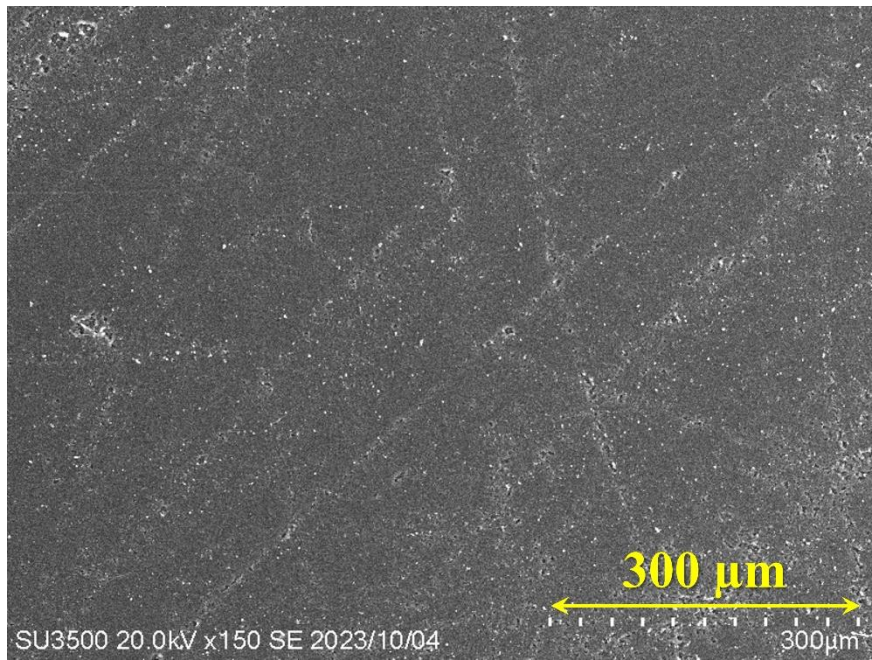
5.3 Experimental Results and Discussions

5.3.1 Physical Structure of Artificially Degraded SiR Surface

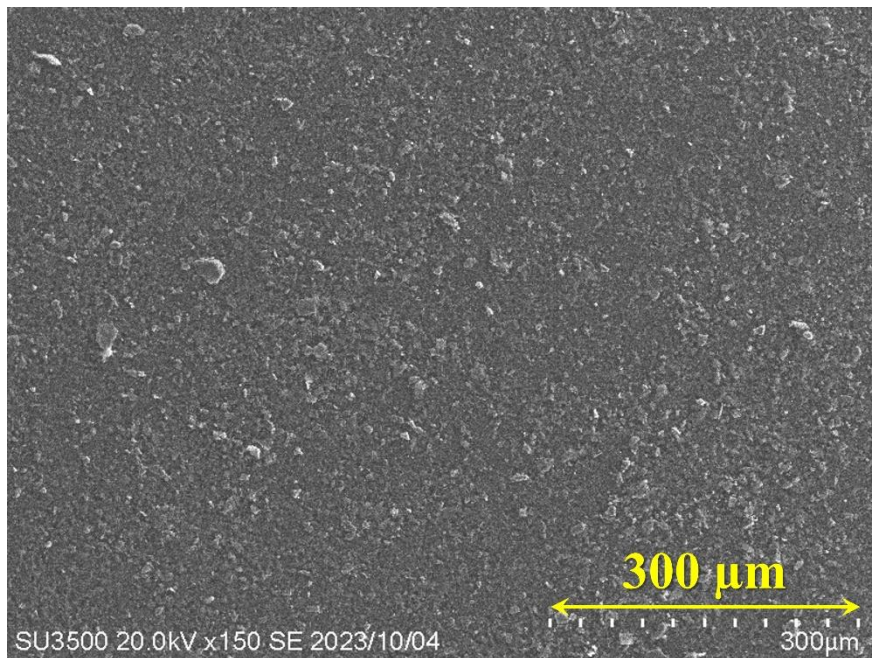
Two kinds of artificially degraded SiR surfaces were fabricated by a 1-cycle test and a 2-cycle test. To investigate the physical structure of the artificially degraded SiR surface, the contact angle was measured on the surface. The initial contact angle on the SiR surface before making the degraded surface was 112.4° . In step 5 of a fabrication cycle shown in Figure 5.1, the red clay adhesion on the SiR specimen is cleaned up by using a writing brush and ionized water, which is the same as a fact of surface cleaning by rainfall. The visible red clay remained on the SiR surface after cleaning by using a writing brush and ionized water. In step 2, the SiR surface with red clay adhesion was irradiated by UV light which made the red clay adhesion stronger on the surface. To measure the contact angles on the artificially degraded SiR surfaces, it was desirable to clean the visible red clay on their surfaces by using a writing brush and alcohol. After cleaning the visible red clay, the measured average contact angles on artificially degraded SiR surfaces made by a 1-cycle test and a 2-cycle test were 98.5° and 104.1° , respectively. The average contact angle on an artificially degraded SiR surface made by a 2-cycle test is larger than that made by a 1-cycle test because the contact angle is dependent on the minute surface roughness owing to adhesive material [49]. SEM images measured on the artificially degraded SiR surfaces made by a 1-cycle test and a 2-cycle test are shown in Figure 5.3. The surface structure on the artificially degraded SiR surface made by a 2-cycle test was different from that made by a 1-cycle test, and the red clay can be well seen on the SiR surface made by a 2-cycle test even after cleaning the surface with alcohol. Additionally, the surface roughness on the SiR surfaces made by a 1-cycle test and a 2-cycle test were $0.14\ \mu\text{m}$ and $0.18\ \mu\text{m}$, respectively. The surface roughness made by a 2-cycle test was larger than that made by a 1-cycle test. Due to the surface roughness of the pollution layer which can be seen in Figure 5.3(b), the contact angle on artificially degraded SiR surface made by a 2-cycle test becomes larger.

On the other hand, the variations in contact angle on artificially degraded SiR surfaces are shown in Figure 5.4. The average contact angles after making degraded surfaces are smaller than the initial value (112.4°). After 30 min from making degraded surfaces, the average contact angles on artificially degraded SiR surfaces made by a 1-cycle test and a 2-cycle test are 109.2° and 105.3° , respectively. They are still smaller than the initial contact angle, and the required times for restoring the average contact angles to the initial values are more than 30 min.

Specifically, in the cases of a 1-cycle test and a 2-cycle test, the required times are 40 min and 60 min, respectively. Thus, an artificially degraded SiR surface made by a 2-cycle test requires longer recovery time because a UV light irradiation process and a surface heating process are repeated two times. Due to UV light irradiation, the molecular structure of SiR is broken and the contact angle decreases [47]. Additionally, a combination of a UV light irradiation process and a surface heating process promotes the dispersion of LMW fluid from the bulk to the surface, and the LMW-enriched surface is newly formed on the surface. As a result, the contact angle of artificially degraded SiR surfaces restores to the initial value. The detailed changes in chemical structure on the SiR surface due to UV light irradiation and surface heating are explained in Section 5.3.2.



(a)



(b)

Figure 5.3. SEM Images Measured on Artificially Degraded SiR Surfaces Made by (a) 1-cycle Test and (b) 2-cycle Test.

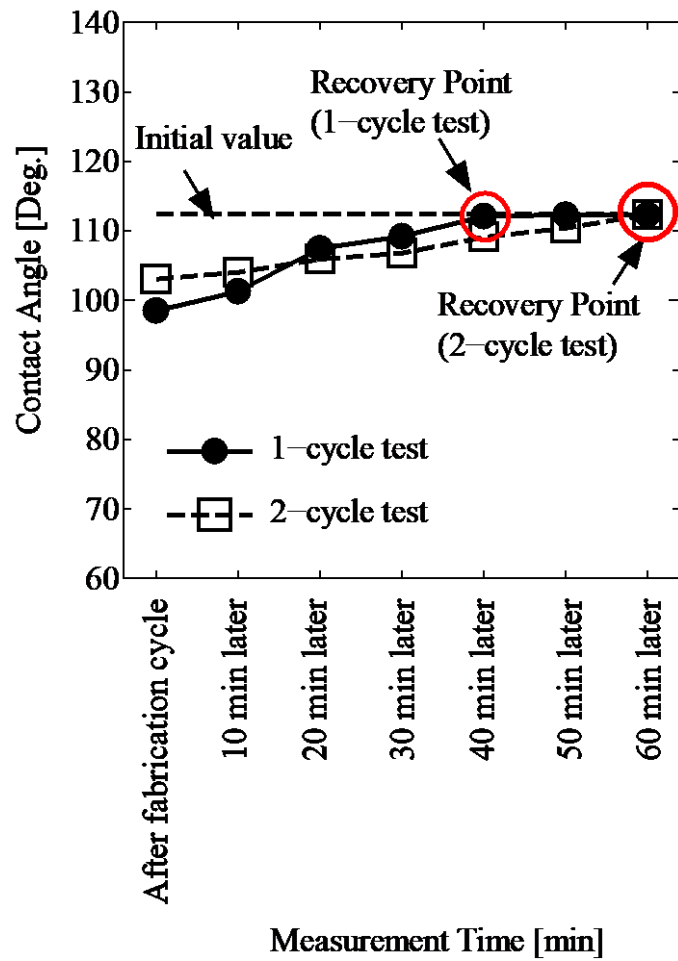


Figure 5.4. Variations in Contact Angle Measured on Artificially Degraded SiR Surface Made by a 1-cycle Test and a 2-cycle Test.

5.3.2 Chemical Structure Change of Artificially Degraded SiR Surface

SiR has siloxane bonds (Si-O) with strong linkage as its backbone of dimethylpolysiloxane. Methyl groups (CH₃) in the side chain of the dimethylpolysiloxane have the responsibility for hydrophobicity [55]. Chemical structure changes of Si-O in siloxane bond, methyl group Si-CH₃, C-H bond in a methyl group and O-H bond in ATH were observed by ATR-FTIR spectroscopy. The variations of Si-O, Si-CH₃, C-H and O-H bonds were measured at wavelengths of 1083 cm⁻¹, 1260 cm⁻¹, 2963 cm⁻¹, and 3434 cm⁻¹, respectively [48]. The peak intensity ratios of chemical bonds on artificially degraded SiR surfaces made by a 1-cycle test and a 2-cycle test were evaluated against those of a SiR specimen before making degraded surface, i.e., the peak intensities on the SiR surface before making degraded surface are set to reference. Figure 5.5 shows the peak intensity ratios on the SiR surfaces before making the degraded surface and the artificially degraded SiR surfaces made by a 1-cycle test and a 2-cycle test. The peak intensity ratios corresponding to Si-O, Si-CH₃, C-H and O-H bonds on artificially degraded SiR surfaces decrease in comparison with those of the SiR surface before making a degraded surface. In particular, C-H and O-H bonds on artificially degraded SiR surfaces significantly decrease. Due to UV light irradiation and surface heating, both the ATH structure and the side chains as C-H and Si-CH₃ are broken as free radicals of H• and CH₃ while the Si-O-Si group splits into free radicals of Si-O and Si [18][51]. These molecular chain breakings may change the original SiR surface into a degraded surface.

In addition, the decreasing rates of the peak intensity ratios on the aged SiR surfaces and artificially degraded SiR surfaces were compared. Figures 5.6(a), 5.6(b), 5.6(c) and 5.6(d) shows the decreasing rates of Si-O, Si-CH₃, C-H, and O-H bonds, respectively. The comparison of decreasing rates of the peak intensity ratios between the artificially degraded SiR surface made by a 1-cycle test and the 10-year-aged SiR surface on the hydrophobicity class 1 (HC1) portion is represented by a blue rectangular bar. The decreasing rates of the artificially degraded SiR surface made by a 1-cycle test are similar to those of the 10-year-aged SiR surface on the HC 1 portion. Also, a red rectangular bar represents the comparison between the artificially degraded SiR surface made by a 2-cycle test and the 20-year-aged SiR surface on the HC 1 portion. The decreasing rates of the artificially degraded SiR surface made by a 2-cycle test are similar to those of the 20-year-aged SiR surface on the HC 1 portion.

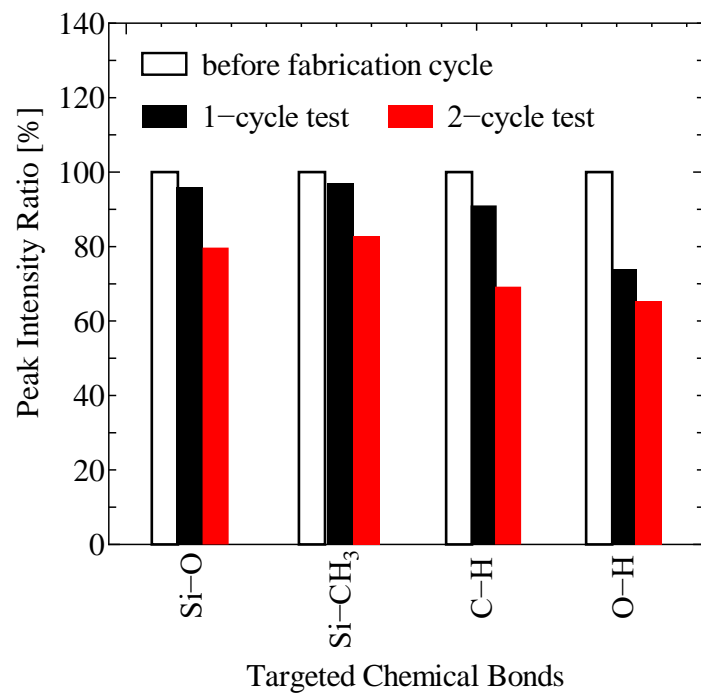
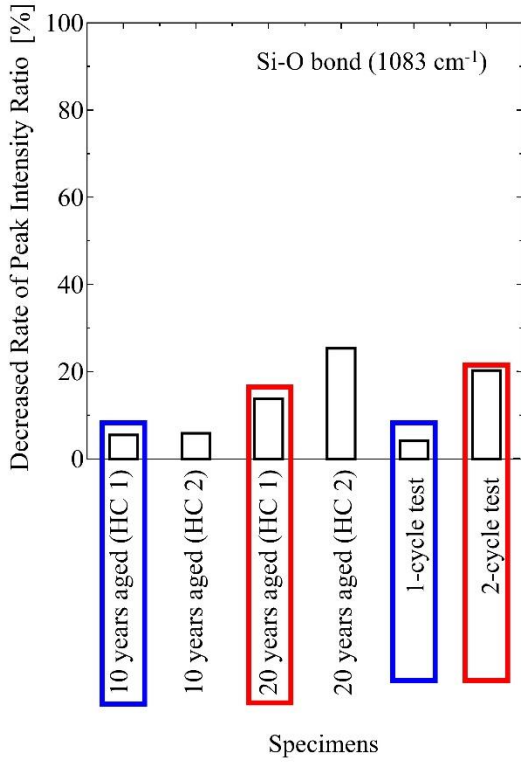
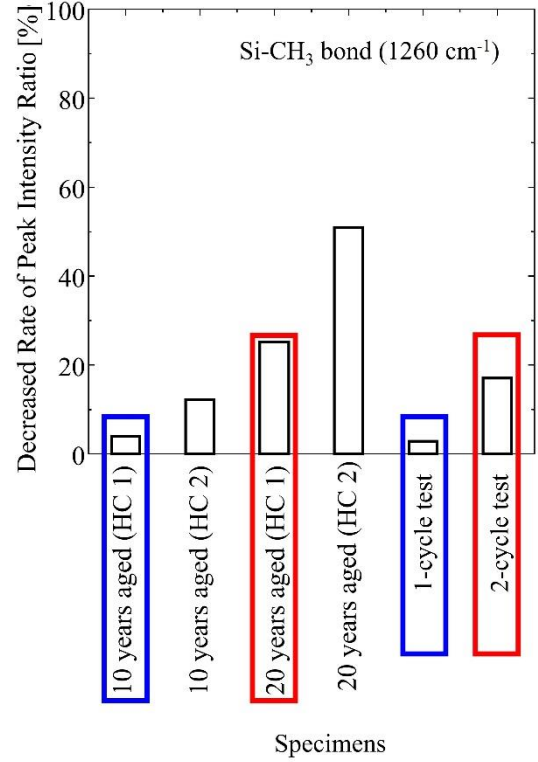


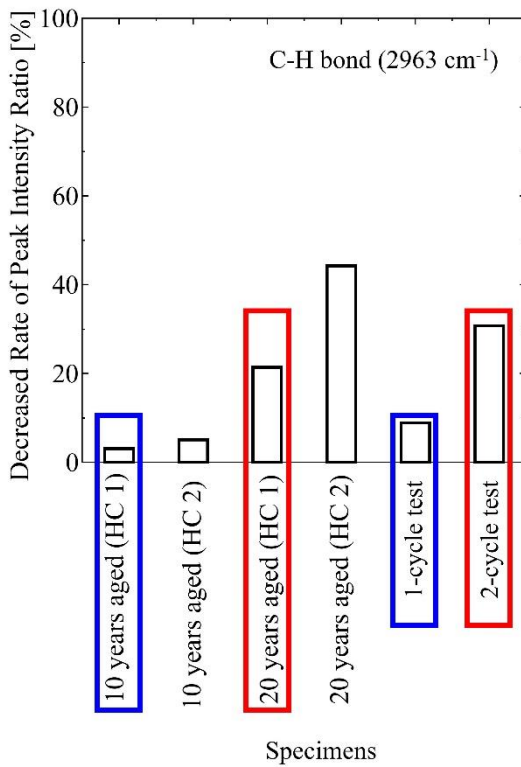
Figure 5.5. Peak Intensity Ratios on SiR Surfaces before Making Degraded Surface and Artificially Degraded SiR Surfaces Made by a 1-cycle Test and a 2-cycle Test.



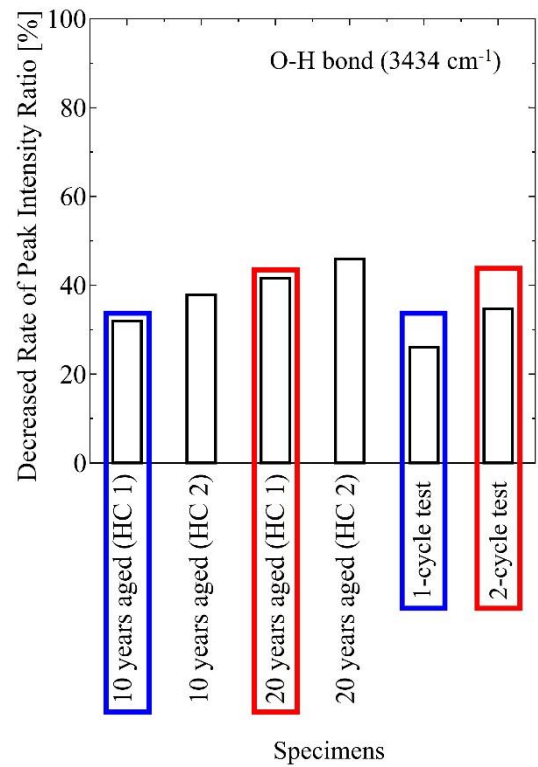
(a)



(b)



(c)



(d)

Figure 5.6. Decreasing Rates of Peak Intensity Ratios of Aged and Artificially Degraded SiR Surfaces (a) Si-O Bond, (b) Si-CH₃ Bond, (c) C-H Bond and (d) O-H Bond in ATH.

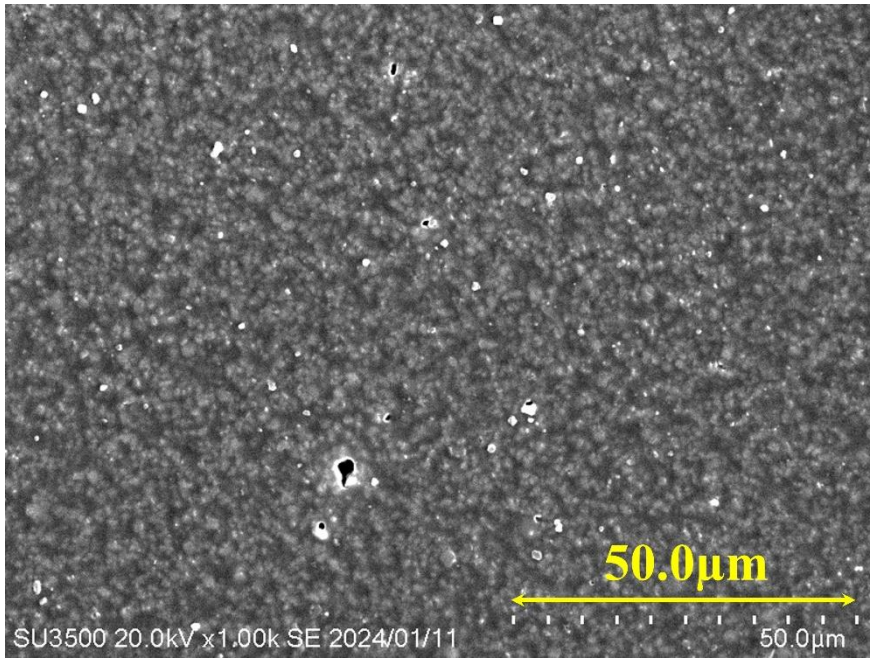
5.3.3 Recovery Characteristics of Hydrophobicity after SD Treatment

To evaluate the degradation degree, artificially degraded SiR surfaces were exposed to SD. The morphologies of the SiR surface states before and after SD treatment for 25 s are represented in Figure 5.7. It can be seen from this figure that there is no significant physical damage on a SiR surface even after the SD treatment. Figure 5.8 shows the temporal variations in contact angle on the SiR surfaces after SD treatment. The contact angles on the SiR surfaces decrease with the increase of SD treatment time. The binding energies of the Si-O bond and C-H bond in CH₃ are 4.6 eV and 4.25 eV, respectively [52][53]. SD is a non-equilibrium atmospheric pressure plasma [7], and it is well known that the electron temperature following the electron energy distribution function is in the range of 1-10 eV. The energy of energetic electrons is higher than the binding energies of Si-O bond and C-H bonds in CH₃. The chemical structure on the SiR surface is easily changed, and then the contact angle decreases. Additionally, after SD treatment, the contact angles on artificially degraded SiR surfaces decreased more than that on a SiR specimen before making degraded surface. Before SD treatment, the chemical structures on artificially degraded SiR surfaces had already been changed because of UV light irradiation and surface heating, which caused a further decrease in the contact angle.

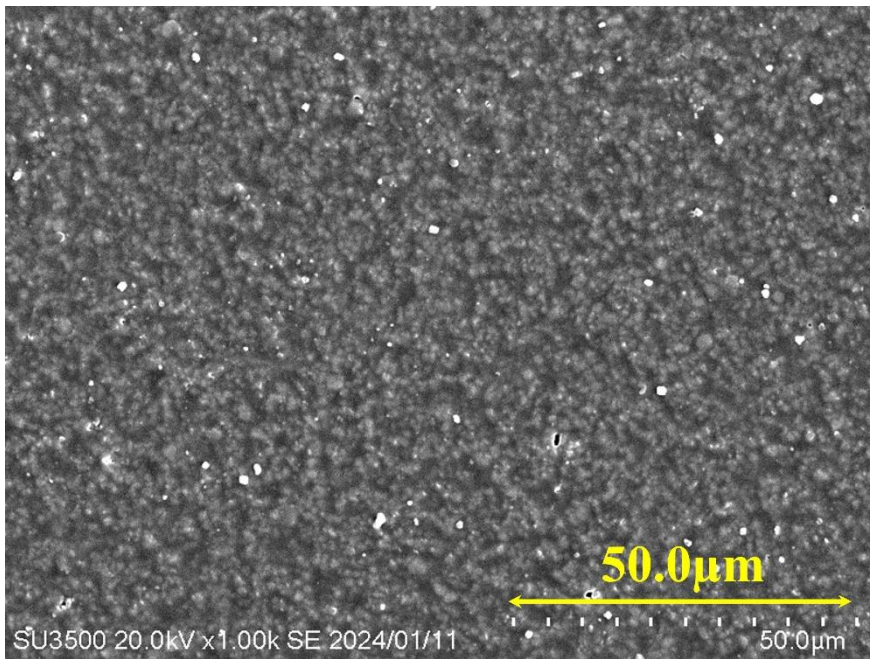
The decreased contact angles on the SiR surfaces after the SD treatment gradually increased as shown in Figures 5.9, 5.10, and 5.11. The hydrophobicity recovery times on the SiR surfaces are shown in Figure 5.12. The hydrophobicity recovery time means the required time for recovering the initial contact angle due to the dispersion of LMW. In the case of an SD treatment for 5 s, the hydrophobicity recovery times on the SiR surfaces made by a 1-cycle test and a 2-cycle test were 20 min and 30 min, respectively. In contrast, the hydrophobicity recovery time on the SiR surface before making a degraded surface is 10 min. In the case of SD treatment for 25 s, 120 min and 140 min are required for recovering the initial contact angles on artificially degraded SiR surfaces made by a 1-cycle test and a 2-cycle test, respectively while that before making degraded surface is 70 min.

Thus, the hydrophobicity recovery time on an artificially degraded SiR surface made by a 2-cycle test is longer than that on the SiR surfaces before making a degraded surface and after a 1-cycle test. The SD treatment promotes the dispersion of LMW fluid in SiR, which makes the surface hydrophobicity restore to the initial state [54]. In Figure 5.3, the red clay obviously remains on the artificially degraded SiR surface made by a 2-cycle test. The

dispersion of LWM on the degraded surface might be disturbed, and then the hydrophobicity recovery time becomes long. Thus, it was found that the hydrophobicity recovery times on artificially degraded SiR surfaces which have similar characteristics on the surfaces of SiR insulators aged in outdoor for 10 and 20 years become longer with the increase in SD treatment time. Additionally, the hydrophobicity recovery time after a short-term SD treatment reflects the degradation degree of the actually aged or the artificially degraded SiR surface.



(a)



(b)

Figure 5.7. SEM Images on SiR Surfaces (a) Before and (b) After SD Treatment.

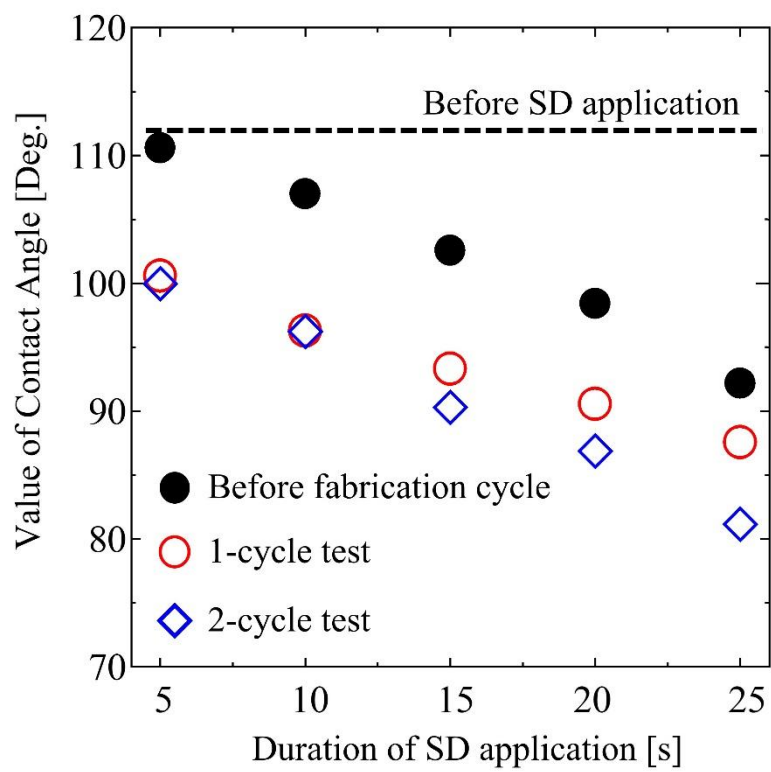
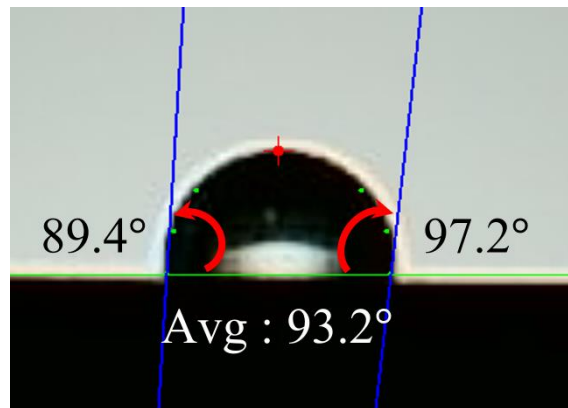
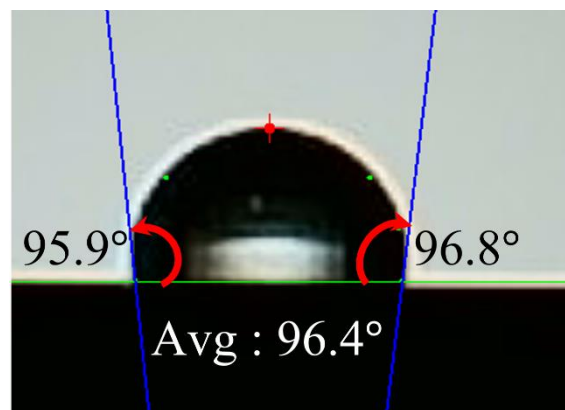


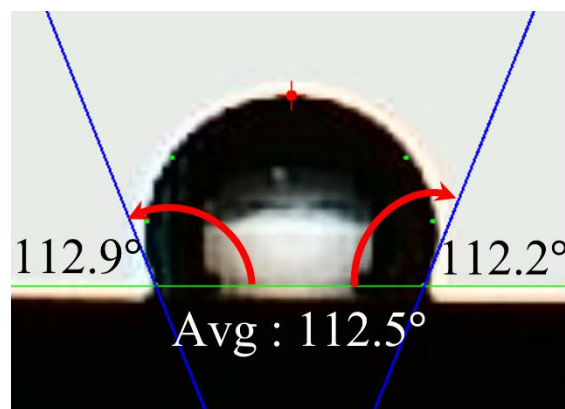
Figure 5.8. Temporal Variation of Contact Angles on SiR Surfaces Before Fabrication Cycle, 1-cycle Test and 2-cycle Test after SD Treatment.



(a)

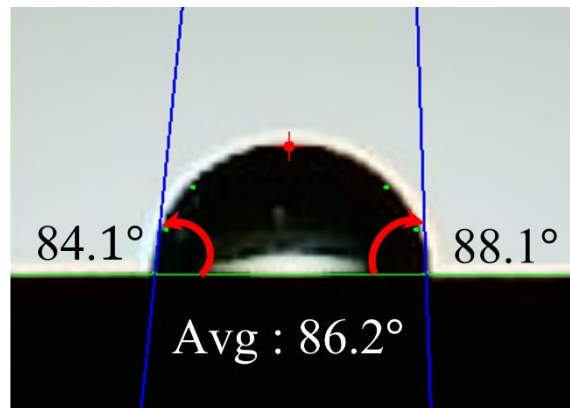


(b)

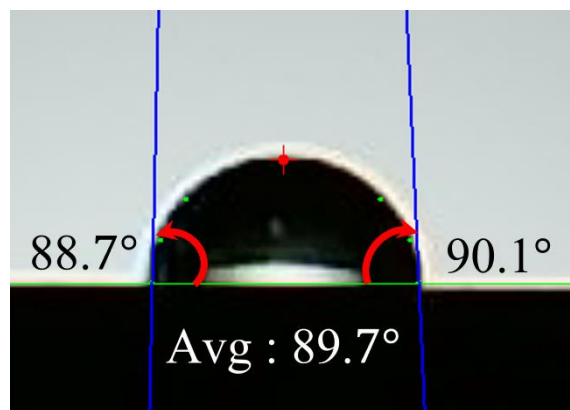


(c)

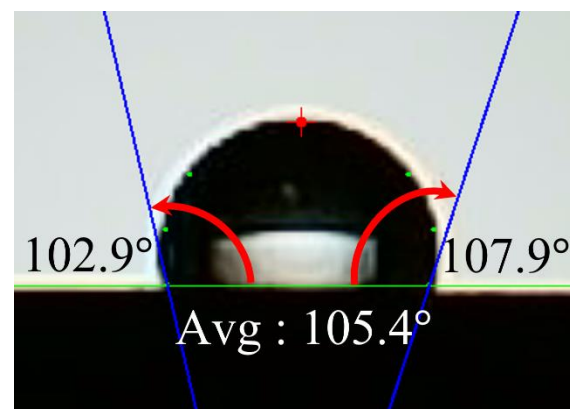
Figure 5.9. Shape Changes of a Water droplet on SiR Surface before Making Degraded Surface (a) just after SD Treatment, (b) 10 min Later, and (c) after Hydrophobicity Recovery (SD Treatment Time = 25 s).



(a)

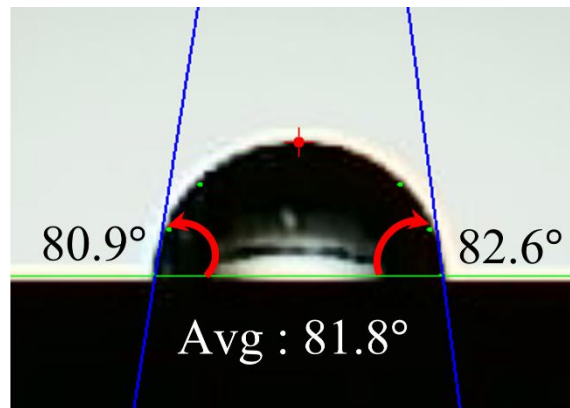


(b)

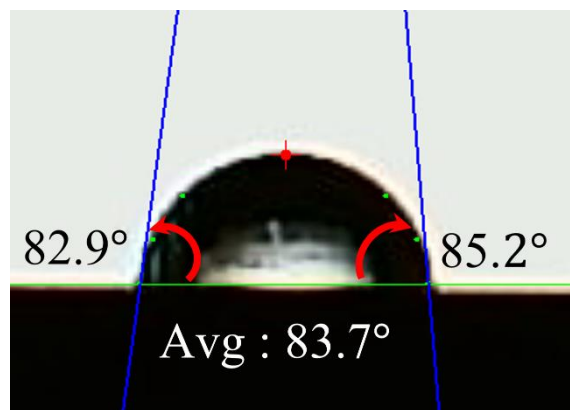


(c)

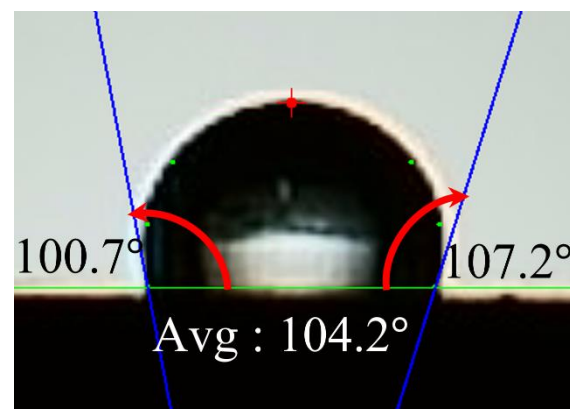
Figure 5.10. Shape Changes of a Water Droplet on Artificially Degraded SiR Surface made by a 1-cycle Test (a) just after SD Treatment, (b) 10 min Later, and (c) after Hydrophobicity Recovery (SD Treatment Time = 25 s).



(a)



(b)



(c)

Figure 5.11. Shape Changes of a Water Droplet on Artificially Degraded SiR Surface made by a 2-cycle Test (a) just after SD Treatment, (b) 10 min Later, and (c) after Hydrophobicity Recovery (SD Treatment Time = 25 s).

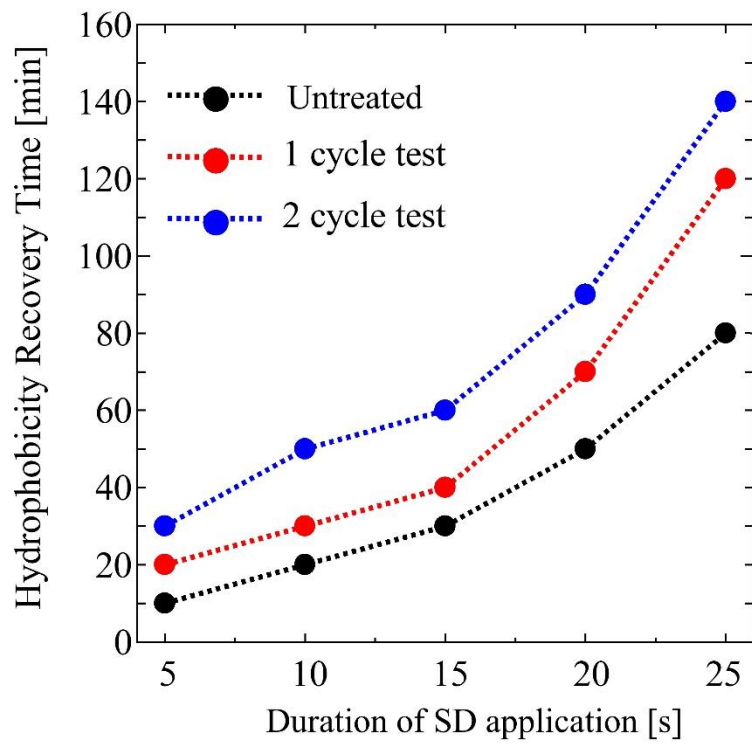


Figure 5.12. Hydrophobicity Recovery Times on SiR Surface before Making Degraded Surface and Artificially Degraded SiR Surfaces Made by a 1-cycle Test and a 2-cycle Test.

5.4 Conclusions

The artificially degraded SiR surfaces, which have similar characteristics of SiR insulator surfaces, were first fabricated by a 24 h fabrication cycle (1-cycle test) and a 48 h fabrication cycle (2-cycle). In addition, in order to evaluate the degradation degree, the artificially degraded SiR surfaces were exposed to SD treatment for 5, 10, 15, 20 and 25 s. Major results are concluded as follows:

- 1) The average contact angle of artificially degraded SiR surfaces decreased after the fabrication cycle due to UV light irradiation and surface heating. In addition, the contact angle on the artificially degraded SiR surface made by a 2-cycle test became larger than that made by a 1-cycle test.
- 2) In chemical structure analysis, the decreased rates of chemical bonds of artificially degraded SiR surface made by 1-cycle test and 2-cycle test are similar to those of 10-year-aged SiR surface and 20-year-aged SiR surface on hydrophobicity class (HC 1) portion, respectively. It can be considered that various degraded SiR surfaces can be made by changing the number of fabrication cycles.
- 3) After an SD treatment, the hydrophobicity recovery time on the artificially degraded SiR surface made by a 2-cycle test was longer as compared with that made by a 1-cycle test. The hydrophobicity recovery time after the SD treatment is useful for evaluating the degradation degree on the artificially degraded SiR surfaces whose characteristics are similar to those of the SiR insulator surface aged in outdoor.

CHAPTER 6

CONCLUSIONS AND RECOMMENDATIONS

6.1 Conclusions

In this study, the characteristics of 22 kV SiR insulators arranged for 10 and 20 years in the coastal area are first investigated. Next, artificially degraded SiR surfaces, which have similar characteristics to actual aged SiR surfaces, are attempted to fabricate. To fabricate the artificially degraded SiR surface, a 24 h-fabrication cycle which consists of a red clay adhesion process, a UV irradiation process, a surface heating process, a heat radiation process, and a surface cleaning process are proposed. Here, the effects of UV irradiation and surface heating on SiR surface are also observed. In addition, the artificially degraded SiR surfaces are fabricated by a 24 h fabrication cycle (1-cycle test) and a 48 h fabrication cycle (2-cycle). After that, the degradation degree of both actual and artificially degraded SiR surfaces is grasped using a 20-time continuous salt-fog aging test and an SD treatment. To grasp the characteristics of both actual and artificially degraded SiR surfaces, the measurement on hydrophobicity class, contact angle of water droplet, surface morphology, chemical structure changes and electric characteristics are performed. On the other hand, to characterize an SD used for measuring the degradation degree of SiR insulator, SD current, surface temperature on the 150-mesh plate during an SD treatment and optical emissions are measured. The major results are concluded as follows:

- 1) *In the analysis of characteristics of aged SiR surfaces*, the contact angle after removing foreign matters capable of wiping became higher than that of an unused SiR surface. On the other hand, although foreign matters on aged SiR specimens exist on their surfaces, hydrophobicity is still high. Additionally, the partial contact angles of the aged specimens are larger than those of an unused SiR specimen. It is found that the minute surface roughness due to foreign matter adhesion makes the contact angle larger. The chemical structures of aged SiR surfaces vary from an unused SiR surface due to multiple stresses such as UV rays and foreign matter adhesion. Peak intensity ratios corresponding to Si-O bond, Si-CH₃ bond, C-H bond, and O-H bond in ATH decrease. Therefore, to artificially fabricate SiR surface having minute surface roughness, it is necessary to introduce fine particles such as red clay into the surface. Additionally, it is necessary to activate the dispersion of LMW by controlling UV irradiation and surface

heating.

- 2) *To fabricate the artificially degraded SiR surface*, the appropriated time of UV irradiation and the effect of surface heating are evaluated. The UV irradiation for 8 h largely decreases the contact angle. However, UV irradiation time for 6 h is observed as the appropriate time from the viewpoint of realizing a short-time fabrication. Next, the surface heating promotes the dispersion of LMW, and the surface heating over 40°C makes the contact angle smaller. However, the red clay on the surface is easily removed and the contact angle recovers to an initial value in a short time. Therefore, it is found that the surface heating process is not enough to artificially make the degraded surface and that a combination of UV irradiation for breaking molecular structure and surface heating for promoting LMW dispersion is necessary. Based on the results, the artificially degraded SiR surface is fabricated by one fabrication cycle (1-cycle test) of 24h and two fabrication cycle (2-cycle test) of 48 h which have the presence of red clay at different surface heating temperatures. The contact angle and the chemical structure on the artificially degraded SiR surfaces decrease like those of the actual aged SiR surfaces. In addition, the decreased rate of chemical structure on artificially degraded SiR surface made by 1-cycle test and 2-cycle test are similar to those of 10-year-aged and 20-year-aged SiR surfaces. Therefore, it can be considered that various degraded SiR surfaces can be made by changing the number of fabrication cycle.
- 3) *In an evaluation of the degradation degree on aged and artificially degraded SiR surface by an SD treatment*, the detected discharge current does not significantly differ from that obtained during the salt fog aging test. An SD treatment can accelerate hydrophobicity loss on the SiR surface. The hydrophobicity recovery times on aged and artificially degraded SiR surfaces are much longer compared to those on an unused SiR surface. Thus, the hydrophobicity recovery time after an SD treatment may be useful for investigating the degradation degree. On the other hand, an SD treatment cannot cause not only physical but also chemical damage to the SiR surface. In addition, it could be confirmed that SD has filamentary discharges. The surface temperature on the 150-mesh plate during an SD treatment cannot promote the decrease of the contact angel on SiR surface because the treatment time of an SD is short. Optical emissions with wavelengths of less than 291 nm which can cut the C-H bond of SiR aren't observed. Therefore, it is thought that the direct energy transfer from energetic particles

with higher energy than the binding energy of C-H changes chemical characteristics and decreases the contact angle on the SiR surface.

6.2 Recommendation

In this thesis, the degradation degree on actual aged and artificially degraded SiR surfaces with ATH 50% is evaluated. According to the results, the artificially degraded SiR surface with ATH 50% can be fabricated by red clay adhesion, UV irradiation and surface heating. However, UV irradiation time and the amount of red clay in a fabrication cycle are constant in this study, and they still have room for improvement. For future work, the fabrication cycle of artificially degraded SiR surface such as changing UV irradiation time or mixing UV irradiation and surface heating should be considered. In addition, SiR specimens with ATH 0% should be considered to investigate the fabrication of degraded SiR surfaces instead of SiR specimens with ATH 50%.

REFERENCES

- [1] E. A. Cherney et al., "Evaluation of and replacement strategies for aged high voltage porcelain suspension-type insulators," *IEEE Transactions on Power Delivery*, vol. 29, no. 1, pp. 275-282, Feb. 2014.
- [2] J. Mackevich, and M. Shah, "Polymer Outdoor Insulating Materials. Part I: Comparison of Porcelain and Polymer Electrical Insulation," *IEEE Electrical Insulation Magazine*, vol. 13, no. 3, pp. 5-12, May. 1997.
- [3] S. Kumara, and M. Fernando, "Performance of outdoor insulators in tropical conditions of Sri Lanka," *IEEE Electrical Insulation Magazine*, vol. 36, no. 4, pp. 26-35, Jun. 2020.
- [4] K. O. Papailiou and F. Schmuck, *Silicone Composite Insulators: Materials Design Applications*. Berlin Heidelberg.: Springer, Nov. 2012.
- [5] J. F. Hall, "History and bibliography of polymeric insulators for outdoor applications," *IEEE Trans. Power Del.*, vol. 8, no. 1, pp. 376-385, Jan. 1993.
- [6] R. Hackam, "Outdoor HV Composite Polymeric Insulators," *IEEE Transaction on Dielectric and Electrical Insulation*, vol. 6, no. 5, pp. 557-585, Dec. 1999.
- [7] Y. Zhu, "Influence of corona discharge on hydrophobicity of silicone rubber used for outdoor insulation," *Journal of Polymer Testing*, vol. 74, pp. 14-20, Apr. 2019.
- [8] C. Ashokrao Fuke et al., "Modified ethylene-propylene-diene elastomer (EPDM)-contained silicone rubber/ethylene-propylene-diene elastomer (EPDM) blends: Effect of composition and electron beam crosslinking on mechanical, heat shrinkability, electrical, and morphological properties," *Journal of Applied Polymer Science*, vol. 136, no. 29, p.47787, Aug. 2019.
- [9] M. Tariq Nazir et al., "Surface discharge behaviours, dielectric and mechanical properties of EPDM based nanocomposites containing nano-BN," *Applied Nanoscience*, vol 9, pp. 1981-1989, Feb. 2019.
- [10] M. Tariq Nazir et al., "Effect of micro-nano additives on breakdown, surface tracking and mechanical performance of ethylene propylene diene monomer for high voltage insulation," *Journal of Materials Science: Materials in Electronics*, vol. 30, pp. 14061-14071, Jul. 2019.
- [11] M. A. R. M. Fernando, and S. M. Gubanski, "Ageing of silicone rubber insulators in coastal and inland tropical environment," *IEEE Transaction on Dielectric and Electrical Insulation*, vol.17, no.2, pp. 326-333, Apr. 2010.

- [12] A. C. Baker et al., "Insulator selection for AC overhead lines with respect to contamination," *IEEE Transactions on Power Delivery*, vol. 24, no. 3, pp. 1633-1641, Jun 2009.
- [13] B. X. Du, and Yong Liu, "Frequency distribution of leakage current on silicone rubber insulator in salt-fog environments," *IEEE Transactions on Power Delivery*, vol. 24, no. 3, pp. 1458-1464, May 2009.
- [14] V. Rajini, and K. Udayakumar, "Degradation of silicone rubber under AC or DC voltages in radiation environment," *IEEE Transaction on Dielectric and Electrical Insulation*, vol.16, no.3, pp. 834-841, Jun. 2009.
- [15] L. Xidong et al., "Development of composite insulators in China," *IEEE Transactions on Dielectrics and Electrical Insulation*, vol. 6, no. 5, pp. 586-594, Dec. 1999.
- [16] X. Jiang et al. "Comparison of DC pollution flashover performances of various types of porcelain, glass, and composite insulators," *IEEE Transactions on Power Delivery*, vol. 23, no. 2, pp. 1183-1190, Apr. 2008.
- [17] M. reza Ahmadi-veshki et al., "Reliability assessment of aged SiR insulators under humidity and pollution conditions," *International Journal of Electrical Power & Energy Systems*, vol. 117, May 2020.
- [18] K. Ning et al., "Study on surface modification of silicone rubber for composite insulator by electron beam irradiation," *Nuclear Instruments and Methods in Physics Research Section B: Beam Interactions with Materials and Atoms*, vol. 499, pp. 7-16, Jul. 2021.
- [19] T. Sakoda et al., "Study on degradation diagnostic method for silicone rubber," *Journal of Electrostatics*, vol. 107, p. 103479, Sep. 2020.
- [20] L. Ying et al., "Effect of different curing parameters on UV aging resistance of silicone rubber," *2018 IEEE International Conference on High Voltage Engineering and Application (ICHVE)*. IEEE, pp. 1-4, Sep. 2018.
- [21] Y. Deng et al., "Hygrothermal ageing performance of high temperature vulcanised silicone rubber and its degradation mechanism," *High Voltage*, vol. 8, no. 6, pp. 1196-1205, Dec. 2023.
- [22] I. Ullah et al., "Impact of accelerated ultraviolet weathering on polymeric composite insulators under high voltage DC stress," *CSEE Journal of Power and Energy Systems*, vol. 8, no. 3, pp. 922-932, May 2022.
- [23] J. Chen et al., "Study on the Influence of Accelerated Aging on the Properties of an RTV Anti-Pollution Flashover Coating," *Polymers*, vol. 15, no. 3, p. 751, Feb. 2023.

- [24] A. H. El-Hag et al., "Influence of shed parameters on the aging performance of silicone rubber insulators in salt-fog," *IEEE transactions on dielectrics and electrical insulation*, vol. 10, no. 4, pp. 655-664, Aug. 2003.
- [25] R. S. Gorur et al., "Polymer insulator profiles evaluated in a fog chamber," *IEEE Transactions on Power Delivery*, vol. 5, no. 2, pp. 1078-1085, Apr. 1990.
- [26] M. Rostaghi-Chalaki et al., "Harmonic analysis of leakage current of silicon rubber insulators in clean-fog and salt-fog," *18th International Symposium on High Voltage Engineering*, pp.1684-1688, Aug. 2013.
- [27] S. Kumagai and N. Yoshimura, "Leakage current characterization for estimating the conditions of ceramic and polymeric insulating surfaces," *IEEE Transactions on Dielectrics and Electrical Insulation*, vol. 11, no. 4, pp. 681-690, Aug. 2004.
- [28] A. H. El-Hag et al., "Fundamental and low frequency harmonic components of leakage current as a diagnostic tool to study aging of RTV and HTV silicone rubber in salt-fog," *IEEE Transactions on Dielectrics and Electrical insulation*, vol. 10, no. 1, pp. 128-136, Feb. 2003.
- [29] M. Rostaghi-Chalaki et al., "A study on the relation between leakage current and specific creepage distance," *18th International Symposium on High Voltage Engineering (ISH 2013)*, pp. 1623-1629, Aug. 2013.
- [30] F. Meghnefi et al., "Temporal and frequency analysis of the leakage current of a station post insulator during ice accretion," *IEEE Transactions on Dielectrics and Electrical Insulation*, vol. 14, no. 6, pp. 1381-1389, Dec. 2007.
- [31] J. Andersson et al., "Properties of interfaces in silicone rubber," *IEEE Transactions on Dielectrics and Electrical Insulation*, vol. 14, no. 1, pp. 137-145, Feb. 2007.
- [32] Z. Farhadinejad et al., "Effects of UVC radiation on thermal, electrical and morphological behavior of silicone rubber insulators," *IEEE Transactions on Dielectrics and Electrical Insulation*, vol. 19, no. 5, pp. 1740-1749, Oct. 2012.
- [33] M. A. R. M. Fernando and S. M. Gubanski, "Leakage current patterns on contaminated polymeric surface," *IEEE Transactions on Dielectrics and Electrical Insulation*, vol. 6, no. 5, pp. 688-694, Dec. 1999.
- [34] R. Ullah et al., "Measuring electrical, thermal and mechanical properties of DC-stressed HTV silicone rubber loaded with nano/micro-fillers exposed to long-term aging," *Applied Nanoscience*, vol. 10, no.7, pp. 2101-2111, Apr. 2020.
- [35] M. Akbar et al., "Multi-stress aging investigations of HTV silicone rubber filled with

- Silica/ATH composites for HVAC and HVDC transmission," *Engineering Failure Analysis*, vol. 110, p. 104449, Mar. 2020.
- [36] T. Sakoda et al., " Characteristics of flashover on polluted polymer surface," *Korea-Japan Joint Symposium on Electrical Discharge and HV Engineering*, p. 81, 2015.
- [37] T. Sakoda et al., "Discharge behavior and dielectric performance of artificially polluted hydrophobic silicone rubber," *Journal of Electrostatics*, vol. 93. pp. 97-103, Jun. 2018.
- [38] Y. Zhu et al., "Distribution of leakage current on polluted polymer insulator surface," *2006 IEEE Conference on Electrical Insulation and Dielectric Phenomena*. IEEE, pp. 397-400, Feb. 2006.
- [39] M. A. Douar et al., "Degradation of various polymeric materials in clean and salt fog conditions: measurements of AC flashover voltage and assessment of surface damages," *IEEE Transactions on Dielectrics and Electrical Insulation*, vol. 22, no. 1, pp. 391-399, Feb. 2015.
- [40] V. J. Narayanan et al., "Analysis of surface condition of polymeric insulators for high voltage power transmission line applications using partial discharge analysis," *International Journal of Engineering And Science*, vol. 4, no. 7, pp. 31-40, Jul. 2014.
- [41] Y. Zhu et al., "Degradation of polymeric materials exposed to corona discharges," *Journal of Polymer testing*, vol. 25, no. 3, pp. 313-317, May. 2006.
- [42] A. J. O'Lenick, "Silicones-Basic chemistry and selected applications," *Journal of Surfactants and Detergents*, vol. 3, no. 2, pp. 229-236, Apr. 2000.
- [43] *Hydrophobicity Classification Guide, Guide 1, 92/1, Ludvika: STRI, 1992.*
- [44] Z. Dong et al., "Hydrophobicity classification of polymeric insulators based on embedded methods," *Materials Research*, vol. 18, pp. 127-137, Jan. 2015.
- [45] J. Kim et al., "Hydrophobicity loss and recovery of silicone HV insulation," *IEEE Transactions on Dielectrics and Electrical Insulation*, vol. 6. no. 5, pp. 695-702, Dec. 1999.
- [46] L. S. Lumba, "Analysis of surface degradation of silicon rubber insulators after 30 years in-service," *International Journal on Electrical Engineering and Informatics*, vol. 12, no. 4, pp. 828-844, Dec. 2020.
- [47] N. Yoshimura et al., "Electrical and environmental aging of silicone rubber used in outdoor insulation," *IEEE Transactions on Dielectrics and Electrical Insulation*, vol. 6, no. 5, pp. 632-650, Dec. 1999.
- [48] Y. Gao et al., "Investigation on permeation properties of liquids into HTV silicone

- rubber materials," IEEE Transactions on Dielectrics and Electrical Insulation, vol. 21, no. 6, pp. 2428-2437, Dec. 2014.
- [49] K. Iida, K et al., "Effect of low molecular weight fluid on the hydrophobicity of silicone rubber," 2008 International Symposium on Electrical Insulating Materials (ISEIM 2008). IEEE, pp. 275-278, Oct. 2008.
- [50] F. Z. Kamand et al., "Self-healing silicones for outdoor high voltage insulation: mechanism, applications and measurements," Energies, vol. 15, no. 5, p. 1677, Feb. 2022.
- [51] S. H. Kim et al., "Chemical changes at the surface of RTV silicone rubber coatings on insulators during dry-band arcing," IEEE Transactions on Dielectrics and Electrical Insulation, vol. 1, no. 1, pp. 106-123, Feb. 1994.
- [52] Y. Zhu et al., "Surface degradation of silicone rubber exposed to corona discharge," IEEE Transactions on Plasma Science, vol. 34, no. 4, pp. 1094-1098, Aug. 2006.
- [53] J. S. Chang *et al.*, "Corona discharge processes," IEEE Transactions on Plasma Science, vol. 19, no. 6, pp. 1152-1166, Dec. 1991.
- [54] H. Homma et al., "Evaluation of surface degradation of silicone rubber using gas chromatography/mass spectroscopy," IEEE Transactions on Power Delivery, vol. 15, no. 2, pp. 796-803, Apr. 2000.
- [55] D. A. Swift et al., "Hydrophobicity transfer from silicone rubber to adhering pollutants and its effect on insulator performance," IEEE Transactions on Dielectrics and Electrical Insulation, vol. 13, no. 4, pp. 820-829, Aug. 2006.